APPLICATION OF FUZZY LOGIC CONTROLLER FOR TRACTING GLOBAL MAXIMUM POWER OF PARTIAL SHADE PV SYSTEM (ASSOSA UNIVERSITY WHETHER CONDITION)

BY

ASSAYE FETENE BAYIH

A Thesis Submitted to the Department of Electrical Power and Control Engineering

School of Electrical Engineering and Computing

Presented in Partial Fulfillment of the Requirements for the Degree of Masters' of Science in Electrical Power and Control Engineering (Power Electronics)

Office of Graduate Studies

Adama Science and Technology University

Adama, Ethiopia

July 2020

APPLICATION OF FUZZY LOGIC CONTROLLER FOR TRACTING GLOBAL MAXIMUM POWER OF PARTIAL SHADE PV SYSTEM (ASSOSA UNIVERSITY WHETHER CONDITION)

BY

ASSAYE FETENE BAYIH

Advisor: TEFERA TEREFE (PHD.)

A Thesis Submitted to the Department of Electrical Power and Control Engineering
School of Electrical Engineering and Computing
Presented in Partial Fulfillment of the Requirements for the Degree of Masters' of Science in Electrical Power and Control Engineering (Power Electronics)
Office of Graduate Studies

Adama Science and Technology University

Adama, Ethiopia
July 2020

Approval of Board of Examiners

We, undersigned, member of the Board of Examiners of the Final Open defense by Assaye Fetene Bayih have read and evaluated his Thesis entitled **"APPLICATION OF FUZZY LOGIC CONTROLLER FOR TRACTING GLOBAL MAXIMUM POWER OF PARTIAL SHADE PV SYSTEM (ASSOSA UNIVERSITY WEATHER CONDITION)**" and examined the candidate. This is, therefore, to certify that the thesis has been accepted in partial fulfillment of the requirement of the degree of Masters' of Science in Electrical and Computer Engineering (specialization in Power Electronics).

______________________	______________	______________
Name of student	Signature	Date
______________________	______________	______________
Advisor	Signature	Date
______________________	______________	______________
External examiner	Signature	Date
______________________	______________	______________
Internal examiner	Signature	Date
______________________	______________	______________
Chairperson	Signature	Date
______________________	______________	______________
Head of Department	Signature	Date
______________________	______________	______________
School Dean	Signature	Date
______________________	______________	______________
Post graduate Dean	Signature	Date

Declaration

I hereby declared that, this M.Sc. thesis entitled **APPLICATION OF FUZZY LOGIC CONTROLLER FOR TRACTING GLOBAL MAXIMUM POWER OF PARTIAL SHADE PV SYSTEM (ASSOSA UNIVERSITY WETHEAR CONDITION)**, has been compiled by me under the supervision of Tefera.T.Y (Ph.D.) at the Department of Electrical and Computer Engineering, ASTU, Adama, Ethiopia. This thesis contains no material which has been accepted for the award of any other degree or diploma, except where due reference is made. To the best of my knowledge, this thesis contains no material previously published or written by another person except where due reference is made in the text of the thesis.

Assaye Fetene Bayih		
Student name	Signature	Submission date

This M.Sc. thesis has been submitted for examination with my approval as a thesis advisor.

Dr. Tefera.T.Y		
Advisor name	Signature	Submission date

Advisor Approval Sheet

To: Electrical Power and Control Engineering department

Subject: M.Sc. Thesis Submission

This is to certify that the thesis entitled "**APPLICATION OF FUZZY LOGIC CONTROLLER FOR TRACTING GLOBAL MAXIMUM POWER OF PARTIAL SHADE PV SYSTEM (ASSOSA UNIVERSITY WETHEAR CONDITION)**", submitted in partial fulfillment of the requirement for the degree of Master's Science in Electrical Power and Control Engineering department (Specialization in Power Electronics), the Graduate program of the department of Electrical Power and Control Engineering, and has been carried out by ASSAY FETENE BAYIH Id. No. A/PR15426/10, under my supervision. Therefore, I recommend that the student has fulfilled the requirements and hence hereby he can submit the thesis to the department.

Dr. Tefera.T.Y		
Advisor name	Signature	Date

Acknowledgment

First and foremost my deepest gratitude goes to the Ultimately God (in Amharic Egziabher), second, I would like to great full thanks to my advisor Tefera.T.Y (Ph.D.) for his guidance and support throughout my thesis Work and also I Would like to thank Benishangul Gumuz Metriology office Workers for giving an important data (sunshine hour and temperature) of Assosa for my study. I would like to thank ASTU, school of Electrical and Computer Engineering, Department of Electrical Power and Control Engineering chairperson Mr. Ensermu and some of the staff members for their support.

Last but not least, I would like to thank all of my families for their incredible support throughout my study.

Finally, I would like to thank all of my classmates' students for their support in my study.

Abstract

A solar photovoltaic (PV) system has been emerging out as one of the greatest potential renewable energy sources and is contributing significantly in the energy sector at present and at large in the future due to its nature of environmental friendly. The main challenge of the PV system is it depends upon the solar irradiation and any changes in the incoming solar irradiation will affect badly on the output of the PV system. Furthermore, solar PV power has large fluctuations due to partial shading condition. This implies, under partial shading conditions, multiple peaks are experienced in the power–voltage (P–V) characteristic curve of a photovoltaic (PV) array, and the conventional maximum power point tracking (MPPT) algorithms (or P&O MPPT algorithm) may fail to track the global maximum power point (GMPP. Furthermore, when the solar panel is directly connected to the load, the power that is delivered is not optimal.

Therefore, this thesis proposes a maximum power point tracking (MPPT) in order to extract the GMPP from multiple peaks of the PV system for a potential maximum efficiency under partial shade conditions. In order to do so; first the PV system with resistive load is discussed, the modeling and the simulation of the PV module and the DC/DC converter (boost converter) are carried out using MATLAB software for different testing conditions. The objective of the proposed algorithm, FLC is to simultaneously solve inherent drawbacks in conventional MPPT algorithms.

The performances of the conventional Perturb & Observe (P&O) algorithm and the proposed algorithm are compared by using MATLAB/Simulink 2015a, and the theoretical advantages of FLC were demonstrated. The results indicated that the proposed algorithm performed with faster tracking time, smaller output power oscillation, and higher efficiency, compared to that of the conventional P&O algorithm. This show that MPPT with FLC can give a big significant improvement on the performance of PV system under the conditions like varying irradiation and temperature, and partial shade. FLC technique gives better and more reliable control for this application.

KEY WORDS: PVs, PV cell, PV Module, PV Array, MATLAB2015a SIMULINK, MPPT GMP, FLC, P&O Algorithm, PWM, Boost Converter, Ideal switches

Table of Contents

List of Tables

Tables……...……………………………………………………………………………...page

Lists of Figures

List of Symbols, Abbreviations and Acronyms

G_n	Solar radiation @ STC
I_d	Diode/dark current
I_{mpp}	PV Current @ maximum power point
I_{mppt}	PV Current of maximum power point tracker
I_o	Saturation current
I_{pv}	Photovoltaic/Module/Panel current
I_{sc}	Short circuit current
N_p	Number of cells connected in parallel
N_{par}	Number of modules connected in parallel
N_s	Number of cells connected in series
N_{ser}	Number of modules connected in series
P_{max}	Power Possible Power from PV array
P_{mpp}	Power @ maximum power point
$P_{mppt}(P_{out})$	Power extracted by MPPT
P_{pv}(P)	Photovoltaic/Module/Panel Power
R_p	Parallel resistance
R_s	Series resistance
T_n	Temperature @ STC
V_{mpp}	PV voltage @ maximum power point

V_{mppt}	PV voltage of maximum power point tracker
V_{oc}	Open circuit voltage
V_{pv}	Photovoltaic/Module/Panel voltage
AC	Alternate Current
COG	Center of gravity
DC	Direct Current
FL	Fuzzy logic
FLC	Fuzzy logic control
GMPP	Global Maximum power point
I	Current
IVTF	Initial voltage tracking function
KW	Kilo-Watt
LMPP	Local Maximum power point
MF	Membership function
MP	Maximum power
MPP	Maximum power point
MPPT	Maximum power point tracking
OCV	Open circuit voltage
P	Power
PSC	partial shade condition
SCC	Short circuit current

SP	Shading Pattern
STC	Standard test condition
T	Temperature
Tri	Triangular
Trimf	Triangular membership function
V	Voltage
W	Watt
ANN	Artificial neural network
D	Duty cycle ratio
DE	Differential evolution
G	Solar radiation
GW	Giga-Watt
$IncCond$ (IN)	Incremental Conductance
K	Boltzmann constant
$P\&O$	Perturbation & Observation
PSO	Particle swarm Optimization
PV	Photovoltaic
q	Electron charge
$\boldsymbol{\alpha}$, α_1	diode identity constant

CHAPTER 1

INTRODUCTION

1.1 Background

It is well established that energy production and use based on consumption of fossil fuels can have an impact on the world ecosystem and human health, including the potential of global warming of the earth through changes in the atmosphere's concentration of carbon dioxide. Beside this, now a day the worldwide conventional energy sources are rapidly depleting at an alarming rate. The energy demand is growing at a rapid rate due to modern industrial society and population growth. This issue has driven interest in research and technological investments related to the optimization of energy efficiency and the use of sustainable and renewable energy either self-sufficient or supplementary to the main source is mandatory [1], [2].

Among various renewable sources of energy solar, wind, biomass, geothermal, hydro are some of them. One of the promising sources of renewable energy which is durable and eco-friendly in nature is solar / photovoltaic energy. Solar energy as a source of electricity using photovoltaic (PV) conversion system has been growing at a faster rate in the last decades because of abundant availability of light energy and an improvement on the PV cell conversion rates.

The predominant features of photovoltaic energy which makes it outstanding from other renewable energy sources are [3]-[5];

- ✓ It is abundant in nature and is free and readily available unlike the fossil fuels.
- ✓ There is no emission of harmful greenhouse gases and is a clean source of energy production.
- ✓ They require minimal maintenance and are reliable as they do not have any moving parts and are free from vibrations.
- ✓ The photovoltaic power generation can be installed in small-scale and distributed manner; near the load center; unlike the conventional power generation systems which require large scale installations to operate.
- ✓ The photovoltaic power is available during the times when there is peak power demand.

However, the solar system have some inherent limitations such as low conversion efficiency, dependent on atmospheric conditions, non-linear characteristic, high initial investment requirement, large area for installation, partial shading effects, and, cell degradation are challenges to investigate techniques for efficient extraction and utilization of PV power [6], [7]. The main purpose of this work is to develop and optimize maximum power point tracking and control of the most promising alternative energy source, a photovoltaic (PV) module. PV power is a renewable energy source that has recently sparked significant interest and may in the near future replace nonrenewable sources such as fossil fuels. However, to achieve this change-over, PV power cost per kilowatt-hour has to be competitive in comparison to fossil fuel energy sources. The material used in the structure of solar cells and the technology used in arranging the solar cells to form a module are considered key factors that affect the efficiency of PV modules. At the present time, PV modules have only about 12-26% efficiency in converting solar irradiance to electricity, which is quite low [8]. Gallium Arsenide solar cells have a high rate of efficiency of 29%, whereas Silicon solar cells have about 12-14% efficiency [9]. Moreover, efficiency can drop due to load conditions, PV module temperature, or decreases in solar insulation.

PV module, dependents of weather conditions (i.e. sunlight), which are subject to frequent change. Consequently, the duration of electric current generation by PVs may be limited, as a result of its dependence on the temperature of its surroundings, and sunlight in particular. In addition, the voltage-current (I-V) and power-voltage (P-V) features of PV cell are not linear, since they vary with irradiance and temperature [3], [4], [10]-[13]. The (P–V) feature of a PV module requires the module to have an optimal operating point (i.e. MPP)) to yield its maximum power output. This point is variable and dependent on local weather conditions and load impedance. Therefore, MPPT methods are necessary for a PV system to maintain the operation of PV panels at their MPP [14]-[18].

This means, the efficiency of MPPT controllers is reduced under PSC, due to the assumption that most MPPT controllers operate in such a way that the PV module can only produce its maximum power a one point within the P–V characteristic. However, the P–V characteristic becomes more complex and exhibits multiple peaks in PSC, which in turn affects the performance of the controller, resulting in a reduction in the complete output power of the system [19], [20]. Recently, a large number of modified MPPT methods have been proposed in the literature related to the accurate tracking of MPP, and the improvement in the dynamic system response, as well as minimizing system hardware [20]-[22]. These methods differ in complexity, accuracy and speed. Yet, even when the tracking was undertaken perfectly with these methods, it resulted in a slow dynamic response speed of the system.

The non-linear I-V/P-V characteristic is a major challenge that results in a unique maximum power point (MPP) on the characteristic curve. In order to capture the maximum-rated power from a PV module, it is necessary to operate the module at its optimal power point. To do this, a controller called a maximum power point tracker is required. Tracking continuously this operating point is known as maximum power point tracking (MPPT) and it is important to maximize the efficient utilization of solar PV power in the given atmospheric condition. The dependence on atmospheric conditions may complicate the continuous tracking because the variation in atmospheric parameters also varies the operating point (MPP). Thus, it is imperative to operate the PV source at MPP so that maximum power can be extracted by using appropriate technique [23, 22]. There are various MPPT algorithms and they vary in complexity, sensors required, convergence speed, cost, the range of effectiveness, implementation hardware, popularity, etc. They range from the almost obvious (but not necessarily ineffective) to the most creative (not necessarily most effective).

The situation of maximum power point tracking is more complicated whenever the P-V characteristic curve comprises of several local and global peaks. This situation usually happens due to non-uniform distribution of irradiance (in the case of partial shade) on the surface of PV modules in a PV array/system. The situation of partial shade on PV modules can be solved using bypass diode that may result in a considerable amount of energy loss because the shaded module is bypassed by the diode. The second possible option to solve maximum power extraction during partial shading is the application of distributed maximum power tracking (DMPPT) [24], [25]. However, use of DMPPT per module or per string basis may increase complexity by which implementation cost increases. In this thesis, the problem of tracking the global maximum power using classical MPPT techniques is proposed to be solved using fuzzy logic controller based MPPT technique.

1.2 Overall Trends in Installations and Market

Almost 1.288 GW of new solar PV capacity came into operation worldwide in 2000, increasing the global total by 99.796% to almost 633.7 GW as shown in fig. 1.1. Solar PV capacity in operation at 2019 was about 6 times the global total just seven years earlier, and the average annual growth rate exceeded more than 58% for the period from the end of 2012 through 2019 [26] as shown in fig. 1.1 bellow. While the market surpassed all previous records, PV-related production ramped up even faster, resulting in a significant oversupply of modules in 2019.

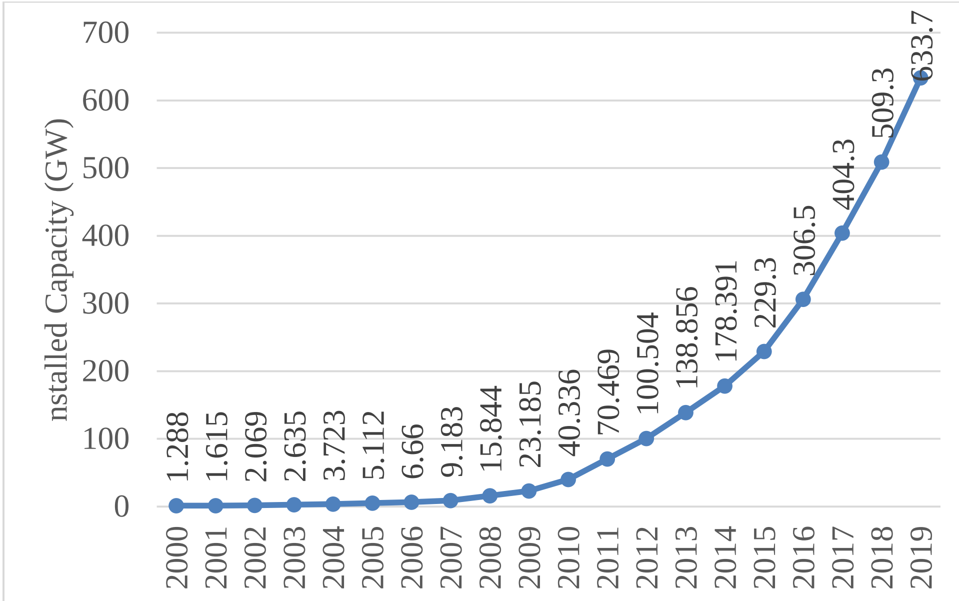

FIGURE 1.1 SOLAR PV EXISTING WORLD CAPACITY 2000-2019

1.3 Photovoltaic History

The history of PV dates back to 1839 when a French physicist, Edmund Becquerel, discovered the photovoltaic effect while experimenting with an electrolytic cell made up of two metal electrodes placed in an electricity-conducting solution-generation increased when exposed to light, Almost 40 years later, Adams and Day were the first to study the photovoltaic effect in solid selenium and were able to build solid cells with 1~2% efficiency. By the 1950s, the Czochralski began to process the first generation of single-crystal silicon photovoltaic.

The real appearance of PVs in practical was in 1958 when they were used in space for the Vanguard I satellite. Today, the production of PV cells is following a rapidly growing curve since technological advancement of late ‘80s that has started to rapidly improve efficiency and reduce cost. The word of photovoltaic divided into two words, Photo means light, and Voltaic means electricity, photovoltaic means getting electricity from light (sun) [27],[28]. PV power conversion technologies has been around for many years, and have been implemented for military, space, commercial and residential applications by taking advantage of the abundant solar energy given off by the sun.

1.4 Architecture of PV system

Solar cell is the fundamental power conversion unit of a PV system. Over the past decades, silicon has been almost the only material used for manufacturing solar cells, although other materials have been developed. Progress in manufacture of solar cells are moving so rapidly, In general, cells can be classified as either wafer-based crystalline (single crystal or Polycrystalline) or thin film [29],[30].

The power produced by a single solar cell is not enough for general use since it produce an output voltage less than 1V; cells must be connected in series, parallel or series-parallel configurations to produce enough power for high-power applications. They are usually assembled into modules. However, there are different sizes of PV modules commercially available; the most commonly used module is 36 to 72 solar cells connected in series to produce enough voltage. For higher power requirement, the modules are interconnected in series/parallel to form arrays as shown in fig. 1.2 [31].

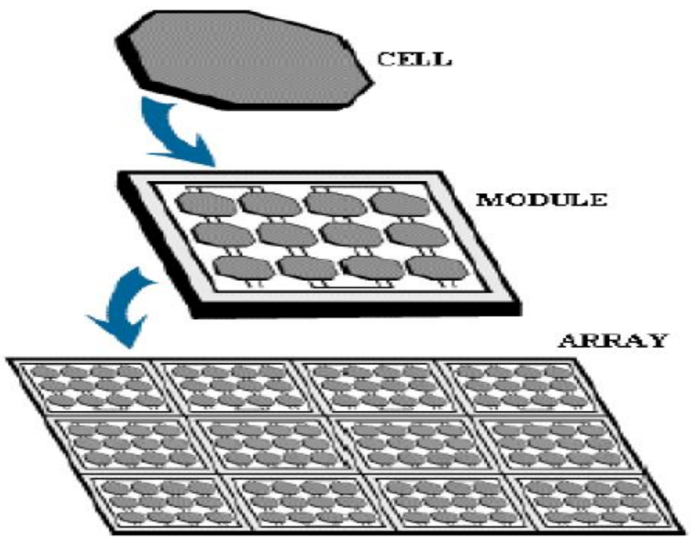

FIGURE 1.2 ILLUSTRATED PHOTOVOLTAIC SYSTEM

In order to be able to compare different PV modules uniform conditions are usually specified for determining the electrical characteristics. These conditions known as standard test conditions (STC) where parameters obtained from the testing are usually provided on the manufacturer's datasheet. These conditions are [30]:

- ✓ Irradiance on cell surface is 1000 W/m2.
- ✓ Operating temperature of 25oC.
- ✓ A specified light spectral distribution with an air mass =1.5.

1.4.1 Advantage and Disadvantage of PV System

The table below illustrated the advantage and disadvantage of the PV system over conventional power sources [32].

Table 1.1 advantages and disadvantage of solar energy generation system over conventional power source.

PV system offers the following advantage over conventional power source	PV has some disadvantages as compared to conventional power system
✓ It is free and inexhaustible.	✓ A high initial investment cost
✓ Low maintenance cost	✓ Low power conversion efficiency
✓ Long lifetime, it can produce power for 25 years.	✓ The non-linear current-voltage (I-V) characteristics exhibited by a PV cell due variations in cell temperature and irradiation
✓ NO fuel cost. Since no fuel source is required, there are on costs associated with purchasing, storing, and transporting fuel.	✓ Required energy storage

1.4.2 Theory of operation

Solar cell is basically a p-n junction. It relies on the process known as the "photovoltaic effect" to produce electricity. When the light irradiates the surface of a solar cell, part of the photons of the light may get reflected or consumed immediately when they impact the surface of the solar cell. This is because the energy that they carry is too weak to be converted into electricity. Only the photons, which are absorbed near the P-N junction of the solar cell, can work for the photovoltaic effect. This phenomenon happens when the energy produced by the photons from sunlight on the exposed solar cell is greater than the band energy of the semiconductor. By absorbing the energy of the photons, the atoms in the P-N junction generates plentiful hole-electron pairs. Under the force of the electrical field of the P-N junction, the holes carry the positive charge and shift from the N-type layer to the P-type layer. The electrons carrying the negative charge, escape from the P-type layer, and eventually migrate to the N-type layer [33]. By connecting an electric load to the P-N junction, such as resistor, the electrons in the N-type layer flow through the load, and finally enter the P-type layer. The holes in P-type layer combine with the coming electrons. The P-N junction of a PV cell is shown on Fig. 1.3 [33]. Thus, electron-hole pairs are created by the breakage and loss of the atoms in the material. The existing electric field of p-n junction of solar cells separate the created charge carriers in the depletion region and lead to a forward bias of the p-n junction, so that a voltage potential is built up. This will cause a current proportional to the incident radiation to flow through the load once it is connected to the cell as shown in fig. (1.3) [34]-[36].

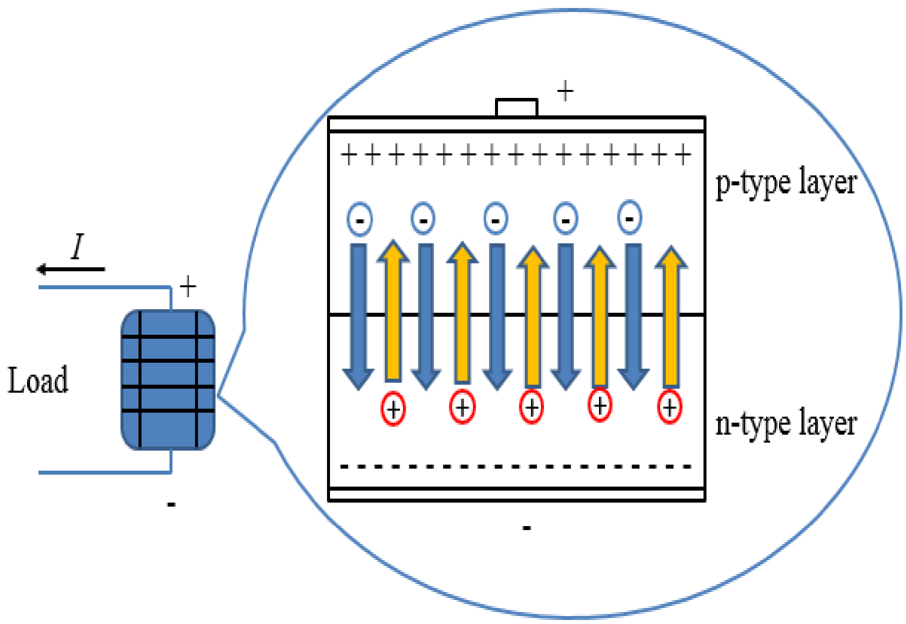

FIGURE 1.3 P-N JUNCTION OF A SOLAR CELL [37]

1.4.3 Types of Solar cell

There are different types of solar panels which differ in their material, price, and efficiency [30].

1.4.3.1 Monocrystalline Solar cell

It has efficiency approximately 12-18% [30],[38]. They are made from a large crystal of silicon. These types of solar panels are the most efficient panels; however they are the most expensive. They do somewhat better in lower light conditions than the other types of solar panels.

1.4.3.2 Polycrystalline Solar cell

It has efficiency approximately 11-16% [30],[38]. Instead of one large crystal, this type of solar panel consists of multiple amounts of smaller silicon crystals; they are the most common type of solar panels on the market today. They look a lot like shattered glass. They are slightly less efficient than the monocrystalline solar panels and less expensive to produce.

1.4.3.3 Thin film Solar cell

It has efficiency approximately 10-13% [30],[39]. Amorphous silicon, copper indium diselenide (CIS) and cadmium telluride (CdTe) are used as semiconductor materials. These types of solar panels have lower efficiency than the other two types of solar panels, and the cheapest to produce.

1.4.4 Balance of Systems (BOS)

BOS are the components which added to the PV array to be able to integrate with systems. These components can be classified into [40]:

- ✓ Wiring components which includes distribution panel, junction box and miscellaneous connectors, lighting protectors, grounding connections, fuse box.
- ✓ Batteries and Battery charge controller: Stand-alone PV systems require energy storage to compensate for periods without or within sufficient solar irradiation, such as during the night or during cloudy weather.
- ✓ Inverter: it is used to convert the direct current output of the array or the battery into alternating current (AC) to be suitable for AC loads.
- ✓ DC/DC converter: it is used to adjust output volt to be suitable for load.
- ✓ MPPT controller: used to extract maximum power of PV array to be transfer to the load.

The main concern of this thesis is to purposes one of the component of BOS, which is MPPT controller, in order to operate the PV system at any atmospheric condition.

1.5 photovoltaic system

The photovoltaic system consists of interconnected components designed in a way to achieve the specific target of delivering the desired electricity from a small device to the required load. It is categorized as gird connected, standalone system and hybrid system which comprises different source of energy such as PV array diesel generator and wind generator. Hybrid and standalone system are used widely in the world especially in the rural areas [25],[26],[41]. Therefore different operating conditions of standalone PV system have been studied in this particular thesis.

1.5.1 Classifications of Photovoltaic Power Systems

As shown in the fig.1.4, PV systems can be divided into two types: (1) a stand-alone system and (2) a grid connected system. Stand-alone systems generally operate independently, and can be used in a number of applications, including: satellites; space stations; remote areas; and water pumping systems. There has recently been an increase in the use of grid-connected systems capable of supplying utilities with solar energy through the grid, with 93% of PV grid connected systems being installed in 2004 [3],[12],[42].

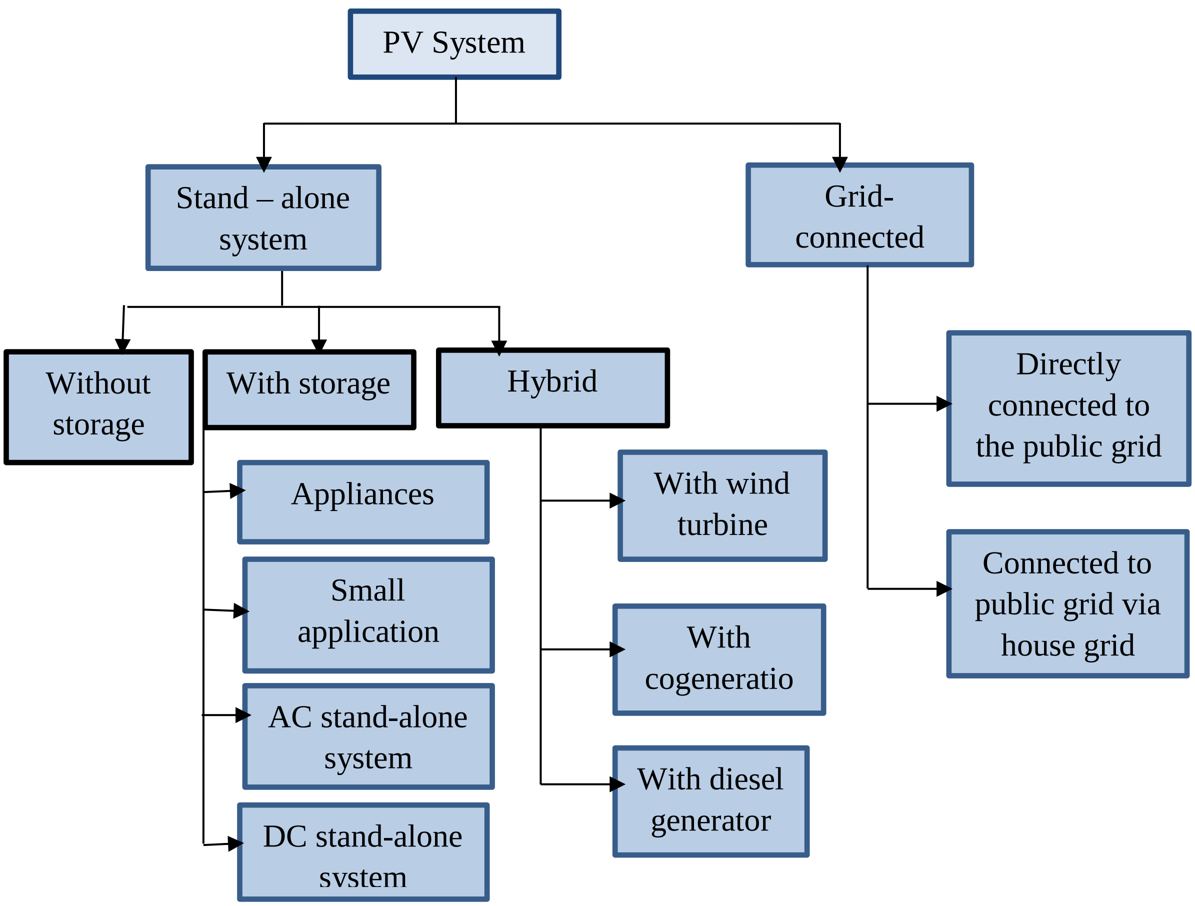

FIGURE 1.4 CLASSIFICATIONS OF PV SYSTEMS [3]

1.5.1.1 Standalone PV system

The power generated from the photovoltaic array in the standalone system is directly fed to the load shown in fig.1.5 without connecting to the grid system, i.e. charging of batteries, water heating systems, solar lighting and water pumping systems. It is considered as one of the most economical way of implementing photovoltaic system especially for application in rural areas that have large period of intense solar radiation and have no access to the national gird [41].

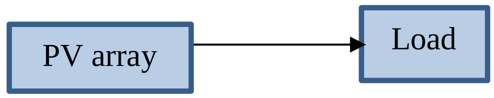

FIGURE 1.5 STAND-ALONE PV SYSTEMS [41]

1.5.1.2 Grid connected PV systems

This form of PV system is appropriate for those regions with plentiful space, combined with lengthy and unsecured periods of sunlight. It consists of a grid connected system, with its output power directly supplied to the grid. However, the output voltage of the PV module is DC, and thus need to be converted to an AC current by means of power electronic devices. The PV output power needs to be initially increased, followed by feeding its output power into a DC link to be inverted into alternative current (AC) through an inverter fulfilling the demand quality of AC voltage [19],[41], [42]. Fig. 1.6 demonstrates the grid connected type when the PV system is connected to other sources in parallel [14].

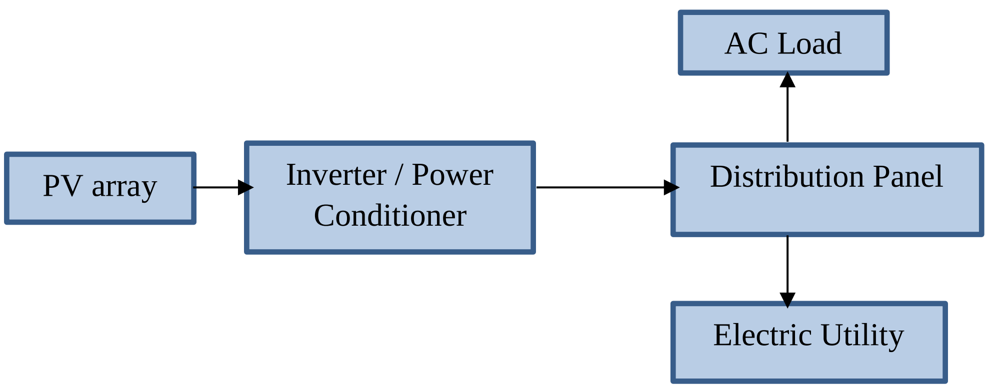

FIGURE 1.6 GRID-CONNECTED TYPE [41]

1.6 The proposed PV system

The proposed system in this thesis is maximum power extraction of partially shaded standalone PV system to obtain the pick power for any atmospheric change at the surface of the PV array. The system mainly comprises photovoltaic module as a source, converting sun light into electrical energy as shown in fig 1.7. To achieve high efficiency system performance and increase the amount of energy extracted from the PV module the load during the day light hours, a maximum power point tracker will be included in the system.

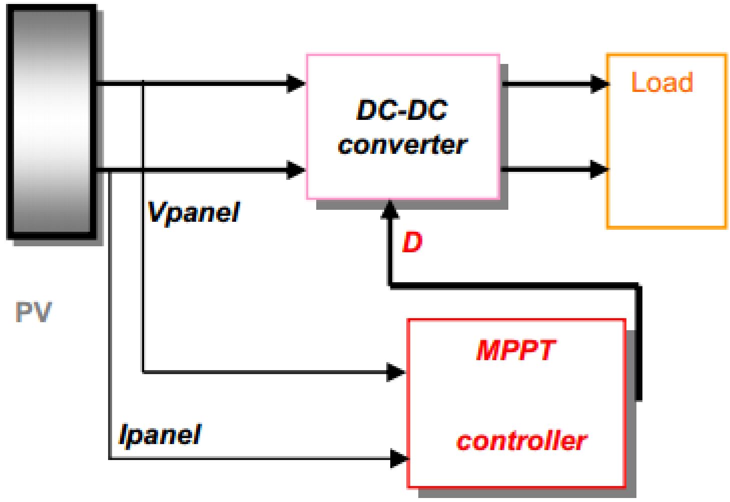

FIGURE 1.7 OVERALL REPRESENTATION OF MPPT CONTROLLER

The components of such photovoltaic system will be described in detail in the remaining parts of this thesis and mathematical models will be developed in chapter 3 to represent the characteristics each component in a complete system simulation.

1.6.1 The PV module

There are different sizes of PV module commercially available (typically sized from 60W to 300W).Usually a number of PV modules are combined as an array to the required energy demands. The size of the system for the proposed system is 3.19KW [29].

1.6.1.1 PV cell model under partial shade conditions (PSCs)

PV panel partial shading is one of the main causes of electrical mismatching of series connected PV cells, and can lead to the eventual avalanche breakdown of shaded cells [43]. The junction temperature increases considerably due to high avalanche current, causing thermal breakdown of the shaded cell.

1.6.2 Maximum power point tracker

A maximum power point trucker is a device capable of trucking the MP, and this device consists of DC-DC power converter its duty cycle adjusted by MPPT controller. While the PV panels may seem like a good source of electricity, their conversion efficiency is not very high. Their ability to convert sunlight energy to electrical power is relatively imperfect, with conversion efficiency typically in range of 12 to 20%. The range of efficiency can drop further during variable solar radiation, panel temperature and load conditions [44]. Therefore, if the load is directly coupled to the PV array, the PV array must be oversized the required power to the load. This causes an oversized expensive system. It is important operate the PV cells of the array at maximum power point, MPP, or as near to it as possible by using an electronic load-matching circuit, since this gives worthwhile improvement in the available power in comparison with direct load connection [44]. The output current and power of a PV array depends on the terminal voltage. The MPPT is now prevalent in gird-tied PV power system and is become more popular in standalone systems. It should not be confused with sun truckers, mechanical devices that rotate and/or tilt PV modules in the direction of the sun. MPPT is a power electronic device interconnecting a PV power source and the load, maximizes the power output from a PV module array with varying operating conditions, and therefore maximizes the system efficiency. MPPT is made up of a switched-mode DC-DC converter and controller.

1.6.3 MPPT controller

Analog controllers have traditionally performed control of MPPT. However, the use of digital controllers is rapidly increasing because they offer several advantages over analog controllers. First, digital controllers are programmable thus capable of implementing advanced algorithm with relative ease. It is far easier to code the equation, $x = y \times z$, than to design an analog circuit to do the same. For the same reason, modification of the design is much easier with digital controllers. They are immune to time and temperature drifts because they work in discrete, outside the linear operation. As a result, they offer long- term stability. They are also insensitive to component tolerances since they implement algorithm in software, where gains and parameters are consistent and reproducible. They allow reduction of parts count since they can handle various tasks in a single chip. Many of them are also equipped with multiple A/D converters and PWM generators, thus they can control multiple devices with a single controller [44].

1.7 DC –DC Converter

DC –DC converters are power electronic circuits that convert a dc voltage to a different voltage level. There are different types of conversion method such as electronic, linear, switched mode, magnetic, capacitive. The types of DC-DC converter used here in this particular thesis is classified as switched mode DC-DC converters. These are electronic devices that are used whenever change of DC electrical power from one voltage level to another is needed to extract maximum power from the PV array.

1.8 Statement of the problem

Solar photovoltaic conversion is widely in use among others alternative sources of electricity due to abundant availability of solar energy, clean, noise and pollution free. However, PV system has low conversion efficiency, dependent on atmospheric conditions, non-linear characteristic and high initial investment requirement are challenges to investigate techniques for efficient extraction and utilization of PV power. However, one of the main challenges of the PV System to operate at its peak is the non-linear behavior of the PV cells under partial shade condition. This varies the operating point of the system accordingly (it means that more than one LMPP and one GMPP is created in the characteristic curves of the PV system) and this arise a difficulties to operate at its optimal operating efficiency (at its GMPP) for the PV system with conventional MPPT algorithm. Therefore, low conversion efficiency and strong dependence on climatic conditions of PV system need techniques for efficient extraction and utilization of available power. Summary of related works on maximum power point extraction (MPPT) techniques showed that classical methods are efficient and simple to implement. However, failure to track the right direction of perturbation, steady-state oscillation and failure to track global MPP under partial shade condition are some of the drawbacks of widely used classical techniques. MPPT algorithm(s) that is comprehensive and applicable for wide range of atmospheric conditions should be developed. The control algorithm follows the excellent approach representation and deduction capabilities of fuzzy logic to fix the operating point the PV array to the GMPP.

1.9 Significance of the study

- To reduce power losses caused by partial shading condition and improve the efficiency of photovoltaic panel.
- Efficiency analysis and optimization of power generated by standalone solar system under variation in atmospheric condition in particular under partially shaded condition.
- To extract the maximum possible power generated from photovoltaic system under any atmospheric condition, especially under partial shade, using fuzzy logic control system.
- To extract the maximum possible power from a PV array.

1.10 Delimitation /Scope of the research

The scope of this research is to maintain global maximum power point for standalone photovoltaic under partial shading condition for a particular location, Assosa atmospheric condition based on fuzzy logic controller, and to study and analyze the MPPT for solar system, by using different analysis techniques. This thesis presents reimplementation of some of the previous techniques. Intelligent control technique using fuzzy logic control is associated to an MPPT controller in order to improve energy conversion efficiency under PSCs and compared with P&O method as one of the most widely used techniques in MPPT because of its simplicity. Simulation and analysis of P&O and fuzzy logic control are presented.

1.11 Objectives

The main aim of the thesis is to apply fuzzy logic algorithm for maximum power extraction of photovoltaic power system under partial shade condition. The successful achievement of the main aim is based on the following objectives.

1) Develop a SIMULINK model of PV module that converts solar energy to electric one and DC-DC boost converter that converts produced DC voltage by the PV module.

2) To study the behavior of PV modules under different environmental conditions, and their modeling techniques in MATLAB using equivalent circuits, suitable for analysis and simulation.

3) To investigate features influencing the performance of MPPT algorithms, i.e. PV capacitance and PSC

4) To investigate the performance of widely used P&O MPPT algorithms in the PV system, comparing their performance and efficiency for varying atmospheric condition.

5) To propose a new MPPT method for a PV system based on FLC method capable of dealing with issues arising when searching for MPP.

6) To investigate the performance of the PV system using the proposed algorithm, comparing it to the existing MPPT algorithm using the MATLAB Tools Simulink

7) Verifying the performance of the proposed method under various shading condition in MATLAB/SIMULINK environment and show that the PV system operates the at/near global maximum power point under partial/uniform shade.

1.12 Thesis outline

In this thesis, a detailed literature review about tracking techniques will be presented in chapter 2. Chapter 3 will focus on PV systems modeling and simulation featuring a MATLAB/Simulink full simulation of the overall standalone PV system. Chapter 4 will discuss the design and implementation of the proposed system, fuzzy logic controller systems and conventional MPPT system, P&O MPPT algorithm. The proposed FLC controller will be fully investigated in chapter 5 highlighting a simulation comparison between the proposed controller and the conventional ones and will verify the proposed technique effectiveness through presenting the PV system experimental results. Finally, chapter 6 will conclude the work discussing the work limitations along with the future work.

CHAPTER 2

LITERATURE REVIEW

In recent years, solar energy has become a significant factor in a number of applications. However, the distribution of electrical energy remains a challenge in remote areas, where applications are relatively small, as can be observed from the small size of generators or utility grid. Electricity acquired from an array of solar systems is more expensive in comparison to that acquired from the utility grid, and it is therefore necessary to undertake in-depth research concerning the efficiency of all aspects, in order to establish an effective PV system capable of satisfying a large number of demands at a lower cost [45],[46].

The efficiency of PV panel functioning is generally influenced by both external and internal factors, of which there are a considerable number, the most significant being ambient temperature, solar irradiance and wind. Such external factors significantly influence the supply of maximum power and the voltage of MPP of a PV panel. In addition, external influences also cause changes in the position of MPP on the voltage of the current (I-V) curve. On the other hand, load is considered as a primary internal factor capable of causing PV to function at a strict point on the I-V curve in directly matched systems. The intersection between the variance in the load line and the I-V curves under different weather conditions demonstrates the functioning point on I-V curves, and is therefore highly important to MPP of the solar array. Conversely, the tracking control of MPP is a highly complex issue, for which a number of tracking methods have been established to curb, including: IncCond; P&O; neural networks; and CV. The setbacks associated with such methods generally include their high cost, complexity, non-stability and difficulty. The use of the MPPT converter is to ensure the maintenance of the function point of the PV array at the MPPT, while the MPPT controller establishes this takes place by itself directing the PV array's voltage of the load [10],[45]-[51] .

It is significant that the relatively high cost of electricity from PV results from the high cost of PV panels and systems. This could explain the reason that inefficient methods of operation of PV panels leads to designers increasing their number, enabling adjustment in accordance with the energy demand for the load. Thus, the high cost of PV panels results in uneconomic system design. Research concerning the influence and maximum effect on power operation contributes to the construction of the maximum size of PV system. This leads to a large amount of energy being spared by the maximum design PV system, masking that this ensures the cost of the PV system falls. The PV system can generally be widely employed in a number of applications, particularly in remote areas [45],[52].

2.1 Classification of MPPT techniques

Weather conditions do not remain constant, and change over time, PV panel MPP also varies. The MPPT controller is required to track the MPP and extract the maximum possible power from the module. The tracking of PV panel MPP becomes more complex during rapidly changing weather conditions, and PSC common in PV systems, due to a number of factors, i.e. a tree shadow, passing clouds and dust. The solar cells in practical systems are connected in series, or parallel configuration, to form the modules /arrays, in order to generate the desired value of the voltage. However, the PV module output voltage will be determined by the output current generated, which primarily depends on solar radiation conditions directly proportional to the irradiance. Therefore, an application such as multiple PV modules (which work at different irradiance conditions) will lead to an opportunity to ensure a number of different, rather than just one, MPP, which can result in a substantial reduction of the output power of the complete system, due to its controller being unable to find the true operating point at MPP. This condition can take place due to PSC.

In the case of shading conditions, the shadow PV panel becomes reverse biased, while the un-shaded PV cells become forward biased. Thus, if the reverse voltage is increased beyond the breakdown voltage, this results in the cell/module temperature being raised. These are known as hot spots, and lead to irreversible damage to the cell. The use of a bypass diode has recently become the most popular technique to protect the PV cell/module from the hot spot when connecting the PV cell/module in series. However, the use of a bypass diode results in multiple peaks on the P-V characteristics, which add additional complexity in tracking MPP.

An in-depth study by [53], concerning a number of different MPPT methods employed in PV systems, has established the presence of at least nineteen MPPT techniques recommended for tracking MPP. These methods have been compared by means of the characteristics noted above. These techniques can be classified into three different categories [54], as outlined below:

2.1.1 Online Technique

The first group is known as direct methods, and includes P&O [55], and IncCond [56]. In these techniques, the PV module operating point is perturbed in order to search for MPP. However, its major weakness consists of its tracking ineffectiveness, which ensure it is not the most appropriate preference to function as MPPT, due to the principle of searching for MPP. A further disadvantage of this group is that it is unable to operate the PV panel at its MPP under rapidly changing solar radiations [54],[57].

A number of investigators have asserted that PVs possess a number of MPPT algorithms. One highly utilized algorithm consists of the P&O technique. It is used extensively, due to being easy to execute, needing only a straightforward feedback regulator, and therefore requiring no previous knowledge of the component features. At the same time, it requires fewer factors, since only two sensors are applied, thus implying a reduction in the expense associated with hardware tools [54]-[57].

The P&O technique has been defined by [5],[60] and is based on the affiliation linking the output energy and the output current of a PV unit, whereas the MPP is acquired by changing the converter's switching disposition (duty proportion) up to when the dp/dvs becomes zero. The drawback of P&O techniques is the production of a fluctuation around the MPP within the stable condition. Xiao et al. [5] are of the idea that the consequence of a constant oscillation within the P&O method in the stable condition creates a noteworthy decrease during the output energy of the PV module. Furthermore, it cannot run the module at its highest output energy in weather circumstances prone to fast alteration.

The technique of hill-climbing is offered in [5] and [58], and is founded on the belief of perturbation and surveillance of the PV output power. In spite of the execution of this technique being both easy and simple, it has some disadvantages, comprising slow tracking pace, causing fluctuations within the stable state, and a low effectiveness under swiftly changing circumstances.

There are three major setbacks associated with the P&O method. Firstly, it needs to take into consideration the measurement of the PV voltage at every stage, resulting in the loss of a considerable amount of energy in the control unit, which causes inefficient functioning of the PV panel. Secondly, the P&O method requires a high number of iterations, to enable the MPP to be monitored, because of the need for oscillation around the MPP. Finally, a variation in MPP also emerges from the difficulties relating to the zero derivative workings of dP/dv or dP/dI. However, there are a number of methods widely believed to correct the issues associated with the P&O method. Hsiao [59] claims to have established a three-point comparison method that distances itself from the oscillation issues of the observation algorithm and perturbation method. Similarly, the observation algorithm and perturbation method is cited in [60], identifying the capacitor for MPP monitoring in a PV power system. As such, the capacitance is worked upon and applied to correct the differences of the duty ratio, and so obtain the highest mark of MPPT alongside the degradation of PV panels.

The IncCond method has been outlined in [56]. This was developed to overcome issues relating to P&O, due to possessing a higher capacity than the P&O algorithm to track efficiency within rapidly changing environmental conditions. This study analyzed the advantages of the P&O method, with the result revealing that the IncCond algorithm has a high efficiency, which successfully tracks MPP of the PV module, even under rapidly changing conditions. However, the result was undertaken through the use of simulation and graphs, and the effect of PSC was not addressed by this algorithm.

A number of researchers have proposed the IncCond method to overcome the drawbacks of the P&O method, and improve system tracking efficiency under rapidly changing weather conditions. However, the conventional IncCond method retains a number of disadvantages, and its tracking efficiency is low, as it generally employs a fixed step size that depends on tracking speed and efficiency. Therefore, the conventional IncCond method must be modified in order to resolve the trade-off between its dynamic responses and reduce the oscillation around the MPP in a steady state.

The IncCond in [12],[56] is considered crucial, since it can be employed to improve the observation algorithm and perturbation method under rapidly changing weather conditions. Thus, the major setbacks associated with the observation algorithm and perturbation method, as well as conductance, consists of a high consumption of energy, resulting from instability due to changes in weather conditions and oscillation around Vmax. Such issues can be avoided in such methods to bring about complexity, particularly in a conventional control unit. The control methods are considered the most popular techniques for reducing setbacks associated with the observation algorithm and perturbation method [56],[61].

Liu et al. [62] have proposed a variable step size IncCond method capable of adjusting the IncCond step size automatically, according to the characteristics of the PV module, and results have revealed that the proposed technique results in high stability in the steady state. However, even if the proposed method results in accurate tracking, its dynamic response will be low, as a result of the threshold of the duty cycle conversion. Although it has a higher level of tracking efficiency than direct methods, it requires additional sensor devices for the relevant computing, leading to its response time for conversion being slower, and thus resulting in greater power losses. The implementation of this method is more complex, leading to it not being the first preference to function as MPPT in many applications [55],[63]-[66].

Dezso et al. [55] note the basic operation principles of different MPPT techniques in PV systems, e.g. Hill Climbing (HC), IncCond; P&O; and Fuzzy Logic Controller (FLC). They present a comprehensive comparison between the techniques studied and their tracking efficiencies under varying weather conditions.

In conventional MPPT methods, a fixed step size is applied within the algorithm to track MPP. However, applying a fixed step size results in oscillation around MPP, and a reduction in overall output power. If a large a step size is used, the system will be unable to produce a stable output power, while if small step size is used, the dynamic response of the system will be slow.

Xiao et al. [3] have undertaken a detailed analysis of the P&O and IncCond MPPT algorithms, in order to clarify a number of common misconceptions relating to these two widely used MPPTs presented in the literature. In this study, the two MPPT methods were analysed mathematically, and their practical implementation was thoroughly introduced. The result was confirmed by the use of experimental tests, which revealed that both P&O and IncCond MPP trackers are equivalent. Ishaque et al. [22] evaluated the performance of the P&O and IncCond MPPT technique according to the European Efficiency Test EN 50530, which is specifically devised for the dynamic performance of PV system. The authors implemented both techniques, using a direct control with buck–boost converter, verified through the use of experimental results. This led to the conclusion that both methods are equivalent, and the dynamic response and MPPT efficiency are practically identical. However, the performance of the IncCond method is found to be slightly higher, and its performance at low insolation levels is indicated to be highly sensitive to its perturbation size.

A number of MPPT methods have been reported in the literature, in order to improve the dynamic behaviour of the conventional methods, i.e. the variable step size and perturbation frequency [50],[67]-[70]. Kobayashi et al. [78] have proposed a variable step-size method to overcome the drawback of the conventional P&O MPPT technique as it oscillates around the MPP at a steady state, resulting in raising the waste of the available output power, and achieving a rapid dynamic response with good tracking performance. However, the variable step-size method also has a number of disadvantages, as a constant value is often used in the algorithm, and the choice of its value is highly significant, since its value cannot be adjusted in response to a change in weather conditions. In addition, its time response is lower in comparison to the conventional method, with less efficiency under PSC and a considerable loss of power during a large variation of solar radiation [63],[64],[67]-[69].

Chen et al. [63] have presented a novel auto-scaling variable step-size MPPT scheme. The main objectives of the controller are to optimize the PV module output power, and to eliminate issues found in the conventional variable step-size method, as it automatically employs a simple judgment to adjust the step size of the proposed method. This leads to the proposed algorithm having no requirement to attain a reference value, as in conventional methods, enabling it to achieve a fast dynamic response with steady state oscillation, even in an extreme range of weather changes. However, its disadvantages include the low response time of the algorithm, low efficiency during cloudy days, and that it can be confused under PSC.

Rodriguez et al. [71] have proposed a new approach, in which a two-stage method is used to track the MPP. In this method, the equivalent load line is estimated during the first step, from which point the IncCond method is employed to track true MPP. However, under PSC, the control may confuse and track the local MPP instead of GMPP, since the load line is estimated under uniform insolation conditions.

Koutroulis et al. [69] have presented a method for detecting the MPP based on the scanning process, in order to search for the region containing the true MP. A P&O algorithm is then employed in the second stage to track the true MP. Although the accuracy of this method is high, and is capable of correctly tracking the MPP, the tracking speed time is slow, due to all local MPPs requiring to be identified during the first stage, in order to establish GP.

2.1.2 Offline Technique

The second group of indirect methods includes the Fractional Short Circuit Current (SCC) and Fractional Open Circuit Voltage (OCV). The main advantages of these techniques are that they are easy to implement without a complex algorithm and have a relatively rapid response. However, they require additional components [72],[73]. The online measurement of the results of OCV and SCC in reducing the output power of the module and its MPP cannot always be matched. Moreover, the measurements of OCV (VOC) and SCC (ISC) are often necessary in this method, implying a shorting of the module at each instance. Nevertheless, this issue can be mitigated with several loads, although additional components will be required, potentially increasing the cost of the system [72]. A further downside of this technique is the estimation of the factors of voltage and current, as these are likely to change during PSC. Additional valves are also necessary in the converter for the OCV and SCC methods, leading to decreased efficiency and greater power losses. Furthermore, the results lack accuracy, and the MPP is not always attained, and therefore this method only yields optimal power at a single temperature [49],[72]. The load is required to be detached from the panel for a set amount of a time for the measurement of the OCV, which wastes a considerable amount of energy [73],[74], and frequently requires the measurement of SCC (ISC), which leads to shorting the module on each occasion. However, this issue may not arise if several loads are employed, but this requires additional components, and thus increases the cost of the system [67],[72].

Tafticht et al. [74] have established a tracker for MPP founded on the computation of the SCC from the measured OCV, since the SCC method possesses greater accuracy than the OCV method, and OCV measurement is easier in comparison to SCC. In this method, it is necessary to measure OCV, resulting in the importance of inserting a switch between the converter and the PV module. Furthermore, additional valves are required for the OCV technique to compute OCV, alongside the insertion of a capacitor between the converter and the module, in order for the load to access power when the circuit opens from the switch. Both the maximum voltage and OCV ratio are variable, and subject to the temperature of their surroundings, and therefore this technique only attains optimum power at a single temperature.

Masoum et al. [67] have proposed a rapid and accurate MPPT algorithm based on the OCV and SCC of the PV module. This method employs mathematical equations used to describe the PV module I-V characteristics in the algorithm. The proposed method has been verified by using MATLAB, and been tested under different atmospheric conditions. The simulation results reveal that the PV module operating points were close to the theoretical value of the PV module, and the developed algorithm was more rapid and accurate than the P&O method.

2.1.3 Intelligent Technique

The third group contains artificial intelligent techniques, including neural networks and planning, and fuzzy logics [69],[75]. These methods have become popular, with studies recommending fuzzy logic MPPT and neural network methods to deal with the downside of conventional methods. Nevertheless, these methods are limited in terms of flexibility, since the features of the PV module need to be defined to formulate rules to control MPPT. Fuzzy logic controls have commonly been used in MPPT, due to their many benefits, e.g. the capacity to work with inaccurate inputs; addressing nonlinearity; and lacking the requirement of a correct mathematical model. In addition, changes in weather conditions do not influence the FLCs. However, the user is required to choose an appropriate method to calculate the error and formulate the table of base rules to ensure they are effective, and FLCs necessitate a large memory to handle the two extremes.

Chin et al. [76] have proposed an initial voltage tracking function (IVTF) for tracking the MPP of the PV array operating under shedding conditions, in which a fuzzy logic MPPT controller was implemented in the conventional P&O MPPT algorithm, in order to vary the step size of the perturb voltage in case of partial shedding conditions. The results indicate that the fuzzy logic MPPT is able to control the operating point of the PV array at its MPP, after IVTF is initialized with a more dynamic response.

Syafaruddin et al. [77] have proposed a method for tracking MPP based on a radial basis function and a three-layered feed forward neural network. The accuracy of this method primarily depends on the training data, and it lacks versatility, as there is a need to create control rules to meet the PV array characteristics. Furthermore, additional time is needed to acquire the correct MP when updating the data of the PV array, and it is also dependent on expert knowledge. Therefore, in order to track GMP correctly, a computational effort will be required under PSC.

More recently, a number of modified MPPT methods have been proposed to accurately tracking MPP and improving the dynamic system response, as well as minimizing the system hardware [78],[79]. However, the conventional P&O and IncCond methods contain a number of drawbacks, including: oscillation around the MPP in the steady state; a failure to track MPP under rapidly changing atmospheric conditions; and a tendency to track the local maxima instead of global MPP in case of PSC. Therefore, a number of researchers have proposed modified P&O and In-Cond methods. However, the associated issues are unable to be completely resolved, particularly under PSC [80]. Improving tracking efficiency, and reduce steady state oscillations, Nguyen et al. [81], have proposed a new method of adaptive reconfiguration of solar PV module operation under PSC. However, this method increases the cost of the system, even if tracking is undertaken perfectly, as it requires additional sensors and switches.

These algorithms have the advantage of working independently, due to knowledge of PV generator characteristics not being a critical factor. Although the majority of these methods are simple to implement [62], they are unable to track MPP correctly during a rapid change of solar radiation. Furthermore, they are unable to operate the system at MPP under PSC, due to their lack of differentiation between the local MPP and the GP [80]-[84].

Alajmi et al. [85] have proposed a fuzzy based P&O MPPT, with the proposed technique being verified using MATLAB/SIMULINK. Simulation results indicate that fuzzy based P&O MPPT has a high rate of efficiency and increases PV output power.

Khaehintung et al. [50] have introduced a new MPPT algorithm using an artificial neural network, with the proposed method developed by a three-layer neural system, using simple functions. The proposed technique was implemented on a PV charging system on a low cost microcontroller without an outer sensor unit prerequisite. The study was verified using experimental results, demonstrating that, in comparison to conventional methods, the proposed algorithm has high efficiency in terms of tracking speed and stability in the steady state condition, and its efficiency is higher than 90% under all test conditions.

According to [75] a neural network is presented to demonstrate the MPP of PV modules, as well as the design of a PI-type controller for real time optimum power tracking. MPP can be discovered through the suggested neural network, through the application of open circuit voltage from the controlling cells. The suggested neural network has established a real calculation of MPP from the PV modules. In general, the neural network views functions with more clarity than simple mathematic computing methods. However, a neural network performs random data without human awareness and, as such; it depends largely on the amount of data available to study the network, eventually leading to tedious, and complex, process. Therefore, neural network research method is applied as an end solution selected to resolve issues associated with a low level of knowledge.

Sheraz et al. [75] have presented a more effective MPPT controller, centered on the Artificial Neural Network (ANN) and Differential Evolution (DE). Outcomes have demonstrated that the use of a combination of these methods yields improved tracking, a more rapid response, and minimal fluctuations in the steady state in comparison with the conventional techniques of MPP. However, due PV panels having various features subject to change, the accuracy of the neural network is dependent on the set rules employed by the concealed layer, and the manner in which the neural network has been instructed. Therefore, the neural network requires periodic instructions in order to warrant an accurate tracking.

Wanget al. [80] , have described a PV system under PSC, illustrating that the use of a conventional MPPT algorithm under partial shadowing conditions has the potential to result in significant loss of power. According to [82], under PSC, the efficiency of MPPT controllers is reduced, due to the majority operating in such a manner that only one point remains at which the PV module is able to produce maximum power within the range of its P–V characteristic. However, when PSC occurs, the P–V characteristic becomes increases in complexity, exhibiting multiple peaks. These, in turn, influence the performance of the controller, resulting in a reduction of the entire output power of the system [82],[86]. A number of modified MPPT methods have recently been proposed in order to ensure the accurate tracking of MPP, to improve dynamic system response and minimize system hardware [71],[83]. These methods differ in their complexity, accuracy, and speed, and even if they resulted in tracking being completed perfectly, the dynamic response speed of the system would remain low [83],[87].

Generally, several studies proved as, on photovoltaic are focusing on various types of MPPT, including circuit components. A wide range of MPPT algorithms and control methods, and the most common approaches are simplified and explained in detail. The design and simulation of a streamlined and highly efficient photovoltaic system is introduced, along with tests, comparisons and valuations of several different MPPT systems. The focusing on issues inherent in MPPT and related system components are shown. For example, The P&O method is less effective than the IC approach mainly because the IC method can sense changes in solar irradiance but P&O cannot. The Short circuit current approach is less effective than the open-circuit voltage method because the former approach alters the step voltage in the least effective direction. The examination of the extracted energy results for both P&O and IC appeared to be more effective than open-circuit voltage and short-circuit current. The best results, however, from approaches that utilize artificial intelligence, such as fuzzy logic is shown. The outputs of fuzzy logic controller results depend on MF and Rule Base Table.

In this thesis, mathematical approach is used to model solar panels that involved mathematical equations for calculating the solar panel current. At the same time, conventional inputs series and shunt resistances were used as additional inputs. It was discovered that MPPT algorithms implementing P&O and fuzzy logic techniques have similar voltages and current variables, and a standard configuration of the boost converter using as a switch was utilized to find a constant DC output voltage. In this setup, the MPPT algorithms pointed to the appropriate duty cycle where gating pulses were given to the switching device, enabling triggering occurs at the MPP and the delivery of maximum power to the load. Furthermore, simulation results were obtained in MATLAB/Simulink based on the developed mathematical and electrical models. A solar PV array was successfully modeled and observed characteristic curves for variations in temperature and irradiance as well as series and shunt resistances. The modeled MPPT controllers based on P&O and fuzzy logic controllers, discovering that the fuzzy logic controller is more effective than the P&O MPPT controller. This justifies the robustness of the fuzzy logic controller [88].

The maximum power point tracking (MPPT) controller for photovoltaic (PV) using fuzzy logic based prototype was discussed and carried out. To control the current that is extracted from the PV, a boost converter controlled by dSpace using DS 1104 board is connected to that prototype, which is related to maximum power at the moment. That is known as the MPPT implementation. In MATLAB simulation, the comparison results of MPPT using FLC and conventional method (Perturbation and observation) is shown, and was done to verify and justify the controller before real time system implementation. The prototype hardware is implemented and shown in real system for 5kW case. The results are illustrated that the MPPT algorithm using fuzzy logic gives faster and stable maximum power tracking as compared to the MPPT using the P&O method. By using MATLAB/Simulink, the FLC has been implemented in dSpace to generate a FLC file, and then the downloading of that file in DS1104 board to control the prototype boost converter is completed and tested with small DC supply [89].

According to previous study of different techniques of MPPT, a fuzzy logic control based MPPT has shown the best results in term of stability and speed response and obtaining global maximum power point (GMPP) from existing local power points. Therefore, this thesis focused on designing of fuzzy MPPT for PV system as a simulation.

The comparison between fuzzy logic control-based MPPT and P&O techniques was simulated and tested in MATLAB/Simulink. The entire system included a photovoltaic panel, boost converter, MPP controller and resistor load. The results were shown that the fuzzy control system gave a better performance than the P&O system. In other words, when the simulation was tested under three different conditions of irradiance, the fuzzy controller was able to give the best duty cycle that could drive the DC-DC converter to produce the maximum power point of the PV system. The efficiency of the overall system was improved by minimizing the energy losses when there was a change in solar irradiance [13].

A fuzzy logic controller (FLC)-based MPPT and a conventional Perturb and Observation (P&O) were implemented in MATLAB/Simulink. The FLC is based on Sugeno's method, which is associated with the max-min composition. Both proposed methods of MPPT have been tested under the same variations of solar irradiance and a constant temperature. The result shows that the FLC response was faster than that of the conventional MPPT, whereas the overshoots of the system are almost the same. Therefore, the FLC can improve the performance of the system more than the P&O [90].

In [91] a fuzzy control-based MPPT of a photovoltaic system has been implemented and represented. The whole system contains a solar panel, DC-DC buck boost converter and load. The implementation was simulated in MATLAB/Simulink with a disturbance in the photovoltaic temperature and irradiation values. The outcomes illustrate that the performance of fuzzy control was done successfully and accurately in all assumed conditions. The oscillation around MPP is decreased and the response is faster in comparison with the P&O technique. Therefore, the proposed fuzzy system gave a higher performance than P&O.

An intelligent fuzzy logic control (FLC) was used to obtain the maximum power point of a photovoltaic system under different temperature and irradiation conditions. The proposed FLC technique was applied to boost the DC-DC converter and was simulated in MATLAB/Simulink. The goal of this work was to control the voltage of the solar panel to get the maximum power that can be produced by observing the PV system under any change in temperature and insolation. The results obtained from the FLC were compared with those obtained from the perturbation and observation controller (P&O) and were discussed. It was clearly shown that the FLC performance was faster than the P&O controller in the transitional state and gave a much smoother signal with fewer oscillations at a steady state. Finally, a faster and steadier FLC of MPPT controller was achieved and this made it possible to find the maximum power point in a shorter time in comparison with the P&O controller [92].

In [93], researchers show how photovoltaic generation systems are continuously under threat by uncontrollable elements such as partial shading that can lead to power loss and hotspots. These problems are further exacerbated by curves showing multiple peaks. Under such operating conditions, conventional MPPT techniques can fail to provide optimum MPP. In light of this crucial issue, several attempts have been made to develop an Adaptive Takagi-Sugeno Fuzzy Inference System-based Fuzzy Logic Control MPPT. The mathematical model of the PV array is simulated by utilizing MATLAB/Simulink. Several cases studies on temperature and in homogeneous insolation and were investigated. However, to determine the appropriateness of the proposed MPPT approach, a comparative analysis is carried out with two common MPPT techniques and the results compared with two other techniques. In this comparison, all the techniques are performed using a grid-connected PV system to measure the efficiency and response of each in tracking the MPP under several different partial shading conditions. The proposed fuzzy logic-based MPPT controller has been shown to surpass other conventional MPPT techniques regarding harmonic reduction, tracking ability, and efficiency. Moreover, the proposed approach demonstrates superior response speed towards the PV system, and the optimal operating point does not oscillate around the MPP, even without knowledge of the actual model.

A fuzzy logic controller uses voltage output as feedback to enhance the dynamic performance of a boost DC-DC using MATLAB/Simulink software. The purpose of this approach is to create a fuzzy logic controller on a control boost DC-DC converter. The fuzzy logic controller is included in the system by devising a fuzzy logic control algorithm. Moreover, the design of the components, including the inductor, has been carried out to enable the converter to function in continuous conduction mode. The output is evaluated and compared as a simulation in MATLAB software between open- and closed-loop circuits. Specifically, the 20 V input on the output voltage for the closed-loop circuit (with fuzzy logic controller) with 0% overshoot indicates better performance than the open-loop circuit (without fuzzy logic controller) with 80% overshoot. Furthermore, the improvement of the output current's valuation corresponds to the system and creates a constant output current valuation of 0.5 A. This could not be possible in an open-loop circuit output current. Thus, using a closed-loop circuit with fuzzy logic controller, the boost DC-DC converter holds an output voltage value that matches the circuit requirement. The results indicate that the voltage output can be controlled in a steady state for boost DC-DC converters by applying this methodology. This approach could solve numerous issues related to stability, as fuzzy logic controller can serve as an intelligent controller for appliances [94].

CHAPTER 3

METHODOLOGY

In this chapter, an explanation of component characteristics, circuit design and mathematical modeling of the PV system are provided. Reviewing the physical structure of semiconductor of the PV cell and basic concept of how does it convert the sun light into electrical energy. The mathematical model of the solar cell and model are represented to show and analyze the effect of the atmospheric conditions on their I-V and P-V output characteristics. This chapter introduces and investigates DC-DC converters, P&O MPPT algorithm and FLC MPPT controller, which are commonly used in MPPT power converter of PV systems.

3.1 Maximum Power Point Approaches for PV panels

It is significant that plays a vital role in the solar array system and it is thus important to accurately establish the functionality of the complete PV system, in order to create an effective system capable of satisfying demand with lower cost. However, wind speed, solar irradiance and ambient temperature are major external factors that determine the highest power capable of being generated from a PV panel. It appears that the position of the MPP on the I-V curve is changed through the influence of external factors. In directly coupled machines, the load forms the major internal factor capable of driving PV panels to operating at a strict point on the I-V curve, as illustrated in Fig. 3.2. In fact, MPP changes its position and operates furthest from the highest power point, decreasing the output power of the PV system as a result of external influences. As such, it is important to track the MPP of a PV solar array. This leads to difficulties in identifying the highest power point mathematically as a function of internal and external factors. MPP of a PV system has been proposed as a control technique for tracking with traditional and artificial techniques. However, research has, over a number of years, focused on many highest power point control algorithms to produce the maximum power of PV panels.

3.1.1 Maximum Power Point Tracking

MPPT is employed to ensure that the highest power is obtained from the PV modules under all environmental conditions (in particular, solar insulations and temperature). This is achieved by matching the functioning voltage and current with the coordination of power converters. Fig. 3.1 shows the outline MPPT block in combination with a DC-DC converter. MPPT purposes concentrate on detecting the present electrical energy of the PV range, with the loads facilitated by the array energy to be added and differentiated with the current MPP value.

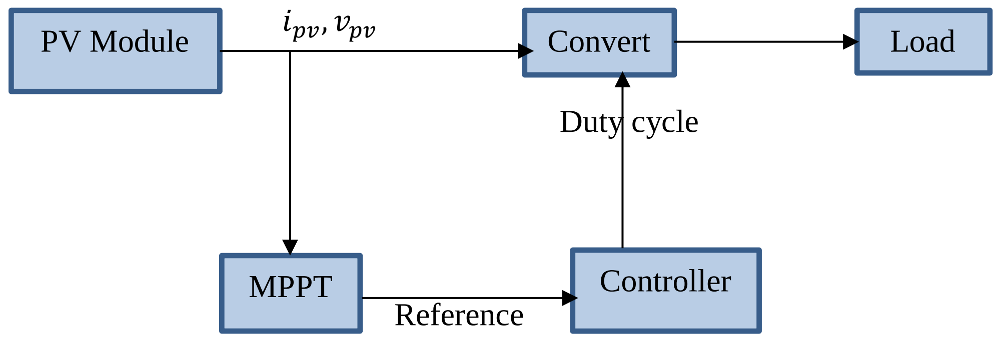

FIGURE 3.1 SIMPLE BLOCK OF MPPT SYSTEM

Similarly, the duty cycle of the converter is set using a FLC to suit MPP, which in turn forces the converter to extract the highest available power from the array. However, an alternative control structure is distinguished by an automatic update of the power converter duty cycle (i.e. direct duty cycle MPPT control).

Despite PV systems containing a number of major advantages, they also have a number of specific disadvantages, i.e. high cost; limited capacity in comparison to other low and zero carbon energy sources; low conversion efficiency; and (as they generally rely on atmospheric conditions) a dependence on weather conditions [12],[14],[42]. Consequently, MPPT is capable of only generating electric current for a short period each day, conditional on both energy from the sun and the prevailing temperature. In addition, differences in climatic setting cause PV systems to have non-linear features, while a PV unit has a position within each climatic condition at which it is capable of generating its highest output current, as well as power, i.e. MPP. It is thus necessary to regulate the PV unit to manage it at MPP [42]. As established by the references, MPPT is capable of rising the generation of electric current to 25% [5],[95]. This illustrates the I-V plus P-V curves shown in the next page fig. 3.2.

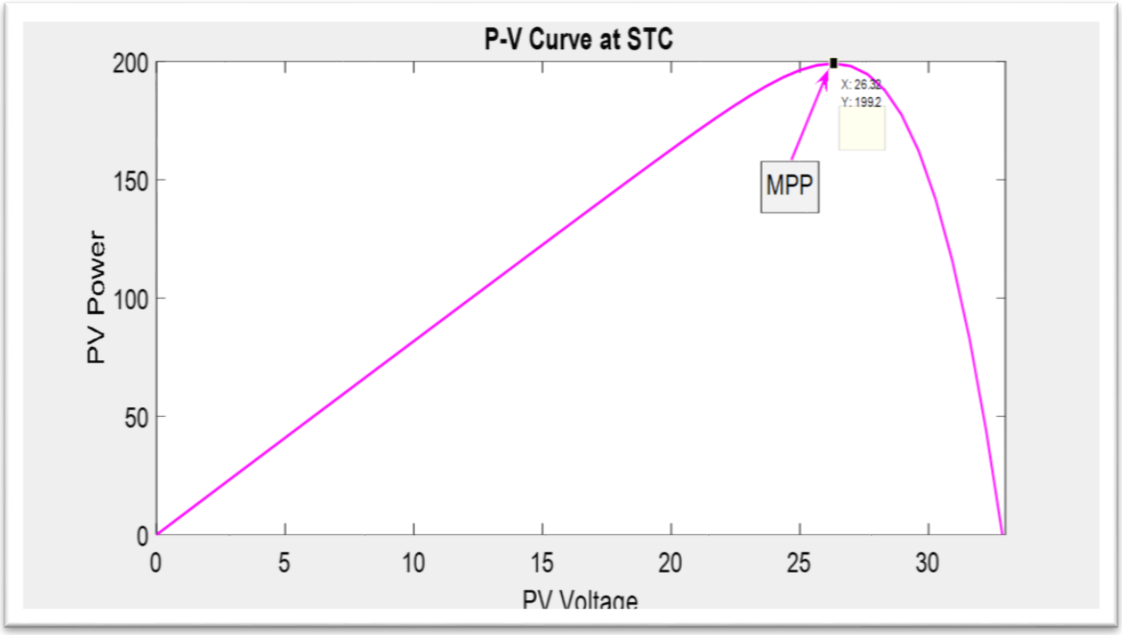

FIGURE 3.2A P-V CHARACTERISTICS OF PV MODULE AT STC (1KW/M2, 25ºC)

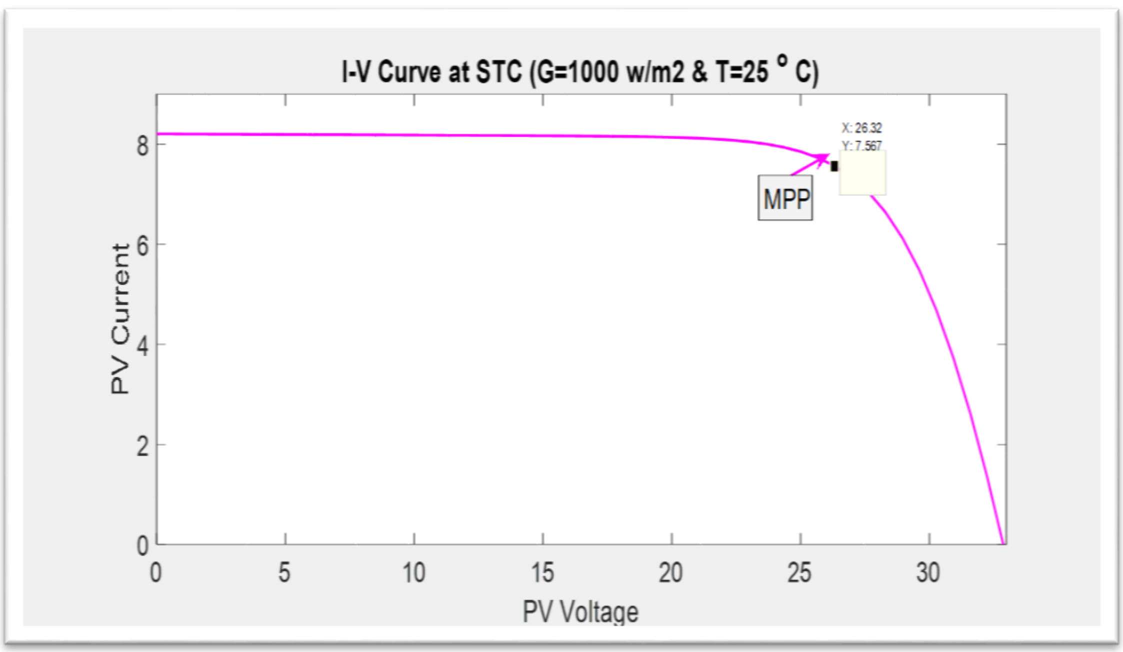

FIGURE 3.2B I-V CHARACTERISTICS OF PV MODULE AT STC (1KW/M2, 25ºC)

3.1.2 Problems of Maximum Power Point controller

Notably, the absolute power point tracking techniques are applicable in the extraction of maximum available power from PV systems in various environmental conditions, with various types of load.

DC-DC converters are employed to interface the highest power point of PV systems with various loads. However, issues that needed to be addressed in MPPT systems include: different shapes of load line; the nonlinearity between the duty cycle and the voltage ratio of most types of converters; and the wide degree of fluctuation in weather conditions.

3.1.3 The restrictions of Maximum Power Point Tracking

This section of the research have been covered a number of important factors capable of affecting the performance of MPPT in the system.

3.1.3.1 Variation of photovoltaic cell materials

Almost all cells can be made from single-crystalline silicon; amorphous silicon; and thin films. These can also classify in terms of their cost, performance and output characteristics [95].

3.1.3.2 Non-optimal conditions

A PV cell is unable to deliver its designated output power under a number of specific conditions. The two major situations influencing MPPT efficiency consist of: (1) partial shading and (2) irradiance variation [5],[34],[95].

3.1.3.3 Partial shading

This thesis has been addressed on the issue of how partial shading affects the maximum power generated from the PV system. Fig. 3.3 A & B demonstrates typical generation features and P-V curve for three series-connected modules under different generating conditions, in particular in relation to irradiance, with a shaded1, shaded2 and non-shaded cell, respectively. The functional features demonstrated in the figure reveal that both shaded and non-shaded module can function effectively in a region in which each single module is able to produce power. However, the capability of producing maximum power varies as irradiance varies.

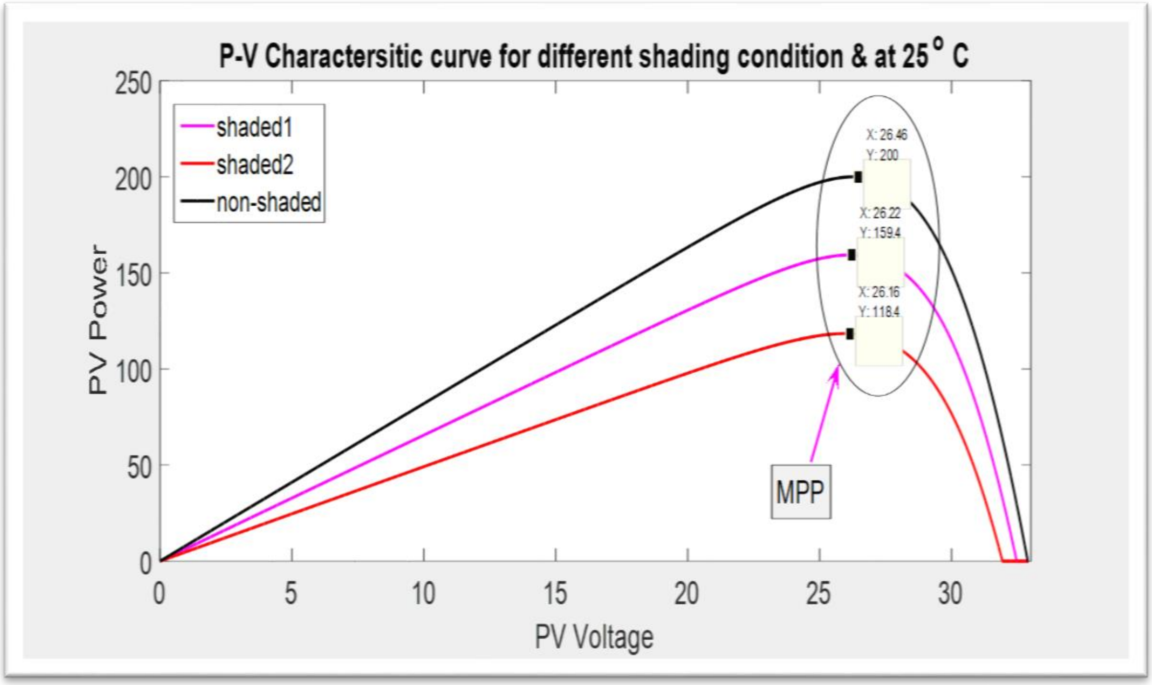

FIGURE 3.3 A. P-V CHARACTERISTIC CURVE OF PV MODULE DURING DIFFERENT RADIATION CONDITION

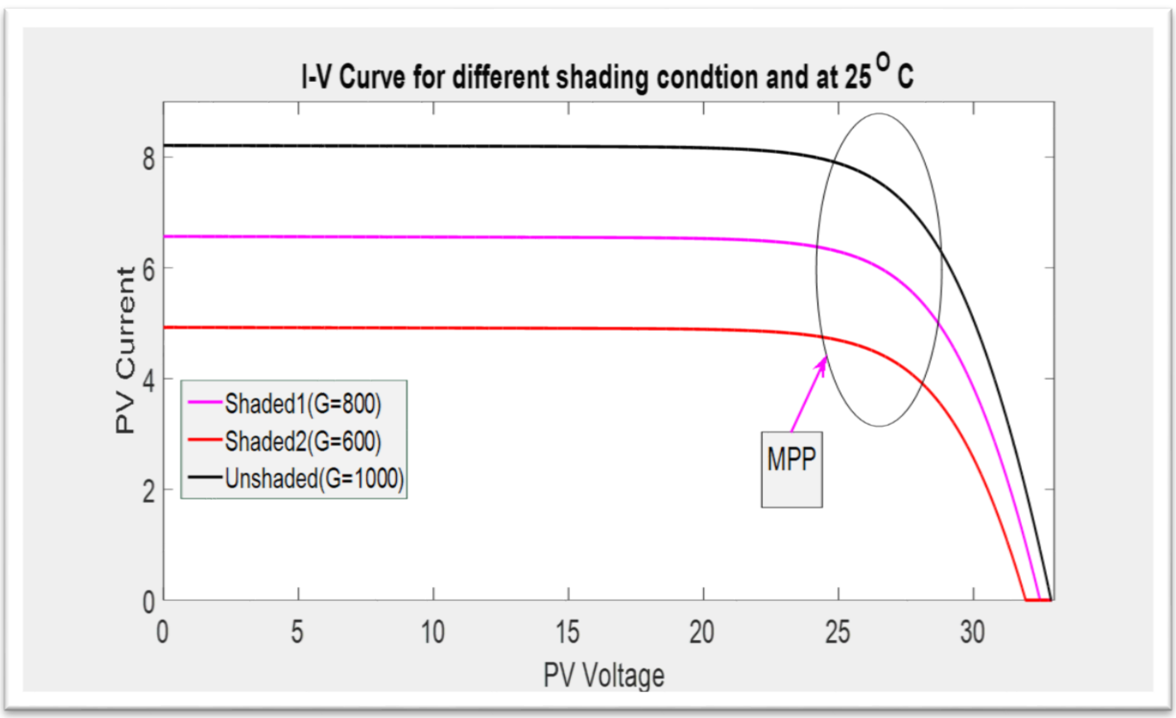

FIGURE 3.3 B. I-V CHARACTERISTIC CURVE OF PV MODULE FOR DURING DIFFERENT RADIATION CONDITION

The fig. 3.3 A & B illustrated above shows the effect of partial shading on the PV system, in which three identical PV module, KG200GT, in series configuration were used. When the two PV modules was shaded, its irradiance was 800 W/m2 and 600 W/m^2, while the others were 1000 W/m2.

In this case, the shaded1 PV and shaded2 PV module reduced the maximum output power of the system from 200 W to 158.4 W, i.e. approximately 79.2 % and to 118.4W, i.e. approximately 59.2% of the maximum output power of the system under normal conditions [3],[95],[96]. According to Ref [82], under PSCs, the efficiency of conventional is an MPPT controller is highly reduced. The assumption made by the majority of MPPT controllers is that there is only one point on the P-V characteristic at which the PV module can produce its maximum power. However, when the PSC occurs, the module will have several MPPs (LMPP and one GMPP), affecting the performance of the controller, resulting in a reduction in the whole output power of the system.

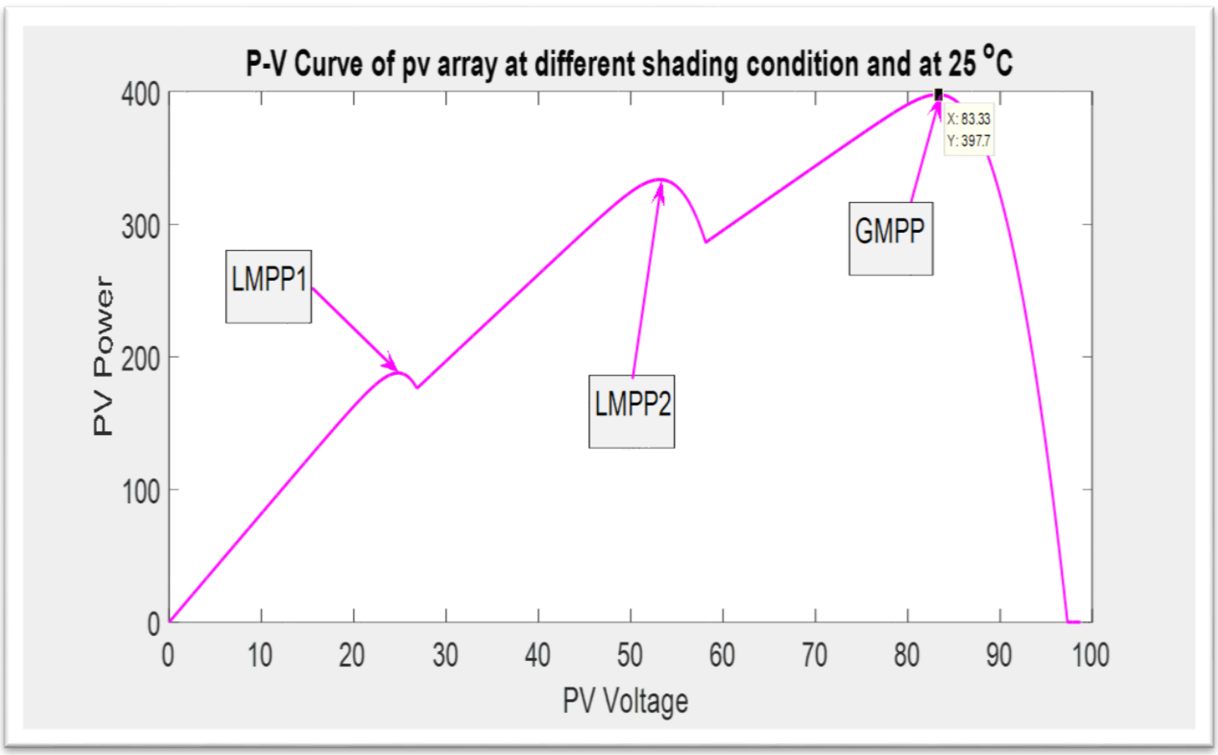

FIGURE 3.4 P-V CHARACTERISTICS CURVE OF PARTIAL SHADE PV ARRAY

3.1.3.4 Variation of solar radiation

The issue of radiance variation can impact on the MPPT controller. It has been highlighted out that a number of MPPT methods (e.g. the perturbation and observation method) have low efficiency as solar radiation varies. Therefore, it is important to improve a suitable MPPT algorithm, whose performance cannot be affected by such condition [97],[98].

3.1.3.5 The effect of load on PV panels curves' operating point

The load is considered to have no effect on I-V features; however, it can affect the functioning point on the I-V curves. The direct load coupling to the PV panel results in a mismatch between the solar generator's optimum, and the actual functioning, voltage, which reduces the generated power from the PV panels. The functioning voltage, along with the functioning current on I-V curves points, relies on the load. The intersection taking place on the different load line and I-V curves under different climatic conditions identify the functioning point on I-V curves. Any change in climate conditions modifies the I-V curve, causing changes in the function voltage and current supply in the PV system. More frequently, the point of intersection is not the Pmax, and therefore the load type influences the range identifying the functioning point in I-V curves.

The sudden increase (or reduction) of the irradiance level during conditions of partial cloud causes a wide range of variance in the production of voltage. The divergences seen in the functioning voltage, as a result of variance in load types, has an effect on the required changes of the duty cycle

3.2 DC-DC converter switching-mode converter

The most important components in the PV system are the DC/DC converter and DC-AC inverter, while their switching-mode generally has nonlinear characteristics variable over time. Therefore, the switching mood converter needs to be closely controlled through the use of appropriate techniques. Furthermore, MP can be extracted from the PV system if the DC-DC converter is well designed and its switching mood is correctly controlled. In addition, the DC-DC converter needs to draw low ripple current to the system, causing conversion loss and reducing the maximum power tracking efficiency. This can be reduced by using high switching frequency [48],[95].

As a result of the recent improvements in electronic devices, PV systems are now able to generate a large amount of energy. They may also be formed into three groups: (1) buck/step-down; (2) boost/step-up; and (3) buck-boost converters [12]. The DC-DC converter method is substantial within MPPT, since MPP may be attained if the converter's button mode is correctly regulated. Thus, the major concern within PV is the creation of an effective regulator for the DC-DC converter.

3.3 Photovoltaic source model

It is important when building a PV system to understand its behavior and ensure system stability, in order to specify its size and its location, as installing the module in a perfect location with widespread sunlight can extract the system's maximum possible power. One of the most common and unavoidable issues with a PV system consists of partial shading, which has a considerable influence on the output power of the PV module. In general, PSCs at a low latitude are less acute than at higher latitudes as, in the latter, the sun is at a considerable distance on the horizon.

Therefore, during installation, the location of a PV system needs to be taken into account, including its direction and installation rise angle. According to [97], a considerable reduction in PV module output power will result in a small shading of the module. Therefore, operating the module in a case of PSC needs to be investigated in order to improve MPPT performance, and extract the maximum power the PV module is capable of generating.

The most important issue when designing a PV system understands PV module behavior, including accurately determining its characteristics. Therefore, modeling a PV module becomes a significant issue when modeling a MPPT of the PV module, and requires considerable knowledge of the characteristics of a PV module, along with its performance under different circumstances, e.g. low solar radiation, temperature, and PSCs. This is necessary to ensure improvements in the design, and to simulate the behavior of the MPPT system. This chapter will therefore: firstly, define the modeling of a PV module, employing a simple equivalent circuit, and secondly, the more accurate module will be used designed to simulate MPPT algorithms. The simulation result will demonstrate the suitability of the proposed model for the design and analysis of the MPPT system.

3.4 The terminal characteristic of photovoltaic cells

3.4.1 Solar Cell Modeling

In PV system, the core elements for converting solar energy into electricity are the PV cells. It can generate DC-power and supply their direct-connected load**.** Throughout photovoltaic effect, photovoltaic cell can generate a power, the electronic characteristics, such as the output current, output voltage and internal resistance of a solar cell are generally determined by the intensity of the received photon, the temperature of the cells' surface, the efficiency of the PV conversion, and the load impedance**.** Different models have been used to represent solar cell varying in their accuracy of modeling, depending on designer need [28],[41],[99].

3.4.1.1 Simplest Model

It consists of an ideal current source in parallel with an ideal diode as shown in fig. 3.5. The current source (Ipv) represents the current generated by solar cell due to photons received from the sun, and is constant under constant temperature and irradiance.

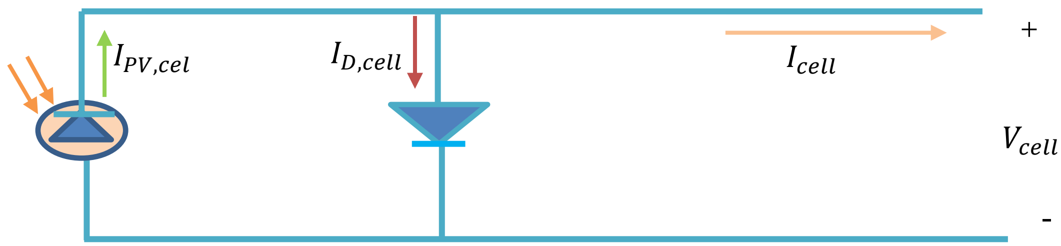

FIGURE 3.5 EQUIVALENT CIRCUITS FOR SIMPLEST PV CELL

There are two key parameters frequently used to characterize a solar cell. The V-I characteristic is generally calculated by computing the following two factors: A) the short-circuit current, which is obtained by shorting the terminals of the V cell (i.e. setting V=0, hence this gives Iph = *Isc*); and B) the open circuit voltage (Voc). The values of these factors are generally provided by the manufactory datasheet [21],[41]. Fig. 3.5 shows the equivalent circuit of the ideal PV cell. The basic equation from the theory of semiconductors that mathematically describes the I–V characteristic of the ideal PV cell is

$$I_{cell} = I_{pv,cell} - I_{d,cell} \qquad 3.1$$

$$I_{d,cell} = I_{o,cell}\left[\exp(\frac{qV_{cell}}{akT} - 1)\right] \qquad 3.2$$

Where, $I_{pv,cell}$ is the current generated by the incident light(it is directly proportional to the Sun irradiation), Id is the Shockley diode equation, $I_{o,cell}$ is the reverse saturation or leakage current of the diode, q is the electron charge (1.60217646 × 10−19 C), k is the Boltzmann constant (1.3806503 × 10−23 J/K), T (in Kelvin) is the temperature of the p–n junction, and $\boldsymbol{\alpha}$ is the diode ideality constant.

By replacing $I_{d,cell}$ of the equation (3.2) into equation (3.1), gives the I-V relationship of the solar cell.

$$I_{cell} = I_{Pv,cell} - I_{o,cell}\left[\exp\left(\frac{qV_{cell}}{akT}\right) - 1\right] \qquad 3.3$$

3.4.1.2 More Accurate Model

There are a few things that have not been taken into account in the ideal model that, it will affect the performance of a PV cell in practice. These include the series resistance, parallel resistance, and recombination factor of solar cell. The system may be enhanced through the addition of a chain resistance to the current path, which symbolizes PV cell wastes.

I. PV Series Resistance

In a practical PV cell, there is a series resistance in a current path through the semiconductor material, the metal grid, contacts, and current collecting bus. These resistive losses are lumped together as a series resister(R_s). Its effect becomes very conspicuous in a PV module that consists of many series-connected cells. The series resistance has no effect on the open-circuit voltage, but reduces the short-circuit current [100],[101].

II. PV Parallel Resistance

It is a loss associated with a small leakage of current through a resistive path in parallel with the intrinsic device. This can be represented by a parallel resistor(R_p). Its effect is much less conspicuous in a PV module compared to the series resistance, and it will only become noticeable when a number of PV modules are connected in parallel for a larger system. The R_p has no effect on the short circuit current, but reduces the open-circuit voltage [100],[101].

III. Recombination

Recombination at the depletion region of solar cells explains non-ohmic current paths in parallel with the intrinsic solar cell. This is relevant at low voltage bias and can be represented in an equivalent circuit by a second diode term with a saturation density current $(I_{o2,cell})$ as shown in fig. 3.6, which is different from the Io of the simplest solar cell diode, and given diode ideality constant (α_2) is most often assumed to 2 [100],[101].

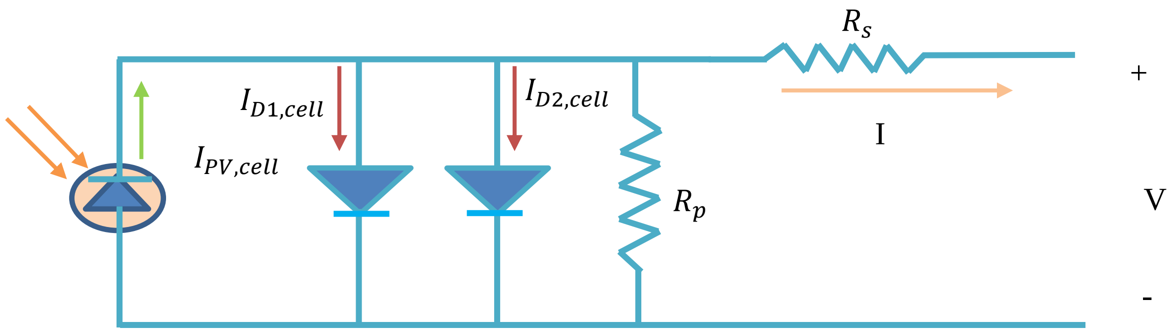

FIGURE 3.6 EQUIVALENT CIRCUITS FOR DOUBLE EXPONENTIAL PV CE11 MODEL

So the I-V relationship of PV cell instead of equation (3.3) can be written as [41],[102],[103]:

$$I_{cell} = I_{Pv,cell} - I_{o1,cell}\left[\exp\left(\frac{q}{a_1 kT}(V_{cell} + I_{cell} R_s) - 1\right)\right] - I_{o2,cell}\left[\exp\left(\frac{q}{a_2 kT}(V_{cell} + I_{cell}) R_S\right) - 1\right] - \frac{V_{cell} + I_{cell} R_s}{R_p} \qquad 3.4$$

The double exponential model is one of the most accurate models, but it exhibits a high complexity due to its double exponential terms. Therefore, the use of this single Exponential model to describe the static I-V characteristic has been considered widely, the main advantage of using the model with single diode is to simplify the electric circuit and consequently the equation that describes the device operation [104]. Fig. 3.7 represent the equivalent circuit of single exponential model.

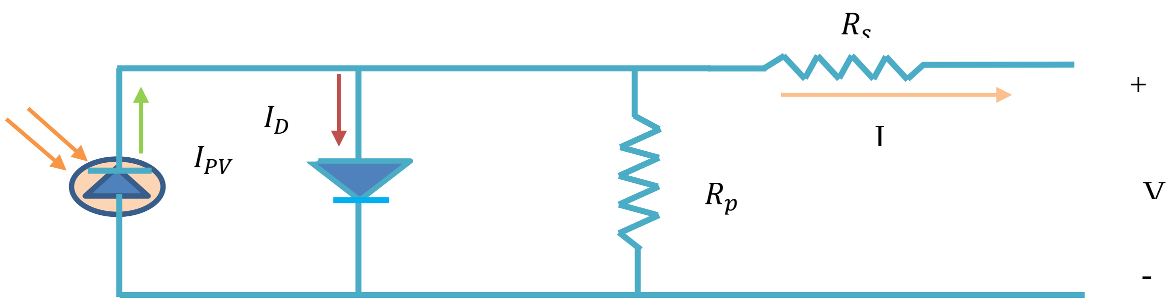

FIGURE 3.7 EQUIVALENT CIRCUIT SINGLE EXPONENTIAL PV MODEL

So the I-V relationship of PV cell instead of equation (3.4) can be written as [102]:

$$I_{cell} = I_{Pv,cell} - I_{o,cell}\left[\exp\left(\frac{q(V_{cell} + I_{ell} R_s)}{akT} - 1\right)\right] - \frac{V_{cell} + I_{cell} R_s}{R_p} \qquad 3.5$$

3.5 PV Module Modeling

The basic equation (3.5) of the solar cell does not represent the I-V characteristic of a practical PV module. PV module is composed of several connected PV cells. The strategy of modeling a PV module is no different from modeling a PV cell. It uses the same PV cell model. The terminal equation for the current and voltage of the module becomes as follows [105],[106]:

$$I = I_{PV} - I_o\left[\exp\left(\frac{(v + I R_s)}{a v_t} - 1\right)\right] - \frac{v + I R_s}{R_p} \qquad 3.6$$

Where Vt $=\frac{N_s kT}{q}$ is the thermal voltage of the module with number of cells connected in series (Ns). Cells connected in series provide greater output voltages while cells connected in parallel (Np) increase the current. If the module is composed of Np cells then the PV and saturation currents may be expressed as Ipv= Ipv,cell*Np, I0= I0,cell*Np, where Np is equal to 1 in this thesis.

3.6 PV Array Modeling

The PV array is composed of several interconnected photovoltaic modules. The modeling process is the same as the PV module from the PV cells. Fig. (3.8) shows a photovoltaic array, which consists of multiple modules, linked in parallel and series. Nser is the total quantity of modules within the series and Npar is amount of modules in parallel. The number of modules modifies the value of Rp and Rs. After extending the relation I-V of the PV modules in equation 3.6 to a PV array, the new relation of I-V of the PV array is calculated by equation (3.7) [105],[106]:

$$I = I_{Pv} N_{par} - I_r N_{par}\left[\exp\left(\left[\frac{v + I R_{ss}\frac{N_{ser}}{N_{par}}}{v_t N_{ser}}\right] - 1\right) - \frac{v + I R_s \frac{N_{ser}}{N_{par}}}{R_p\left(\frac{N_{ser}}{N_{par}}\right)}\right] \qquad 3.7$$

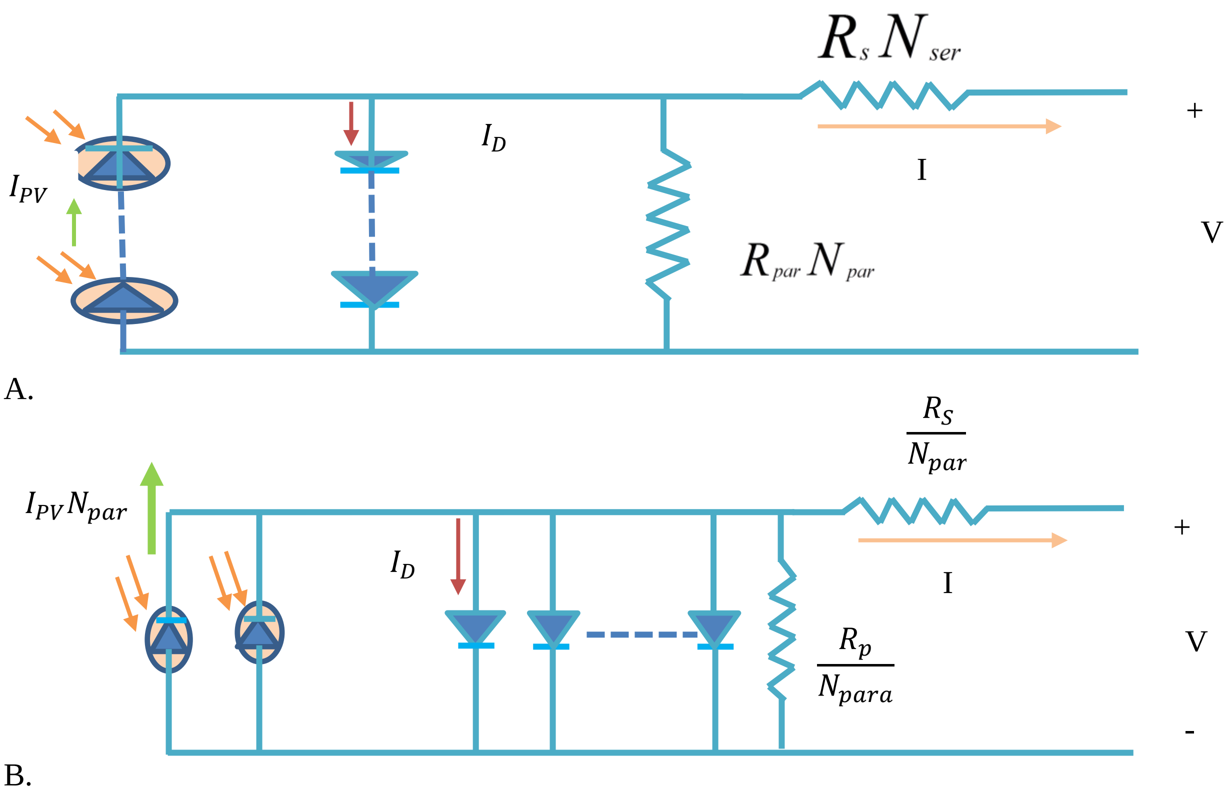

FIGURE 3.8 (A) ARRAY OF PV MODULES CONNECTED IN SERIES, (B) ARRAY OF MODULES CONNECTED IN PARALLEL

Where, N_{ser} =number of PV module connected in series configuration.

N_{par} = number of PV module connected in parallel configuration.

3.7 conventional (fixed step-size) Perturb and Observe algorithm

The conventional P&O algorithm operates by periodically perturbing the PV output voltage v_{pv} and the change in PV output power p_{pv} by comparing the instantaneous power with that of the pervious perturbation cycle. If the change in power is positive, the perturbation will continue in the same direction in the next perturbation cycle, otherwise the perturbation will move to the opposite direction. By repeating this process, the operating point will gradually move toward the maximum power point. The perturbation variable chosen in this proposed algorithm is the duty-cycle with fixed step-size.

3.8 Fuzzy logic

3.8.1 Introduction to fuzzy logic

Fuzzy logic is the area of artificial intelligence associated with reasoning algorithms. Its primary purpose is to mimic human thought patterns and decision-making abilities in machine applications. It was introduced by Lotfi Zadeh in 1965 and is a mathematical tool for dealing with uncertainty associated with vagueness, imprecision, and lack of information regarding a problem or a plant, etc. Unlike binary logic, it is considered as a 'gray' logic, it describes values that are somewhere in the middle between two distinct features. In other words, fuzzy logic creates a data range by assigning two distinct values – namely, 1 (indicating a maximum degree) and 0 (indicating a minimum degree) [99].

Fuzzy control emerged on the foundations of Zadeh's fuzzy set theory. It is a methodology of intelligent control that mimics human thinking and reacting by using a multivalent fuzzy logic and elements of artificial intelligence (simplified deduction principles). It must be feed by the relevant information in order to process and function properly. The information is provided by whoever understands the functioning of the process and is held within the fuzzy system.

Fuzzy logic functions by designating and enacting rules that combine an expert's inputs with the wanted outputs. There are four main determining factors of fuzzy logic:

- ✓ fuzzy sets
- ✓ membership functions
- ✓ linguistic variables, and
- ✓ fuzzy rules.

These four factors are explained in detail below and Figure (3.9) shows the main structure of a fuzzy logic system.

1) **A rule-based system**

It described by 'If-Then' designations. These rules generally include fuzzy logic quantification made by an expert on how to achieve the finest control.

2) **An inference mechanism**

That optimally mimics expert decision-making by both 'understanding' the information and then applying it, again on the way to best control of the input factors.

3) **A fuzzification interface**

It changes inputs into knowledge that the inference mechanism (#2) can then utilize when designating and following rules.

4) **A defuzzification interface**

It changes the outcomes of the inference mechanism (#2) into useable inputs that will 'feed' the process and move it forward.

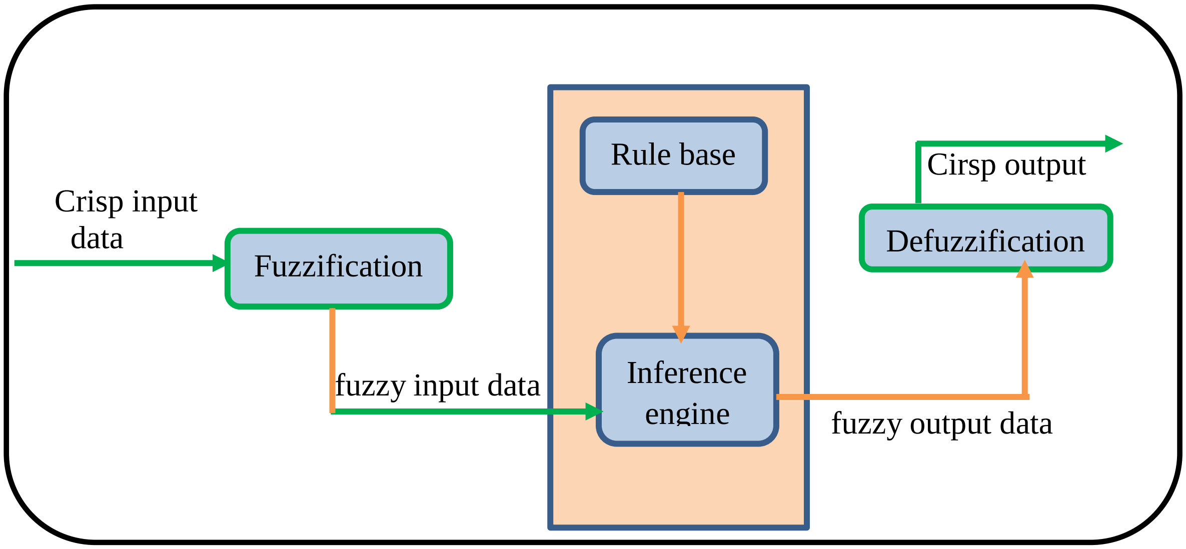

FIGURE 3.9 STRUCTURE OF A FUZZY LOGIC SYSTEM [99]

3.8.2 Fuzzification

It is a process in the fuzzy logic whereby clearly specified values are made fuzzy. To accomplish fuzzification, the linguistic variables and terms to be utilized must first be defined. Numerical values are not used in this process; rather, words and/or phrases from a natural language comprise both the input and output variables. To start the process, a specific linguistic variable is broken down (i.e., decomposed) into its composite linguistic terms. For example, in an air-conditioning system, temperature (T) is the linguistic variable that designates the room's temperature, which can be described (qualified) in general linguistic terms as "hot" or "cold". As this point of view, Temperature (T) = {too cold, cold, warm, hot, too hot} can then serve as the decomposition set for the linguistic variable temperature which is called linguistic values. The individual features of this decomposition are labeled as linguistic terms and represent a part of the temperature's total values. Then, in order to translate the "crisp" (i.e., non-fuzzy) input data to fuzzy linguistic terms, we can apply membership functions, as explained below [99].

3.8.3 Membership Functions

The membership function is a way to express graphically the participation level of individual inputs. It allocates a value to the inputs that can also serve as functional overlaps between the inputs. In so doing, the membership function strongly influences the output response. A critical determining factor of the membership function is configuration or, as it is usually termed, “shape”. The various potential shapes include Gaussian, triangular, trapezoidal, generalized bell and sigmoidal. Of these, the triangular and trapezoidal shape are the most commonly applied, and the degree of membership function is usually in the [0 1] range. The definitions and graphs of the various membership function given bellow.

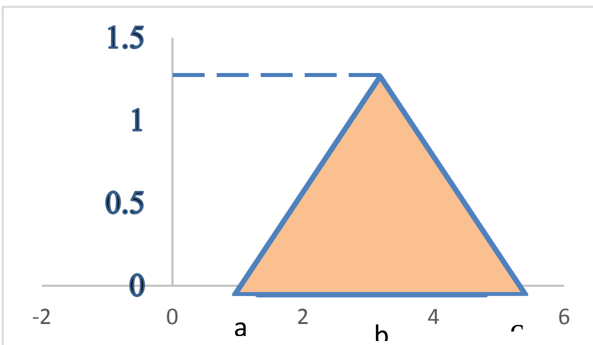

Triangular membership function

$$\text{Trimf}(x;a,b,c) = \begin{cases} 0 & if\ x \le a \\ \frac{x-a}{b-a} & for\ a \le x \le b \\ \frac{c-x}{c-b} & for\ b \le x \le c \\ 1 & for\ x \ge c \end{cases}$$

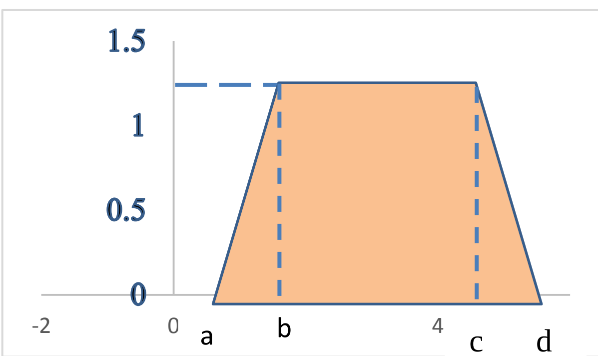

Trapezoidal membership function

$$\text{Tramf}(x;a,b,c,d) - \begin{cases} 0 & if\ x \le a \\ \frac{x-a}{b-a} & for\ a \le x \le b \\ 1 & for\ b \le x \le \\ \frac{d-x}{d-c} & for\ c \le x \le d \\ 0 & for\ x \ge d \end{cases}$$

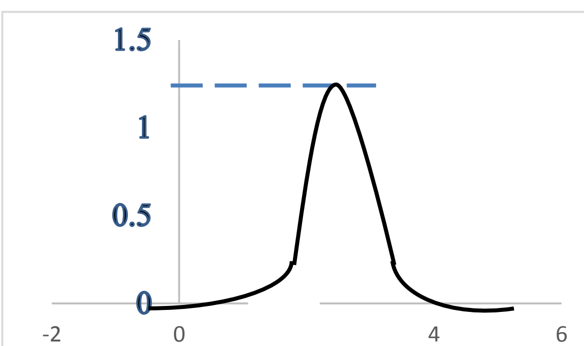

Gaussian membership function

$$\text{Gaumf}(x;c,s,m)=\exp[-\tfrac{1}{2}\left|\frac{x-c}{s}\right|^{m}]$$

Where c, s & m represents the mean , Standard deviation and fuzzification factor respectively

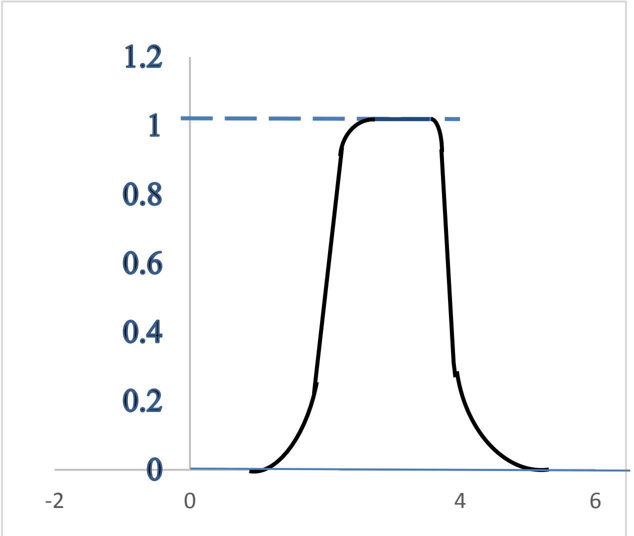	Generalized bell membership function gbellmf (x;ab,c)= $\frac{1}{1+\left\|\frac{x-c}{b}\right\|^{2a}}$ Where, a is widith, b is slope & c is its center
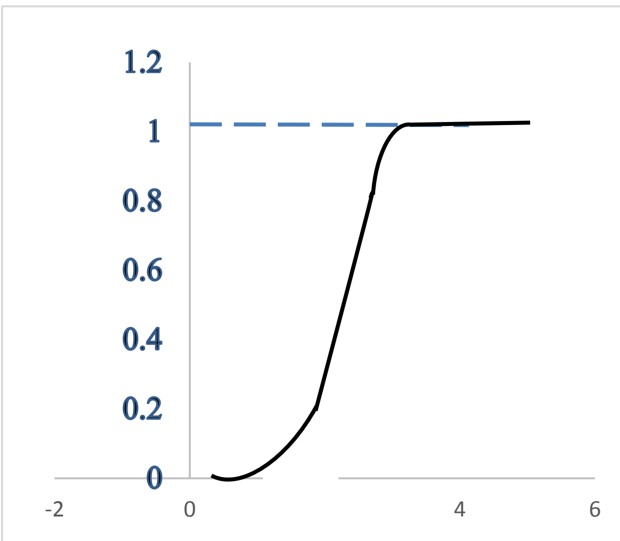	Sigmoid membership function Sigm f(x;a,c)= $\frac{1}{1+e^{-a(x-c)}}$ Where a represents it's slope at the crossover point x=c & c is it's crossover point
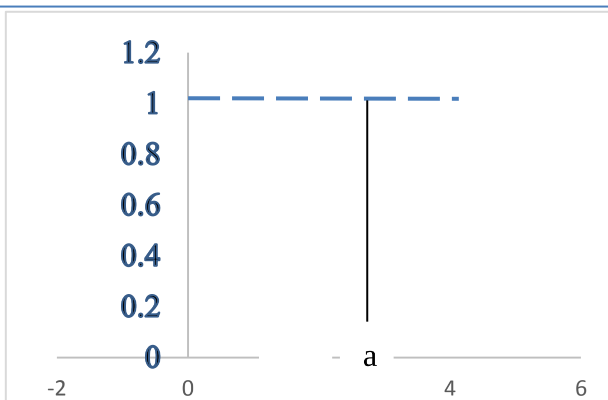	Singleton membership function Sing(x;a)=a

FIGURE 3.10 DIFFERENT TYPES OF MEMBERSHIP FUNCTION [107]

Furthermore, the membership functions designate the various elements in a set as being either discrete or continuous. Discrete form membership function is in a list (vector) format, whereas the continuous form is a mathematical function. Overall, the discrete form is more commonly applied. A triangular membership and trapezoidal membership function comprises straight line segments and is thus easy and practical to apply under fuzzy control and those membership functions are appropriate to be applied in this particular work. However, the Gaussian membership function approach is better suited when smooth and continuous output is desired.

3.8.4 Fuzzy Rules

As touched on briefly above, rule bases are developed to control output variables in a fuzzy logic system. The main aim of fuzzy systems is to create a theoretical foundation to make logical assumptions and associations among inexact terms of reference. In fuzzy logic technological systems, this is called approximate reasoning. The main subjects and verbs of fuzzy logic are comprised of fuzzy sets and fuzzy operators, or so-called "If-Then" rule statements. These are applied when developing the "If-Then" conditionality statements that are the hallmark and basis of fuzzy logic. So, for instance, if a fuzzy rule states that if x is A, then y must be B if A and B are values designated by fuzzy sets specifying a range of X and Y, respectively. In this rule, the "If" part is considered as the antecedent or premise, while the "Then" part is referred to as the conditional consequent or conclusion. Eventually, a fuzzy rule is, at its core, an If-Then rule that features both conditions and a conclusion.

The process of fuzzy logic control proceeds from a set of input data derived from any number of sensors; these data are then 'fed' into the control system. Concurrently, the values of these input variables undergo a change known as "fuzzification", which transforms the discrete values into a broad range of values. Fuzzified inputs are then measured beside a series of production rules, and the rules selected generate the outputs. Lastly, output data are "defuzzified" through control commands [99],[107].

3.8.5 Inference engine

Inference is a process whereby novel information is resulting via existing information. In fuzzy logic control systems, inference refers to a process whereby the final result is derived by combining the outcomes of each rule in terms of fuzzy values. There are several different methods that can be followed to obtain inference, the most popular of which are Mamdani, Larsen and Takagi-Sugeno-Kang.

The Mamdani approach was developed by Ebrahim H. Mamdani as a means to modifying the behavior of a steam engine and boiler in 1975. Mamdani's (1975) control method derives from Lofti

Zadeh's (1973) paper describing fuzzy algorithms for complex systems and decision processes. In Zadeh's (1973) method, the minimum operation Rc is applied as a fuzzy implication, while the max-min operator is applied to obtain the composition. For instance, let us assume that the following form comprises a designated rule base. Hence:

IF input x = A AND input y = B

THEN output z = C

3.8.6 Defuzzification

It is the process of changing the fuzzy output of the inference engine to a clearly defined crisp output by applying membership functions such as those utilized by the fuzzifier. Examples of defuzzification approaches include (in no particular order) Centroid of Gravity (COG), Bisector of Area (BOA), Weighted Average, Mean of Maximum (MOM), First of Maxima and Last of Maxima. While each defuzzification procedure is based on the application's properties, choosing a suitable defuzzification strategy is an art rather than a science (i.e., there is no fool-proof method, but instead tends to proceed by "feel"). Centroid of Gravity (COG) is currently the most commonly applied defuzzification approach, mainly for its relative simplicity. The base equation for COG is:

$$u_o = \frac{\int \mu_u(u)u\,du}{\int \mu_u(u)\,du} \qquad 3.8$$

Where u_o is the finest/optimal output obtained from COG defuzzification method of FLC.

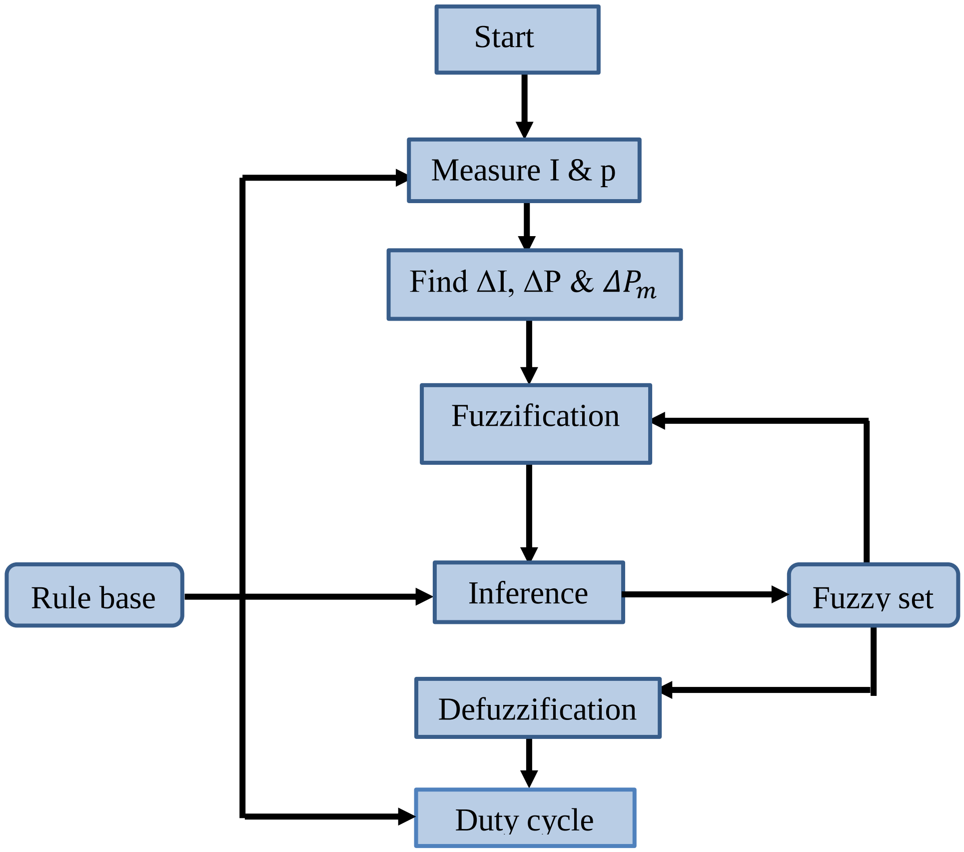

FIGURE. 3.11 FLOW CHART OF FLC

3.9 Modeling of photovoltaic by MATLAB

3.9.1 Introduction

This particular section of the thesis discusses the modeling of PV cell, module and array according to manufacturer supplied data for a specific module, and then the model is used to study characteristics of PV under different atmospheric conditions.

Solar panels can conveniently convert the received light energy to electricity without any pollution. A solar panel normally consists of numbers of inter-connected solar cells. The pattern of the connection can be cascaded, paralleled or both. The size and rated power of a solar panel is determined by the number of its solar cells, by the area of each solar cell, and by the efficiency of each solar cell. However, the potential maximum power generated by a solar panel heavily depends on irradiation and temperature conditions.

3. 9.2 Modeling a PV Module by MATLAB

Manufacturers of PV arrays, provide only a few experimental data about electrical and thermal characteristics, instead of the I–V equation. Unfortunately, some of the parameters required for adjusting PV array models cannot be found in the manufacturer's datasheets, such as Ipv or I, Rs, Rp, $\boldsymbol{\alpha}$, and Io.

All PV array datasheets bring basically the following information: the nominal open circuit voltage (Voc,n), the nominal short-circuit current (Isc,n), Vmp, Imp, the open-circuit voltage/temperature coefficient (KV), the short circuit current/temperature coefficient (KI), and the maximum experimental peak output power (Pmax,e). This information is always provided with reference to the STC (1000 w/m2 and 25 o_C) of solar irradiation and temperature. Some manufacturers provide I–V curves for several irradiation and temperature conditions. These curves make easier the adjustment and the validation of the desired mathematical I–V equation. Basically, this is all the information one can get from datasheets of PV arrays.

KC200GTS PV module, pictured in fig. (3.12), is chosen to design in this work. The module is taken as a reference module for this thesis to designing this work. It is of made of 54 multi-crystalline silicon solar cells in series and provides 200W of nominal maximum power as shown in datasheet in [108]. The single diode model with moderate complexity, and provides fairly accurate results is used, which described by equation (3.6) and (3.7) for simulation. To solve these equations the following parameters must be defined. Table 3.1 shows the electrical characteristics of KC200GT PV module, which here is a selected module. In this thesis, PV arrays of four KC200GTS module have been connected in series configuration shown in fig. 3.17.

FIGURE 3.12 PICTURE OF KC200GTS PV MODULE

Table 3.1 Electrical characteristic data of KC200GT PV module

Rated power	200w
current at maximum power (Impp)	7.61A
voltage at maximum power (Vmp)	26.3V
short circuit current	8.2A
open circuit voltage	32.9V
total number of cells in series	54
total number of cells in parallel	1

The test condition electrical specifications are: cell temperature at 25°C; spectrum at 1.5 air masses and irradiance at 1 kW/m2.

3.9.3 The light-generated current

The amount of incident light directly affects the generation of the current generated by the device. Ipv of the elementary cells, without the influence of the series and parallel resistances, is difficult to determine. The assumption Isc ≈ Ipv is generally used in the modeling of PV devices because in practical devices the series resistance is low and the parallel resistance is high. The Ipv of the PV cell depends linearly on the solar irradiation and is also influenced by the temperature according to equation (3.9) [37],[109].

$$I_{Pv} = \left(I_{sc,n} + k_I \Delta T\right)\frac{G}{G_o} \qquad 3.9$$

Where

- $I_{sc,n}$ is short circuit current at STC
- $\Delta T = T - T_n$ (Tn being nominal temperatures [in Kelvin]) (298.15 k).
- G_n is the nominal solar irradiation (1000 W/m2).
- G is solar irradiation (W/m2)

T denotes the solar cell's actual temperature and G denotes the actual received irradiation on the solar cell. The open circuit voltage (v_{oc}) is the voltage between the positive lead and negative lead of a solar cell when the current that flows through the connected load is almost zero. The value of

k_I is relatively small and this makes the cell output current linearly dependent on solar radiation level more than temperature.

3.9.4 Diode reverses saturation current

The value of the reverse saturation current I_o is rarely provided by the manufactures. It is strongly dependent on the temperature. However, it may be approximated by using equation (3.10) [37],[109].

$$I_o = \frac{I_{sc,n} + k_I \Delta T}{\exp\left[\left(\frac{k_v \Delta T}{a V_t}\right)\right] - 1} \qquad 3.10$$

Where k_I is short circuit current coefficient

k_v Open-circuit voltage coefficient

3.9.5 Parameter determination of PV array

Rs and Rp are the unknown parameters in equation (3.12). Those parameters are determined accurately to get an accurate characteristic I-v curves that is similar to experimentally measured I-V curves provided by manufactures. Thus parameters are calculated accurately at actual temperature and irradiance of the PV module. Therefore, find the value of Rs and Rp that makes the peak power of the mathematical P–V curve (Pmax,m) coincide with the Pmax,e at the (Vmp , Imp) point through keep increasing the value for *Rs*, while simultaneously calculate the value for Rp. Equation (3.11) can be used for manipulation of this procedures [37],[110].

$$R_p = \frac{v_{mpp}(v_{mpp} + I_{mpp} R_s)}{v_{mpp}\left(I_{mpp} - I_d\right) - P_{mpp}} \qquad 3.11$$

By using equations (3.6) through (3.10), the parameters of a single solar cell can be reasonably computed. However, those equations may not be sufficient for solving the parameters of a solar panel or a solar array, which is a matrix of inter-connected solar cells. Fig. 3.13 illustrates the equivalent circuit of a photovoltaic matrix (PV array). The photovoltaic current of a solar panel/array can be calculated by using equation (3.12).

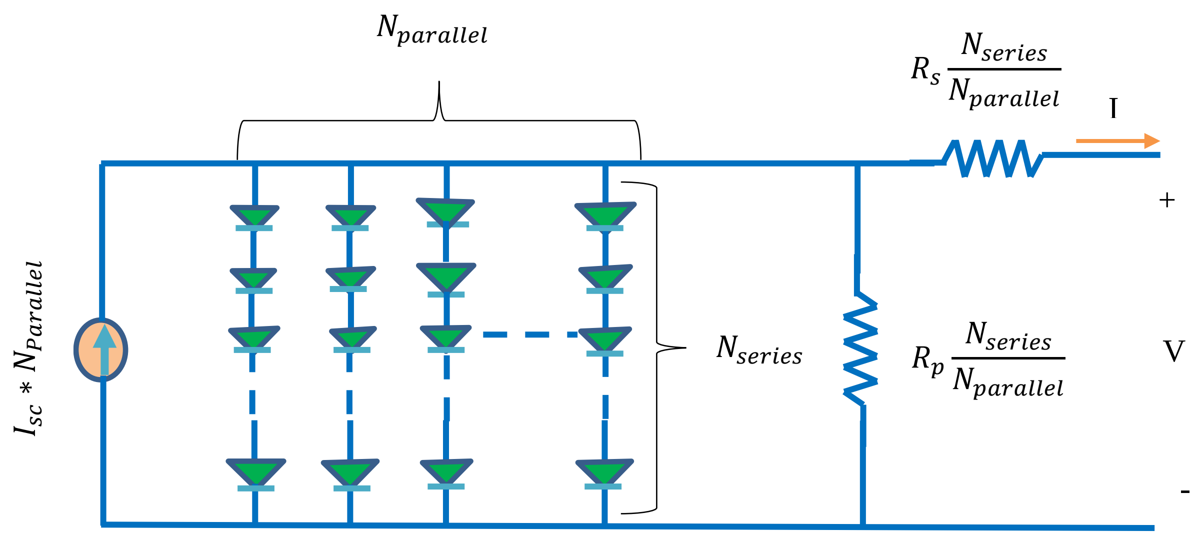

FIGURE 3.13 ELECTRICAL EQUIVALENT CIRCUIT MODEL OF PV ARRAY [37]

$$I_{Pv} = I_{sc} N_{par} - I_o N_{par} \left[\exp\left(q \frac{v + IR_S \frac{N_{ser}}{N_{par}}}{akTN_{ser}} \right) - 1 \right] - \frac{v + I \frac{N_{ser}}{N_{par}}}{R_p \frac{N_{ser}}{N_{par}}} \qquad 3.12$$

By reviewing the equation (3.10), which is provided by [37], [111] , the relationship between the Rs and Rp in a matrix of solar cells may not be sufficiently accurate. Therefore, according to the equations (3.11), (3.12), and the structure of the photovoltaic array, the Rp can be computed by using equation (3.13).

$$R_P = \frac{v_{mpp}\left(v_{mpp} + I_{mpp} R_s \left(\frac{N_{ser}}{N_{par}} \right) \right)}{\left(\left[v_{mpp} \left(I_{sc} - I_d \right) \right] \left(\frac{N_{ser}}{N_{par}} \right) \right) - P_{mpp}} \qquad 3.13$$

Therefore, the significant step for modeling PVs is applying the above calculations for finding a solution pair of $\{Rp, Rs\}$, which can best match the calculated maximum power to the provided $Pmpp$.This is done through an iterative process by the principles of Newton Rahpson method in

Appendix I, Rs must be slowly incremented starting from Rs = 0. Adjusting the P–V curve to match the experimental data requires finding the curve for several values of Rs and Rp [37], [109].

Finally, the PV module can be simulated with an equivalent circuit model based on the PV model of fig. 3.14, where it shows a circuit model using one current source (Im) and two resistors (Rs and Rp). This circuit can be implemented by MATLAB simulator. The value of the model current Im is calculated by the computational block that has V, I, Io, and Ipv as inputs. Io is obtained from equation 3.10 and Ipv is obtained from equation (3.9). The photovoltaic array can be simulated with the modified I-V equation (3.12). The simulation circuit presented previously must be modified according to the number of associated modules as shown in fig. 3.14.

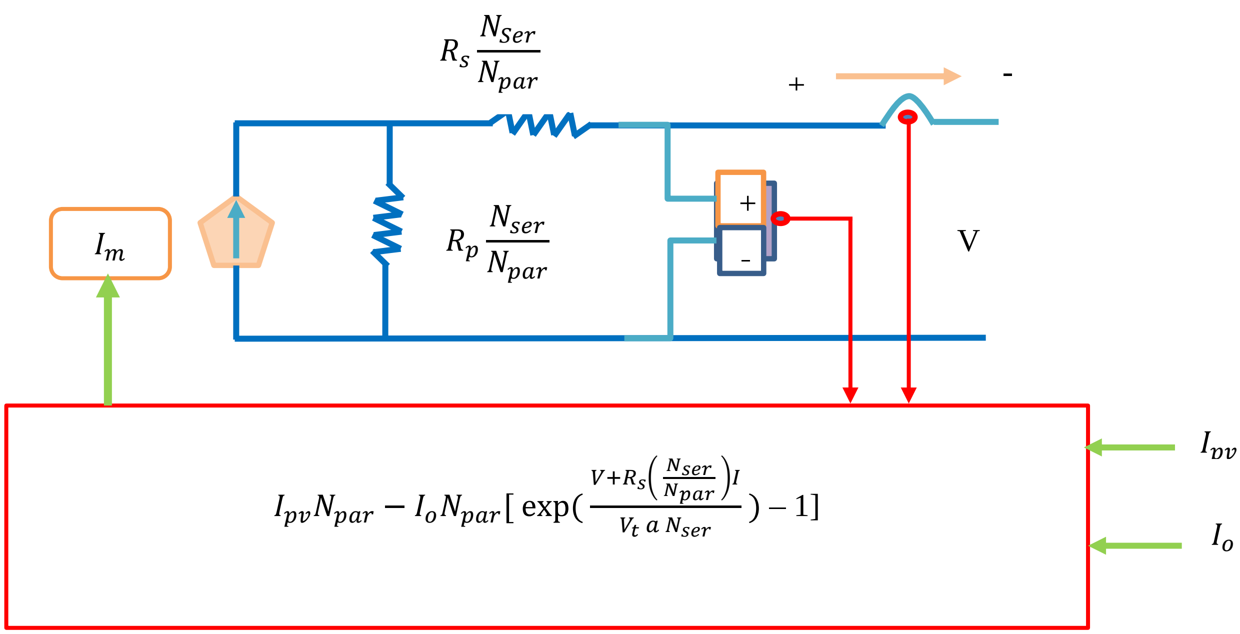

FIGURE 3.14 CIRCUIT MODEL OF THE PHOTOVOLTAIC ARRAY BY MATLAB

3.10 Factors affecting the PV characteristic

The major factors influencing the functioning of the PV systems consist of irradiance level, wind speed, and the ambient temperature. Isc, Vmax, Voc, and the max are the commonly known factors assisting in the specification of the I-V curves of the PV panels systems. I-V curve features and the cell junction temperature of PV panels are able to function well in response to climate change conditions. The illustration below demonstrates the ways in which PV output features, and the cell-junction temperature, changes because of climatic conditions. At the same time, this section the research also discusses the impact of cell junction temperature on electrical features of PV curves panels. To understand characteristic of photovoltaic, several factors must be taken into considerations which are:

3.10.1 Temperature effect

A PV module's temperature has a great effect on its performance. It is observed in fig 3.15 a and b, that the temperature mainly affects the terminal voltage; it increases with increasing temperature. This is somewhat surprising as one would typically expect the PV array to operate more efficient as temperature increases. However, one of the reasons the PV array operates more efficient with decreasing temperature is due to the gap energy of semiconductor materials varies with temperature. An increase in temperature will cause the band gap energy of the material increase. With higher band gap energy, the electrons in the valence band will require more energy from the photons to move to the conduction band. This means that a lot more photons will not have sufficient energy to be absorbed by the electrons in the valence band resulting in fewer electrons moving to the conduction band and a less efficient solar cell [112].

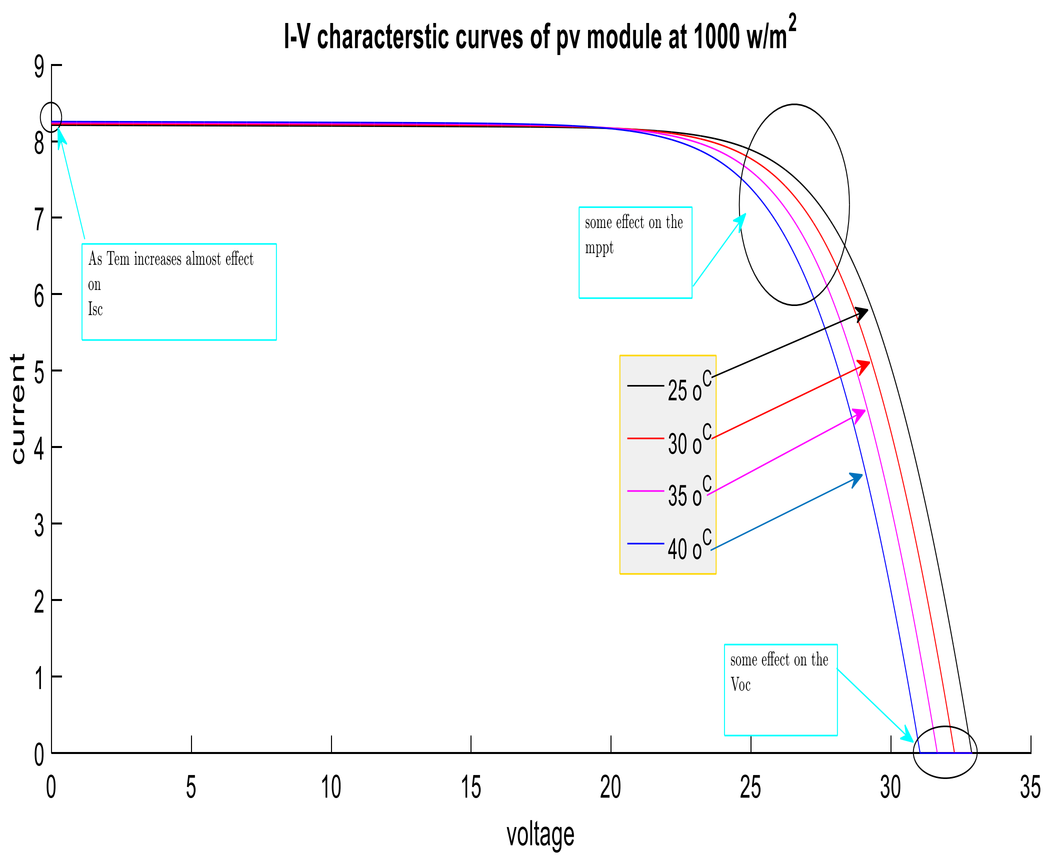

FIGURE 3.15 A. I-V CURVE OF PV MODULE OPERATING AT 1000 W/M2 AND DIFFERENT TEMPERATURE

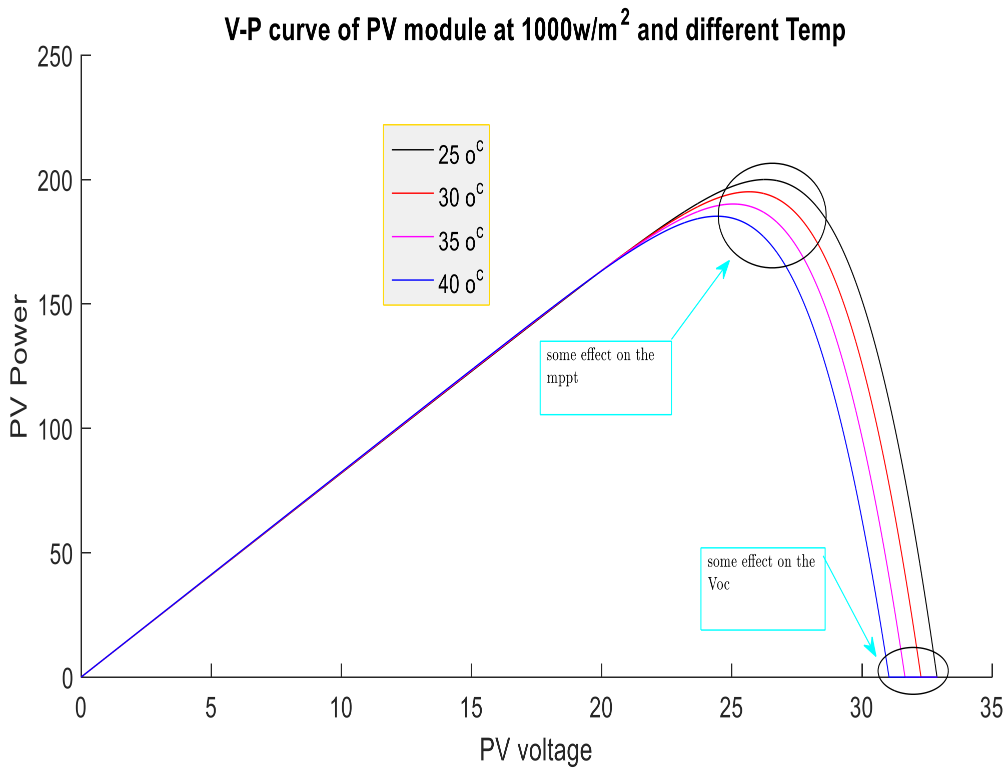

FIGURE 3.15 B. V-P CURVE OF PV MODULE OPERATING AT 1000 W/M2 AND DIFFERENT TEMPERATURE

The cell's temperature can affect the characteristics of photovoltaic. Fig. 3.15a and 3.15b illustrate I-V and P-V curves of the KC200GT PV module, operated under different temperature conditions and a fixed irradiation condition of 1000 W/$m2$.The various temperature conditions do not heavily change the $Impp$ of the KC200GT modules, while they obviously affect the $Vmpp$ and $Pmpp$. This can be explained in detail in the table below.

Table 3.2 a. The effect of change of actual temperatures of the PV module with constant solar radiation of the 1000 w/m2 on the PV module parameters based on the Appendix.

Temp	10 oC	20 oC	35 oC	45 oC	60 oC	75 oC	90 oC
Pmax_m	199.8105	200.1036	199.9094	200.0746	199.7066	200.123	200.004
Isc	8.1623	8.1941	8.2418	8.2736	8.3213	8.369	8.4167
Ipv	8.442	8.4494	8.65584	8.7477	8.893492	9.0456	9.2074
Rs	1.73	1.89	2.14	2.3	2.55	2.78	3.02
Rp	50.8131	46.9245	42.393	39.7709	36.5265	33.6626	31.2874

3.10.2 Irradiance effect

It is a high influence in the possible production of energy of the PV modules energy that can produce. Because PV array rely on conditions that are never constant, the amount of power extracted from a PV module can be very inconsistent. Irradiance is an important changing factor for a solar array performance. It is used to describe the density of the radiation incident on a given surface. In PV system, it is the amount of solar energy that is absorbed by the array over its area. Irradiance is expressed typically in watt per square meter (W/m2). Given ideal conditions, a PV array should obtain an irradiance of 100 W/m2 up to 1000 W/m2.

Unfortunately, this value that is obtained by a PV array will vary greatly depending on geographic location, angle of the sun.

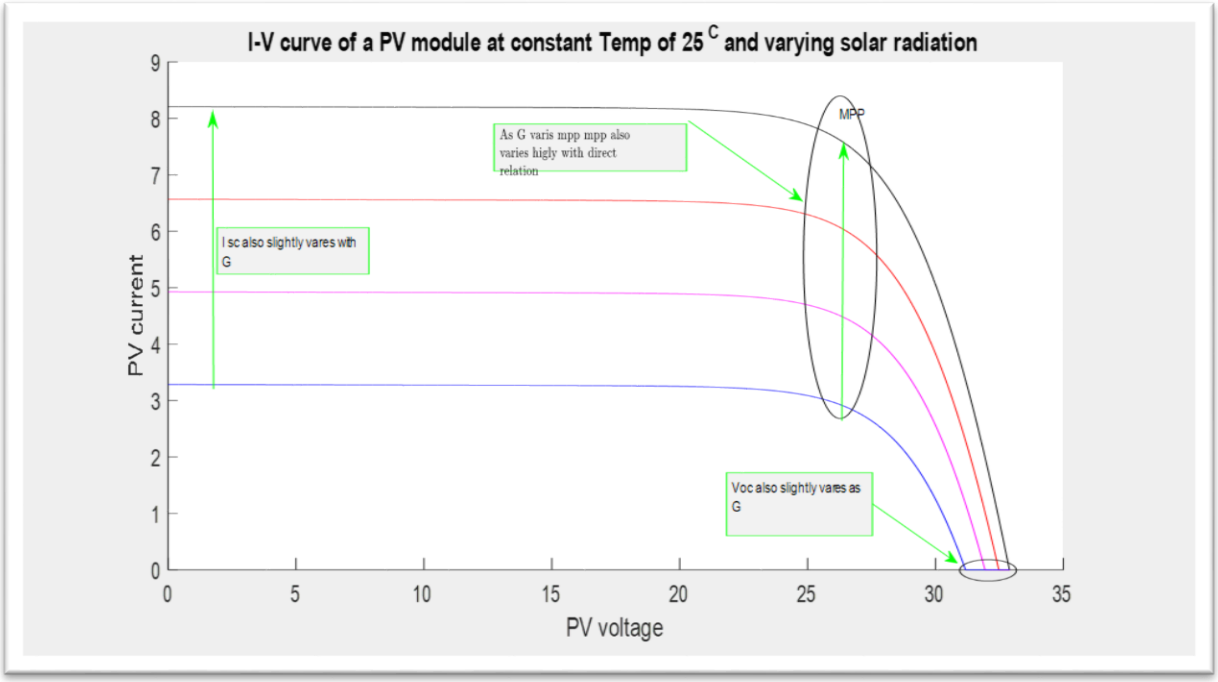

a.

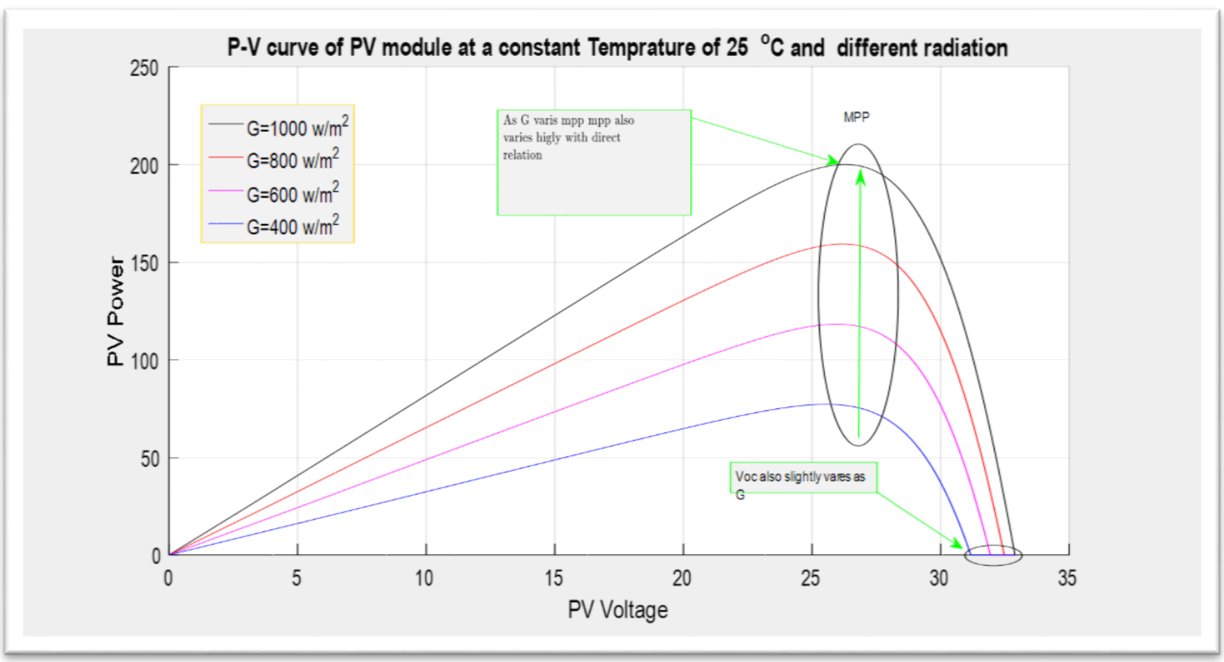

b.

FIGURE 3.16 EFFECTS OF RADIATION ON THE MPP OF THE PV MODULE.(A) I-V CURVE OF THE PV MODULE; (B) P-V CURVE OF THE PV MODULE.

Fig. 3-16 (a) and (b) illustrate the simulated I-V curves and P-V curves of the KC200GT module operating under the same temperature condition and different irradiation conditions, respectively. Fig. 3.16(b) shows that the output of PV array is directly proportional to irradiance. This makes sense where by the principle of operation of the solar cell the generated current is proportional to the flux of photons. When the irradiance or light intensity is low, the flux of photon is less. When the sun is bright, the light intensity is high, more current is generated. The change in voltage is minimal with varying irradiance and for most practical application; the change is considered negligible [112]. This can be more elaborated by the table below.

Table 3.2 b. The effect change of solar radiation with a constant temperature of 25 o_C on the solar PV module parameters using the algorithm in the Appendix.

G	4211	4000	2000	1000	800	600	400
Pmax,m	198.4791	199.7102	199.7842	199.9251	199.7734	200.0870	199.95
Isc	34.5723	32.2083	16.42	8.21	6.5680	4.926	3.284
Ipv	49.9659	45.2083	16.4748	8.4454	5.8779	3.910193	2.338
Rs	0.31	0.3	0.2	2.28	2.28	2.27	2.27
Rp	0.6837	0.7602	2.9839	84.0735	-21.3104	-10.9029	-7.8249

3.10.3 Shading effect

The main objective of this work is study and analyzes the effects of partial shading on the outputs of the PV module for a series configuration of four KC200GT modules. Performance of a series connected string of solar cells is adversely affected if all its cells are not equally illuminated (partially shaded). In a PV array spread over vast area, it is likely that shadow may fall over some of its cells due to tree leaves falling over it, birds on the array, shade of a neighboring construction etc. In a series connected string of cells, all the cells carry the same current. Even though a few cells under shade condition produce less photon current but these cells are also forced to carry the same current as the other fully illuminated cells. The shaded cells may get reverse biased, acting as loads, draining power from fully illuminated cells. If the system is not appropriately protected, hot-spot problem can arise and in several cases, the system can be irreversibly damaged. To overcome this problem a bypass diodes offer an easy current path around any shaded cells shown in fig. 3.17.

Ideally there would be one bypass diode for each solar cell, but this is rather expensive. Many PV modules therefore incorporate one diode per small group of cells or one bypass diode for per PV module for a PV array. [112].

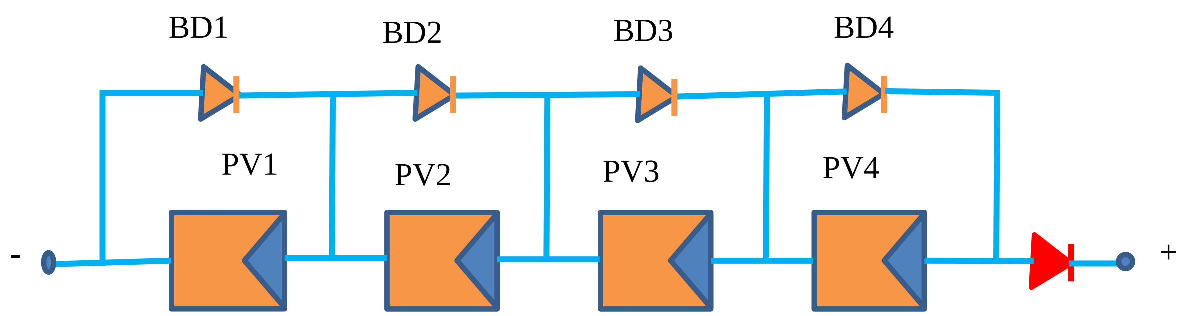

FIGURE 3.17 AN ARRAY WITH FOUR MODULES AND BYPASS DIODE

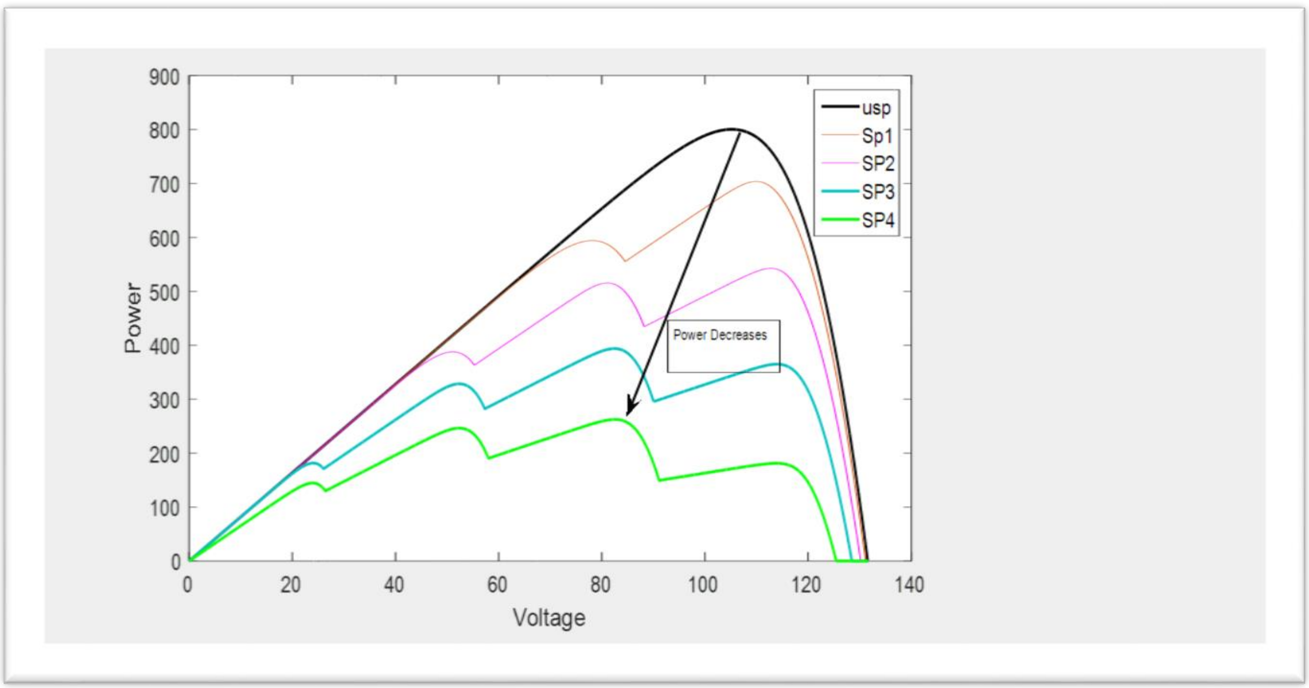

FIGURE 3.18 P-V CHARACTERISTIC CURVES FOUR KC200GT PV ARRAY CONNECTED IN SERIES UNDER DIFFERENT PARTIAL SHADING PATTERN AND ONE UNIFORMLY SHADED PV MODULE.

Fig. 3.18 illustrates as the PV array with large number of modules receives unequal illumination on the surface of it (SP4); less amount of energy produced. Additionally it is difficult to extract available power due to a number of local maximum outputs and one global maximum power.

3.10.4 Reflection effect

A photon can be reflected, absorbed or it can pass through a semiconductor. Since only the photons that are absorbed contribute to the generation of electrical energy, it is important to reduce the percentage of photons that are reflected. An anti-reflective coating is usually applied to the surface of the solar cell in order to decrease the number of photons that are reflected [112].

3.11 Modeling and output characteristics of PV Panel under PSCs

3.11.1 Effect of shadow on the module

PV panel partial shading is one of the main causes of electrical mismatching of series connected PV cells, and can lead to the eventual avalanche breakdown of shaded cells [112]. The junction temperature increases considerably due to high avalanche current, causing thermal breakdown of the shaded cell. Consequently, a shadow falling on a group of cells will reduce the total output by two mechanisms: 1) by reducing the energy input to the cell, and 2) by increasing energy losses in the shaded cells. The Problems become worse when shaded cells get reverse biased.

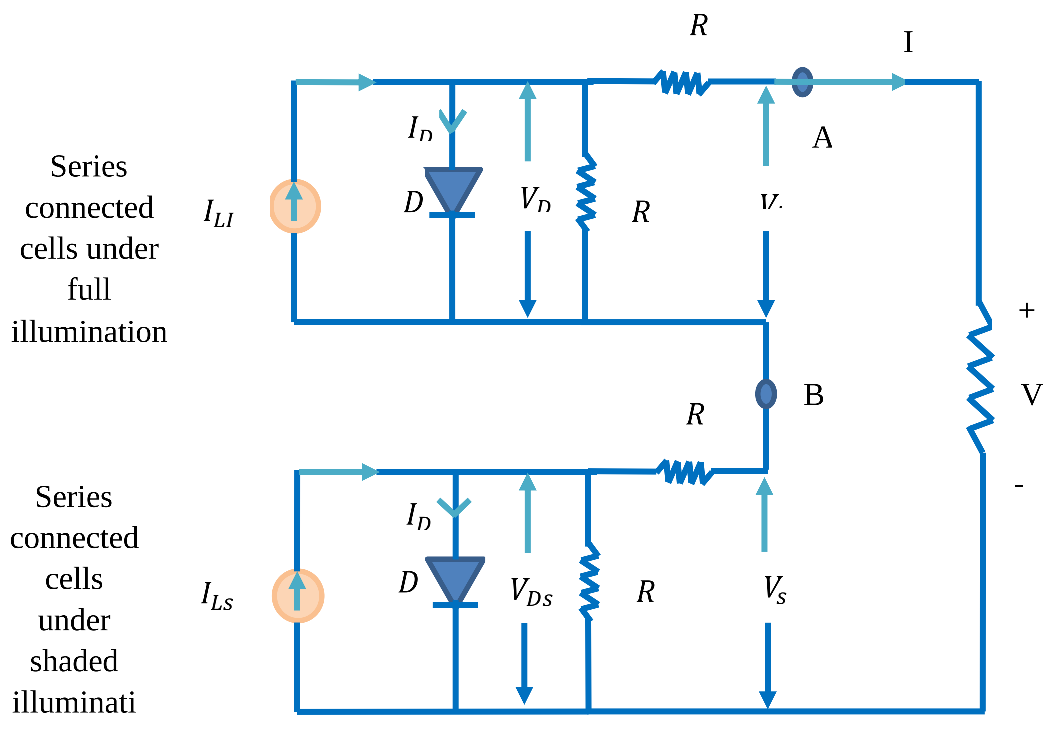

FIGURE 3.19 EQUIVALENT CIRCUIT OF SPV MODULE CONSISTS OF 54 CELLS IN SERIES WITH NO UNIFORM ILLUMINATION

In Fig.3.19, a group of cells under full illumination is connected in series with another group of cells under shaded illumination. The photon current of fully illuminated cells *Iphi* is high compared with that of the shaded illuminated cells *Iphs*. If the module current $I < Iphs$, diode Ds is forward biased and there is no risk for the shaded cells. But if *I* > *Iphs*, then the diode current *IDs* = *Iphs*-*I* flow through the diode in the reverse direction. Reverse biased diode Ds offers high resistance will consume power and will significantly reduce the load current *I* itself. The point B will assume negative potential. If the difference in illumination levels is high, Ds may get damaged due to overheating.

3.11.2 Parameters affecting the performance of SPV

3.11.2.1 Mathematical modeling of PV module under partial shading

The photo current generated by the shaded illuminated cell is *FIph*, where *F* is the ratio of photo current generated by the shaded cell to that of the fully illuminated cell. *F*=0 means, fully shaded and *F*=1 means fully illuminated. The output current of solar illuminated solar cell given in eqn (3.6) can be modified to a solar cell in a series array under shadow as:

$$I = FP_{Pv} - I_o\left[\exp\left(\frac{v_{ds}}{av_t} - 1\right)\right] - \frac{v + IR_{ss}}{R_p} \qquad 3.14$$

Where

$$v_{ds} = v_s + R_{ss} I_s \qquad 3.15$$

$$V_{di} = v_i + R_{si} I_i \qquad 3.16$$

Vds=diode voltage of shade PV cell Rss is series resistance of shaded cell

Vdi=diode voltage of illuminated PV cell Rsi is series resistance of illuminated cell

As the shaded and illuminated cells are connected in series, the same current is forced to flow through both. So in the equations (3.6), (3.14), (3.15) and (3.16), *Ii* and *Is* replaced by the same current *I*. Therefore,

As the value of F decreases from 1 to 0, $\exp\left(\frac{v_{ds}}{v_t}\right)$ tends to zero. Therefore (3.15) can be simplified as, therefor, the output current equation can be reduced to

$$I = FI_{ph} + I_o - \frac{v_s - IR_{SS}}{R_{ps}} \qquad 3.17a$$

Rearranging (3.17α), the expression for the voltage across the shaded cell v_s can be obtained as,

$$v_s = (FI_{ph} - I)IR_{ps} - IR_{ss} \quad 3.17b$$

In the above equation3.17b *IRss* is neglected in comparison with larger terms. The total module output voltage is the sum of voltages across each cell operating at the same current *I*. So the module consists of 54 identical series connected cells, the output voltage can be expressed as,

$$V = \sum_{j=0}^{i} V_{ij} - \sum_{k=0}^{b} V_{sk} \quad 3.18$$

Where a+b=total number of cells in the module/array depending on the PV system.

The power dissipated by the shaded cell is obtained by using (3.19) as:

$$P_{ds} = IV_s = I\lfloor FI_{ph} - I \rfloor R_{ps} - IR_{ss} \quad 3.19$$

Power dissipation in the shaded cell may be substantial leading to increase in its temperature. Due to increased temperature, the cell current gets concentrated in an increasingly small region of the cell, producing the hotspot. This can damage the cell encapsulation and eventually produce module failure. [113]-[116].

3.11.3 Output characteristics of PV array under PSCs

As a result of the partial shading, the generated current of a PV array having multiple modules connected in series is limited by that of the shaded PV ones. The terminal voltages corresponding to the peak power points of a PV array is a key piece of information for the MPPT algorithm under PSCs. This work considers a PV array consisting of four PV modules of identical type, and all having 54 chained cells in series and one string in parallel. The irradiation levels on the modules may be different, and are taken to range from 1000 to 4211 W/m2.

3.12 DC/DC Converter

It is an electronic device that changes input dc voltage to a different output dc voltage level. There are three common topology of dc – dc converter. Boost converter have been used for this work.

3.12.1 Boost converter

It is a medium of power transmission to perform energy absorption and injection from solar panel. This process in the boost converter is performed by a combination of four components which are inductor, electronic switch, diode and capacitor. Those components in the boost converter are shown in figure bellow. In other word the average output voltage is controlled by the switching on and off time duration. This can be realized by PWM signal. It is adjusting the ON and OFF duration of the switch at a constant frequency. The switching duty cycle, D is defined as the ratio of the ON duration to the switching time period. The energy absorption and injection with the relative length of switching period will operate the converter in two different modes known as continuous conduction mode (CCM) and discontinuous conduction mode (DCM) [4], [37].

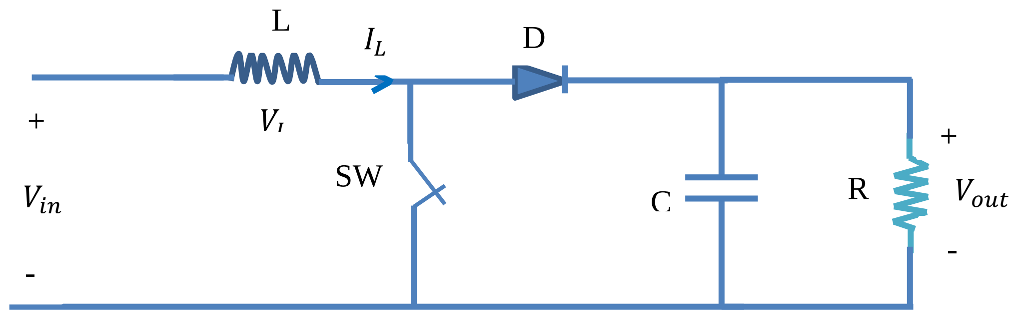

FIGURE 3.20(A) CIRCUIT DIAGRAM OF BOOST CONVERTER

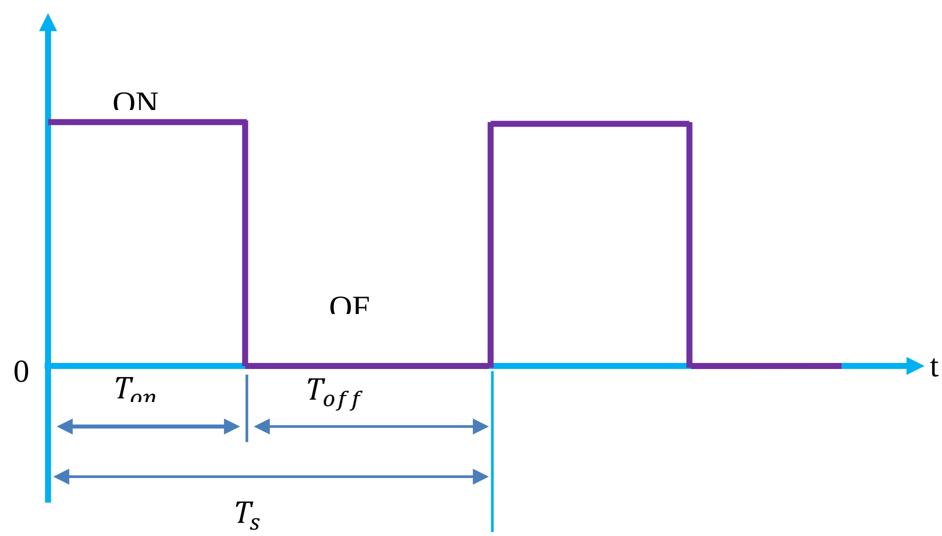

FIGURE 3.20 (B) WAVEFORM OF PWM.

3.12.2 Steady state analysis of the boost converter

Under CCM, boos converter operation divided into two modes:

Mode 1 the switch SW1 is turned on at t=0 as shown in the fig. 3.21. The input current which rises flows through inductor L and switch SW. During this mode, energy is stored in the inductor and load is supplied by capacitor current.

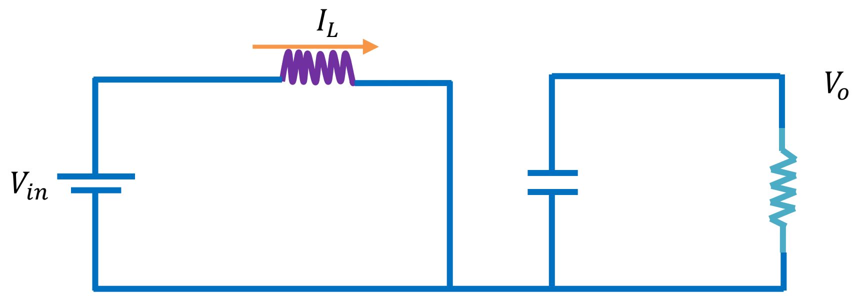

FIGURE 3.21 THE ON STATE CIRCUIT DIAGRAM OF THE BOOST CONVERTER

When the switch is ON, the inductor is charged from the input voltage source Vg and the capacitor discharges across the load. The duty cycle, D=$\frac{T_{on}}{T}$, Where T=$\frac{1}{f_s}$

Mode 2 begins when the switch is turned off at t = DT. The current that was flowing through the switch would now flow through inductor L, diode D, output capacitor C, and load R as shown in Fig. 3.22. The inductor current falls until the switch is turned on again in the next cycle. During this time, energy stored in the inductor is transferred to the load together with the input voltage.

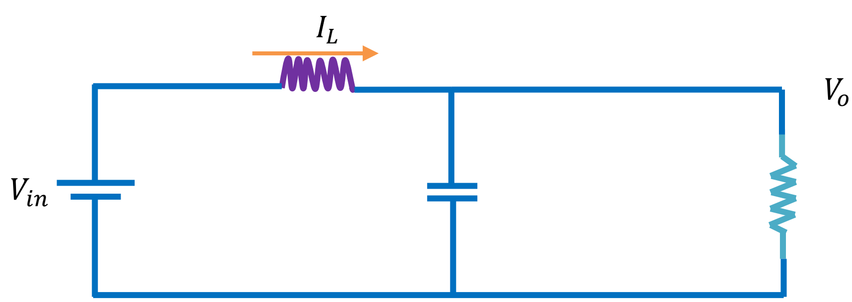

FIGURE 3.22 THE OFF STATE CIRCUIT DIAGRAM OF THE BOOST CONVERTER

When the switch is off, the sum total of inductor voltage and input voltage appear as the load voltage.

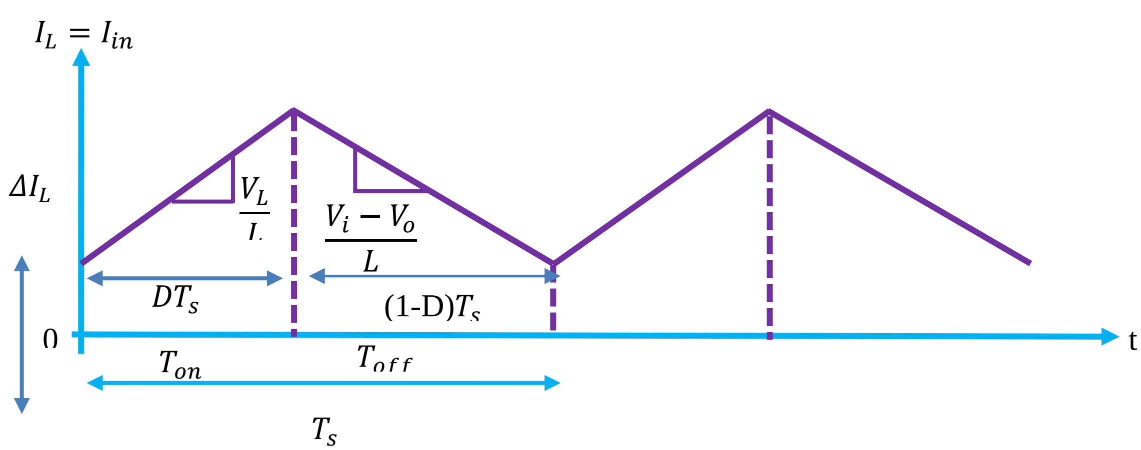

FIGURE 3.23 INDUCTOR CURRENT WAVEFORM

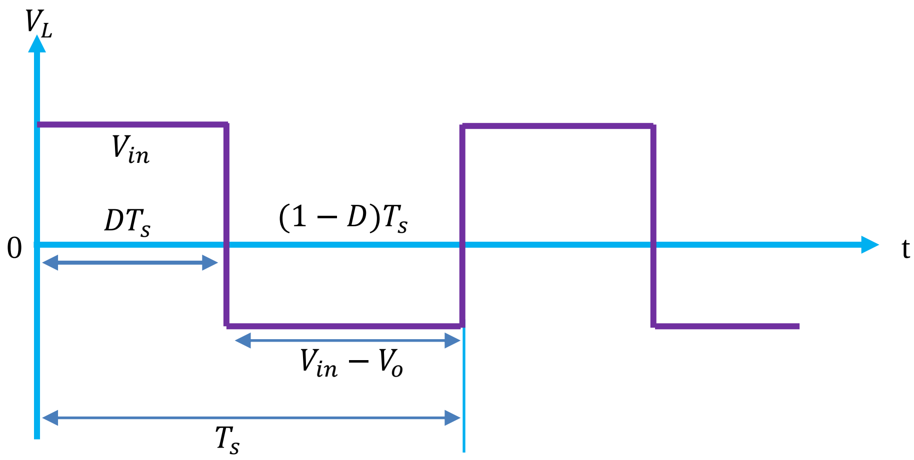

FIGURE 3.24 INDUCTOR VOLTAGE WAVEFORM

As a result the operating principle of the boost converter explained above; the following equations are formulated.

From the inductor voltage balance equation, have:

$$V_{in}(DT_s)+(V_{in}-V_o)(1-D)T_s=0 \qquad 3.20$$

$$V_{in}(DT_s)-V_{in}(DT_s)-V_{in}T_s+V_o(DT_s)-V_oT_s \qquad 3.21$$

$$V_o=\frac{V_{in}}{1-D} \qquad 3.22$$

Therefor; the duty cycle is: $D=1-\frac{V_o}{V_{in}}$ and the converter output voltage is $V_{out}=\frac{1}{1-D}*V_{in}$

Where V_{out} is the output voltage, D is duty cycle, and V_{in} is input voltage [37]

From the inductor current ripple analysis

$$\Delta I_L=I_{\max}-I_{\min} \qquad 3.23$$

$$\Rightarrow \Delta I_l = \left(\frac{V_{in}}{L}\right) * \left(DT_s\right) \qquad 3.24a$$

$$\Rightarrow \Delta I_l = DVin \ * \left(Lf_s\right) \qquad 3.24b$$

$$\Rightarrow L = \left(\frac{DV_{in}}{\Delta I_L f_s}\right) \qquad 3.25$$

The boost converter operates in CCM (continuous conducting mode) for L> Lb where

$$L_b = \frac{\left(1-D\right)^2 * D * R_{load}}{2 f_s} \qquad 3.26$$

The minimum value of the filter capacitor that results in the voltage ripple (V_r) is given by:

$$C_{\min} = \frac{DV_o}{V_o * R_{load} * f_s} \qquad 3.27$$

In order to operate the converter in CCM, the inductance is calculated such that the inductor current IL flows continuously and never falls to zero.

$$L_{\min} = \frac{\left(1-D\right)^2 * D * R_{load}}{2 f_s} \qquad 3.28$$

Where *L*min is the minimum inductance, *R* is output resistance, and *f* is the switching frequency of switch SW [4]. The output capacitance to give the desired output voltage ripple is given by

$$C_{\min} = \frac{DV_{out}}{\Delta V_o R_{load} f_s} \qquad 3.29$$

When the value of the inductance is lower than the minimum value calculated by the above eqn. (3.28), the inductor gets into dcmany values of *L*min below than the minimum inductance will result in the boost converter to operate in DCM.

CHAPTER 4

DESGIN OF FUZZY LOGIC CONTROLLER FOR PV SYSTEM UNDER PARTIAL SHADE CONDITION

4.1 Description of the case study area

Assosa University is one of the third generation public **universities** in Ethiopia which was established in May2011 by the Council of Ministers. The university is located in **Asosa** town, in western Ethiopia and the capital of the Benishangul-Gumuz Region (or *kilil*) of Ethiopia with a latitude of 10.06541 and longitude of 34.507. It has an elevation above sea level of 1,570 meters and 664.6 Kilometers North of Addis Ababa. The area has high concentration of sunshine insulation.

FIGURE 4.1 OVER VIEW OF ASSOSA UNIVERSITY BACKGROUND

4.2 Solar Radiation analysis of the site

The first input in the designing process is study and analyze the metrological data collected at Assosa metrological agency. Sunshine hour and temperature (Maximum temp and minimum temp) are the two important information used to find solar irradiance of the PV system going to be designed in this research.

Table 4.1 average sunshine hours for Assosa, Ethiopia (2009-2018) using Campbell-Stokes recorder

YEAR	J	F	M	A	M	J	J	A	S	O	N	D
2009	9.3	7.7	7.9	7.7	7.2	5.9	3.4	4.2	4.6	5.5	8.5	8.9
2010	8.3	8.1	7.7	8.4	5.6	4.1	3.3	2.7	3.9	4.6	7.9	8.3
2011	8.4	8.8	7.8	7.7	5	4.2	4.1	3.4	3.2	4.5	8.1	6.3
2012	9.4	9.3	8.2	8.9	6.1	4.9	2.1	3.4	3.7	4.8	8.4	8.6
2013	9.3	8.3	7.9	5.9	5.6	4.8	3.2	3.7	4.9	4.6	7.7	9.8
2014	8.9	6.8	7.2	6.7	4.7	4.1	3.5	2.9	4.5	4.5	8.6	9.1
2015	9.4	9.1	7.7	8.4	4.8	5.4	3.6	4.1	5.8	4.9	9.1	7.4
2016	9.8	9.1	7.8	8.1	4.6	5.2	3.2	4.7	4.8	5.3	9.2	9.2
2017	9.8	6.9	7.9	6.6	5.1	5.7	3.1	4.2	5.2	5.6	8.5	9.3
2018	9.7	8.5	8.8	8.1	6.3	4.1	3.6	3.9	6.1	3.5	7.6	8.5
Ava	9.23	8.26	7.89	7.65	5.5	4.84	3.31	3.72	4.67	4.78	8.36	8.54

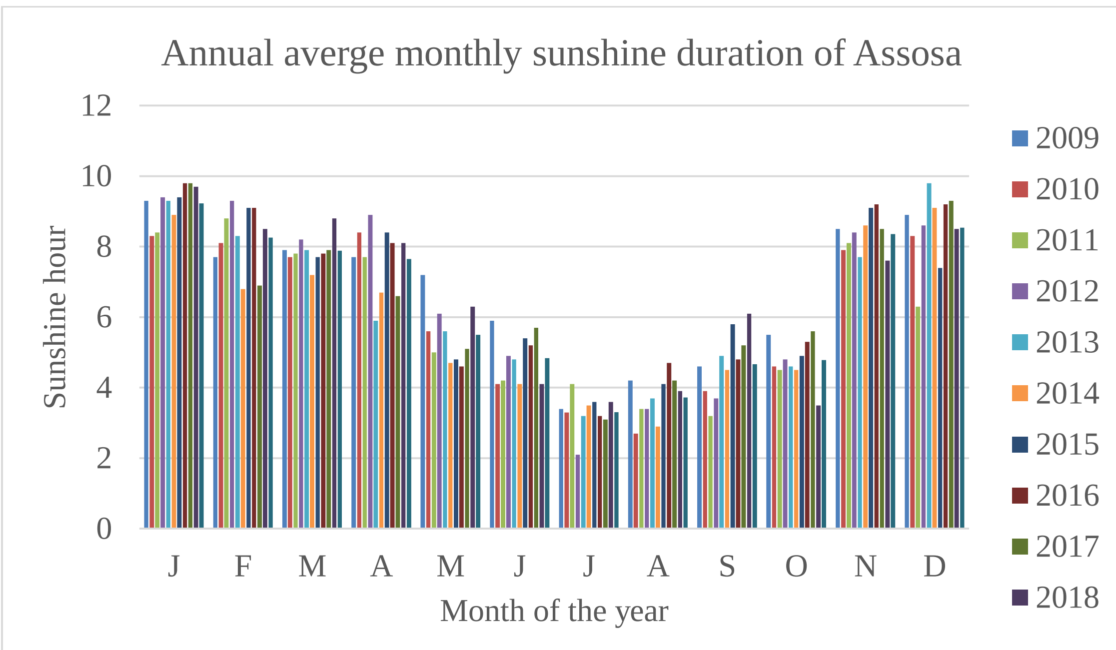

FIGURE 4.2 GRAPHICAL REPRESENTATION OF ANNUAL AVERAGE MONTHLY SUNSHINE DURATION OF ASSOSA, ETHIOPIA

The series of the procedure provided bellow have been used to converting the sunshine hour to available solar irradiance, which is used as an input to the PV system.

Solar irradiance is most commonly measured; a more common form of radiation data used in system design is the solar insolation. The solar insolation is the total amount of solar energy received at a particular location during a specified time period, often in units of kWh/ (m2.day). While the units of solar insolation and solar irradiance are both a power density (for solar insolation the "hours" in the numerator are a time measurement as is the "day" in the denominator), solar insolation is quite different than the solar irradiance as the solar insolation is the instantaneous solar irradiance averaged over a given time period. Solar insolation data is commonly used for simple PV system design while solar radiance is used in more complicated PV system performance which calculates the system performance at each point in the day. Solar insolation can also be expressed in units of MJ/m2 per year and other units and conversions are given in the unit's page [113].

Solar radiation for a specific location can be given in the form of one the following ways:

- ✓ Typical mean year data for a particular location
- ✓ Average daily, monthly or yearly solar insolation for a given location
- ✓ Sunshine hours data
- ✓ Solar Insolation Based on Satellite Cloud-Cover Data
- ✓ Calculations of Solar Radiation

Solar constant variation with time over the year St is given by [113]

$$S_t = S\left(1 + 0.033\cos\frac{360n}{365}\right) \qquad 4.1$$

Where n=n^{th} day of the year with first January being n=1

S=solar constant

The declination angle of the sun insulation can be given by [113]

$$\delta = 23.34 Sin\frac{360}{365}(284 + n) \qquad 4.2$$

The relation between the incidence angle and other angles is given by [113]

$$Cos\theta = \sin\Phi(\sin\delta\cos\beta + \cos\delta\cos\gamma\cos\omega\sin\beta) + \cos\phi(\cos\delta\cos\omega\cos\beta - \sin\delta\cos\gamma\sin\beta) + \cos\delta\sin\gamma\sin\omega\sin\beta \qquad 4.3$$

Condition 1: when the collector surface is lying flat on the ground, its angle with horizontal plane will be zero, i.e., β=0°. Thus, for the horizontal surface, Eq. (4.3) can be written as: [113]

$$Cos\theta = \sin\phi \sin\delta + \cos\varphi \cos\delta \cos\omega \quad 4.4$$

Condition 2: When the collector surface is facing due south, the surface azimuth angle becomes zero, i.e., γ=0°. In the situation, Eq. (4.3) can be written as: [113]

$$Cos\theta = \sin\delta \sin(\phi - \beta) + \cos\delta \cos\omega \cos(\phi - \beta) \quad 4.5$$

As just shown above, equations (4.3), (4.4) and (4.5) can be used to find out the incident angle on solar collector under any conditions, which then can be used to determine the solar radiation falling on the surface of collector.

The sunrise and sunset hour angle will be the angle for which the incidence angle of sunrays is 0^o or zenith angle is 90°. Substituting ϴ = 0° in Eq. (4.3), we get

$$Cos\omega_s = -\tan\phi \tan\delta \quad 4.6$$

$$\omega_s = \cos^{-1}(-\tan\phi \tan\delta) \quad 4.7$$

$\omega_s = hour\ angle$ (It may give positive or negative value)

The positive value is representing sunshine hour angle and the negative is sunset hour angle. It can be converted into hour by the relation 1hr=15^o .

If the collector surface is inclined and south facing, the sunrise and sunset hour angles will be obtained from Eq. (5). Using θ=90o, we get:

$$\omega_s = \cos^{-1}(-\tan(\phi - \beta)\tan\delta) \quad 4.8$$

For the inclined surface the sunrise and sunset hour angles will be smaller, which means the day length for inclined collector surfaces will be smaller than the horizontal surface. The day length is the duration from the sunrise hour angle to the sunset hour angle. Due to symmetry both angles are same for the horizontal collector. Thus, the day length will be equal to $2\omega_s$ **.** In terms of the number of hours, the day length S_{max} (day length or maximum number of sunshine hours) will be given as [113]:

$$S_{max} = \frac{2}{15}\cos^{-1}(-\tan\phi\tan\delta) \quad 4.9$$

$$S_{max} = \frac{2}{15}\omega_s \quad 4.10$$

4.3 Estimation of Total Solar Radiation

The amount of solar radiation falling on a solar collector at a given time and location, the direct or beam radiation and diffuse radiation should be either measured or estimated using empirical equations. The monthly average daily global radiation on a horizontal surface Hga is [113]

$$\frac{H_{ga}}{H_{oa}} = a + b\frac{S_a}{S_{max}} \quad 4.11$$

Where H_{oa} =monthly average extra-terrestrial solar radiation at horizontal surface

S_a =monthly average daily sunshine hours

S_{max} =maximum possible daily sunshine hours at a given location

a and b are constants.

In Eq. (4.11), needs to have a value of Hoa which can be estimated from the instantaneous value of extra-terrestrial solar radiation. Integration of extra-terrestrial radiation over a day will give the daily value of extra-terrestrial solar radiation, Ho (=H_{oa} if it is estimated for a given day of a month), which can be written as [113]:

$$H_a = S_t\int\cos\theta dt \quad 4.12$$

$$= S\left[1 + 0.033\cos\frac{360n}{365}\right]\int_{sunrise}^{sunset}(\sin\phi\sin\delta + \cos\phi\cos\delta\cos\omega)dt \quad 4.13$$

Where t=time in hour. It can be converted into time in angles (in radian) by $dt = \frac{180}{15}d\omega$, Therefore,

$$H_o = \frac{12}{\Pi} S\left[1 + 0.033\cos\frac{360n}{365}\right]\int_{-\omega_s}^{\omega_s}(\sin\phi\sin\delta + \cos\phi\cos\delta\cos\omega)d\omega \quad 4.14$$

Integrating eqn. (4.14) will give the values of Ho: [113]

$$H_o = \frac{12}{\Pi} S\left[1 + 0.033\cos\frac{360n}{365}\right]\omega_s(\sin\phi\sin\delta\cos\phi\cos\delta\cos\omega_s) \quad 4.15$$

Where S is in w/m^2

Ho will be in w-h/m^2

The multiplying term in eqn. (4.15) ω_s should be in radians.

The declination angle in the equation represents the day of the year. It has been shown by Klein (1977) that of Ho is calculated for a particular day of the month, its value will be equal to its average value over the month (i.e., H_{oa}).

Hence, the dates at which Ho is equal to H_{oa} are: January 17, February 16, March 16, April 15, May 15, June 11, July 17, August 16, September 15, October 15, November 14 and December 10 [113].This can be represented in the table 4.2 bellow.

Table 4.2 recommended average days for months and values of n by months

Month	n for i^{th}, Day of the month	Date	n, day of the year
JUN	I	17	17
FEB	31+i	16	47
MAR	59+i	16	75
APR	90+i	15	105
MAY	120+i	15	135
JUNE	151+i	11	162
JULY	181+i	17	198
AUG	212+i	16	228
SEP	243+i	15	258
OCT	373+i	15	288
NOV	304+i	14	318
DEC	334+i	10	344

Therefore using this series of procedures, now convert the collected sunshine data into usable solar irradiation for developing the PV system that can be designed in this thesis.

Table 4.3 annual average monthly daily maximum sunshine hour, annual average monthly sunshine angle and annual average monthly daily solar radiation of Assosa, Ethiopa (2009_2018) determined by applying the above series steps depend using average sunshine hour.

Month	Jan	Feb	Mar	Apr	May	Jun	July	Agu	Sep	Oct	Nov	Dec
I	17	16	16	15	15	11	17	16	15	15	14	10
N	17	47	75	105	135	162	198	228	258	288	318	344
Ava sunshine	9.23	8.26	7.89	7.65	5.5	4.84	3.31	3.72	4.67	4.78	8.36	8.54
$\boldsymbol{\delta}$	-20.94	-13.018	-2.49	9.34	18.74	1.56	21.23	13.54	2.327	-22.734	-18.838	-23.025
$\boldsymbol{\omega}$s	86.162	87.6989	89.60	91.716	93.488	90.323	93.98	92.49	90.458	85.79	86.58	85.73
S_{max}	11.488	11.693	11.947	12.228	12.465	12.043	12.531	12.332	12.061	11.439	11.544	11.431
Ho	37669606	37695638.24	37598021	37726733	37573792	37716512	37515960	37586082	37727383	37585315	37516372	37501769
H	24771896	23069922.59	22197575	21655770	18312630	17684814	15161836	15852886	17429330	17905284	23273473	23668154
H	6.88	6.408	6.16	6.01	5.08	4.91	4.211	4.40	4.84	4.97	6.46	6.57

$\boldsymbol{\omega}$s(deg); Ho(wh/m2_day); $\boldsymbol{\delta}$(deg) and H(kwh/m2_day

Where I is the date at which $H_o = H_{oa}$ of the month.

n is the date at which $H_o = H_{oa}$ of annual monthly beginning from January n=1

Ava. Sunshine is S_a

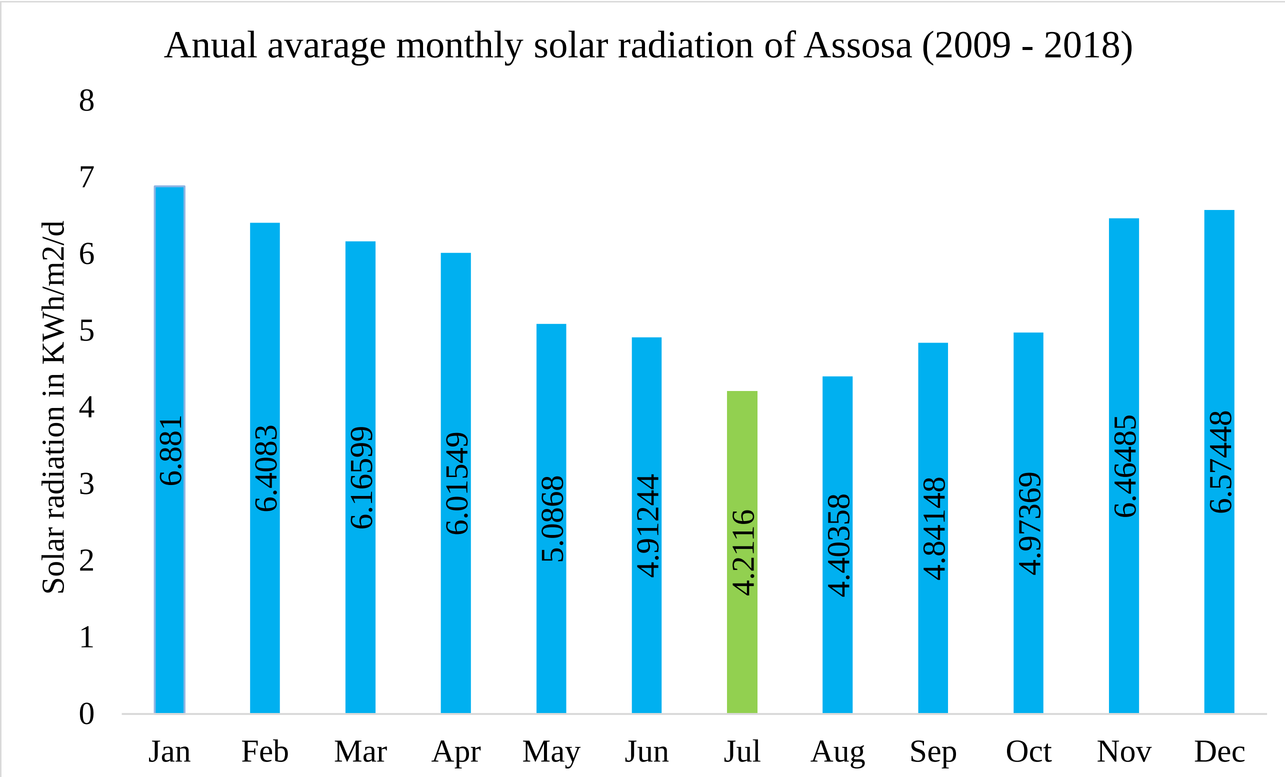

FIGURE 4.3 GRAPHICAL PLOT OF ANNUAL AVERAGE MONTHLY SOLAR RADIATION OF THE SITE

Table 4.4 Allsky Insolation Incident on Horizontal Surface of Assosa, Ethiopia (Kwh/m^2/Day)

PARAMETER	JUN	FEB	MAR	APR	MAY	JUN	JUL	AUG	SEP	OCT	NOV	DEC	ANN
ALLSKY_SFC_SW_DWN	6.1	6.45	6.64	6.54	5.7	4.82	4.62	4.79	5.07	5.13	6.01	5.94	5.65

Source: NASA@Latitude10.06541 degree and Longitude 34.50701

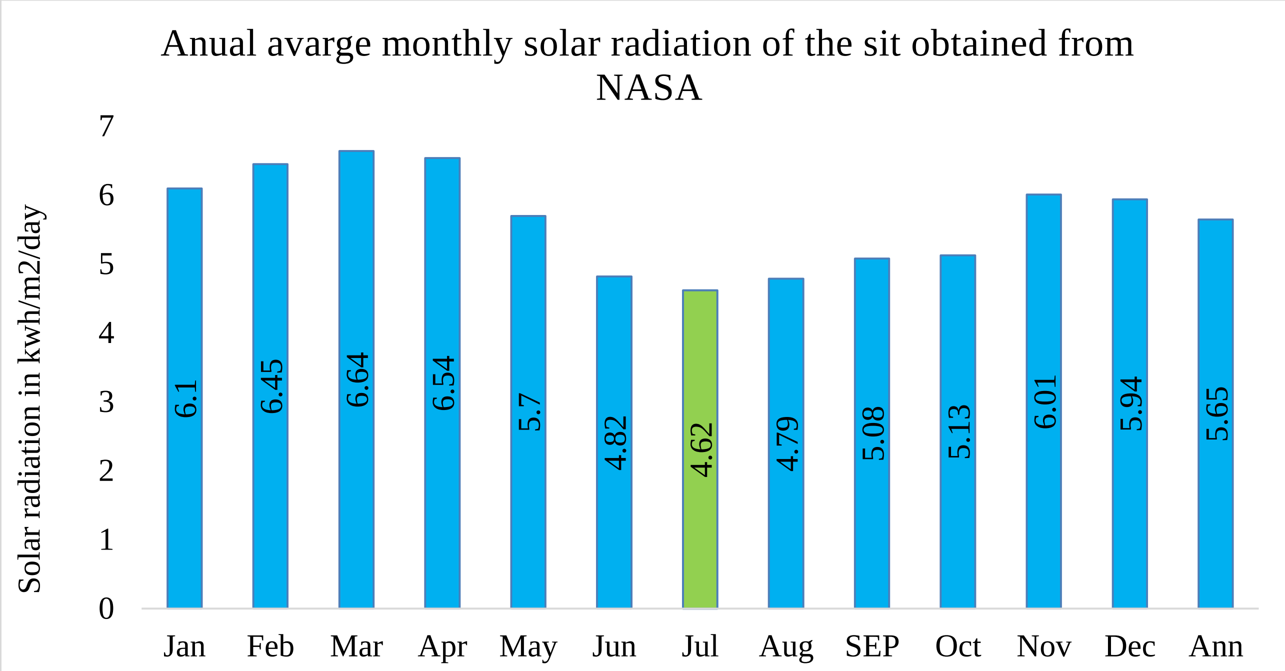

FIGURE 4.4 GRAPHICAL REPRESENTATION OF AVERAGE MONTHLY SOLAR RADIATION OF THE SITE (ASSOSA, ETHIOPIA) (NASA)

Table 4.4 is horizontal solar irradiation (Kwh/m^2/Day) data for the selected site, Assosa, Ethiopia, is obtained from NASA at latitude of 10.06541 and longitude of 34.507 for 30-year Meteorological and Solar Monthly & Annual Climatologies (January 1984 - December 2013).

It is compared with the calculated solar radiation, done in the above sections of this particular thesis in table 4.3, of the site which is implemented by converting sunshine hours into solar radiation by using Empirical Equation [Duffle. and Beckman, 1991]. For the comparison, the root means square error (RMSE) formula can be applied to the equation below.

$$RMSE(\%) = 100\frac{1}{H_{ob}}\left(\sum \frac{s_i^{\,2}}{u}\right)^{1/2} \qquad 4.16$$

Where, $S_i = H_{estimated} - H_{obtained}$

For x= 1, 2, 3… u, U is the total number of observation point, H_{ob}= the arithmetic mean value of the obtained data (data from NASA [NASA, 2008]. The correlation coefficient, r by which the depth of the correlation of the two radiation levels is compared is given by the following statistical formula [Nguyen and Pryor, 1997].

$$R = \frac{\sum (H_{estimated} - H_e)^2 * (H_{obtained} - H_{ob})}{\sqrt{(H_{obtained} - H_{ob})^2 * \sum (H_{estimated} - H_e)^2}} \qquad 4.17$$

Where He is the arithmetic mean value of the estimated value of the solar radiation and Hob, is the arithmetic mean value of u obtained a value of the solar radiation. The solar radiation, calculated from the daily sunshine hour is almost approximately equal to the solar radiation obtained from NASA comparing fig.4.3 and fig.4.4. Therefor for better reliability of the solar radiation for the given purpose: the worst condition is taken, i.e. for any photovoltaic system in order to meet the required demand. From fig4.3 the worst condition is on July with green color (G=4211W/m2) is taken for modeling the PV system.

4.4 Design of boost converter parameter and steady state analysis

In this work, a boost converter operated in CCM is designed to boost up fluctuating solar array voltage to a higher constant output voltage of 230 V (d.c) the input voltages to the boost converter is the minimum PV voltages generated by the PV array. The boost converter is designed to maintain a constant output of 230 V (d.c).

(1) CURRENT RIPPLE FACTOR (CRF):

According to IEC harmonics standard, CRP should be bounded within 20% to 40%.

i.e. $\frac{\Delta I_L}{I_{out}} = 25\%$

(2) Voltage ripple factor (VRF):

i.e. $\frac{\Delta V_o}{V_o} = 1\%$

(3) Switching frequency (fs):

f_s= 25 kHz

GIVEN DATA FROM THE PROPOSEEED SYSTEM:

- Input voltage, Vin=140.8V
- Output voltage, Vo=230V
- Output power Po=3190W

Step 1: Calculation of Duty cycle (D):

$$D = 1 - \frac{V_{in}}{V_{out}} \quad 4.18$$

$$D = 1 - \frac{140.8}{230} = 0.38778$$

Step 2: Calculation of Ripple Current (ΔI_L):

$$\Delta I_L = 0.25 * \frac{P_{out}}{V_{out}} = 0.25 * \frac{3190}{230} = 2.94$$

Step 3: Calculation of Inductor value (L):

$$L_{\min} = \frac{V_{in} * D}{f_s * \Delta I_L * \left(\frac{V_{out}}{V_{in}}\right)} \quad 4.19$$

$$L_{\min} = \frac{140.8 * 0.3878}{25000 * 2.94 * \left(\frac{230}{140.8}\right)} = 742.887\mu\text{H}$$

Step 4: Calculation of Voltage Ripple Factor (V_r):

V_r= 0.01* 230 = 2.3

Step 5: Calculation of capacitor value(C):

$$C_{\min} = \frac{I_{out} * D}{f_s * \Delta V_{out}} \quad 4.20$$

$$C_{\min} = \frac{230 * 0.3878}{25000 * 2.3} = 48.579\mu F$$

Step 5: Calculation of Load Resistance (R_{Load}):

$$R_{load} = \frac{V_{out}}{I_{out}} \quad 4.21$$

$$R_{load} = \frac{V_{out}}{I_{out}} = \frac{230}{7.205} = 32.204\Omega$$

4.4.1 Selection of the component of boost converter

4.4.1.1 Selection of electronic switch

The electronic switch SW in has been chosen based on its voltage and current rating which have to be higher than the maximum input voltage and current. From the proposed system, the rating of the converter is 3 KW with an input voltage ranging from 50 V to 200 V. Therefore, electronic switch such as power MOSFET, IGBT, BJT and thyristor handling capability should meet the specification of the proposed design. In this proposed system Power MOSFET has been selected.

4.4.1.2 Selection of inductor

Equation (4.19) is the minimum inductance for boost converter to operate in CCM, therefore the selection of the inductor should be higher than the calculated value. Inductors with a ferrite core or equivalent are recommended.

4.4.1.3 Selection of diode

Diode reverse voltage rating is the main consideration for selecting the diode. Other important consideration is its ability to block the required off–state voltage stress and have sufficient peak and average current handling capability, fast switching characteristics, low reverse–recovery, and low forward voltage drop.

4.4.1.4 Selection of capacitor

Equation (4.20) is the calculation for output voltage ripple using capacitance. The selection of capacitor should be higher than the calculated value to make sure that the converter's output voltage ripple stays within the specific range. Another important consideration is its equivalent series resistance (ESR). Since the capacitor's ESR affects efficiency, low-ESR capacitors will be used for best performance. ESR can be reduced by connecting few capacitors in parallel.

Therefore, the specification of the proposed design to acquire is shown in the next page.

Table 4.5 shows the components used in the proposed design based on the equations and consideration mention previously.

Mode	CCM
Power rating	3190W
Output voltage	230V
output current	7.203A
Switching frequency	25000 Hz
Input voltage	50-140.8 V
Calculated parameter	
Inductor	742.588µH
Output Capacitor	48.579µF
Load	32.2Ω

4.4.2 Modeling and simulation of Boost converter in MATLAB

The fig. 4.5 is a circuit diagram for MATLAB simulation of boost converter. Thus is used to analyze the characters tics of boost converter and to measure the output voltage waveform.

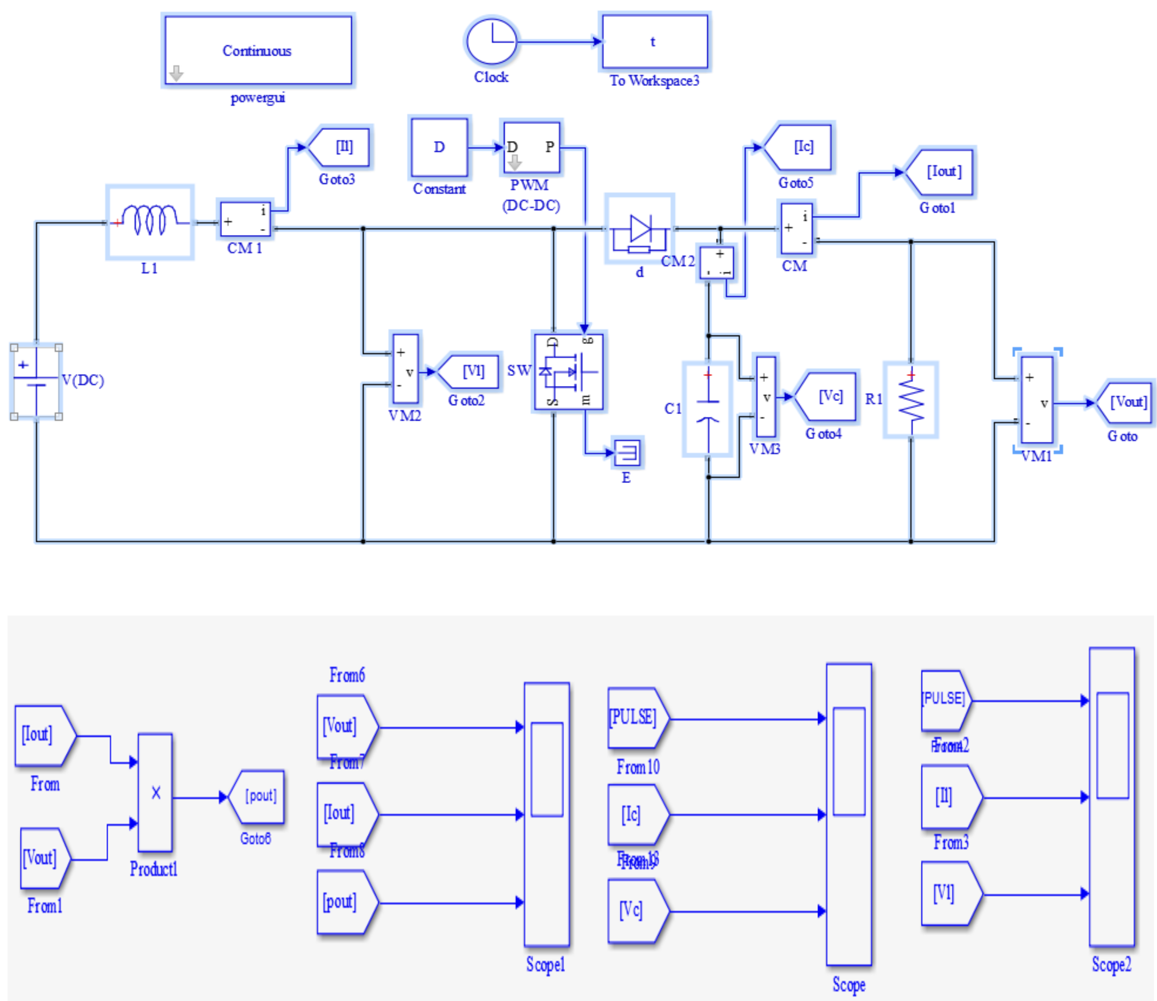

FIGURE 4.5 CIRCUIT DIAGRAM OF BOOST CONVERTER USED IN MATLAB 2015A FOR SIMULATION

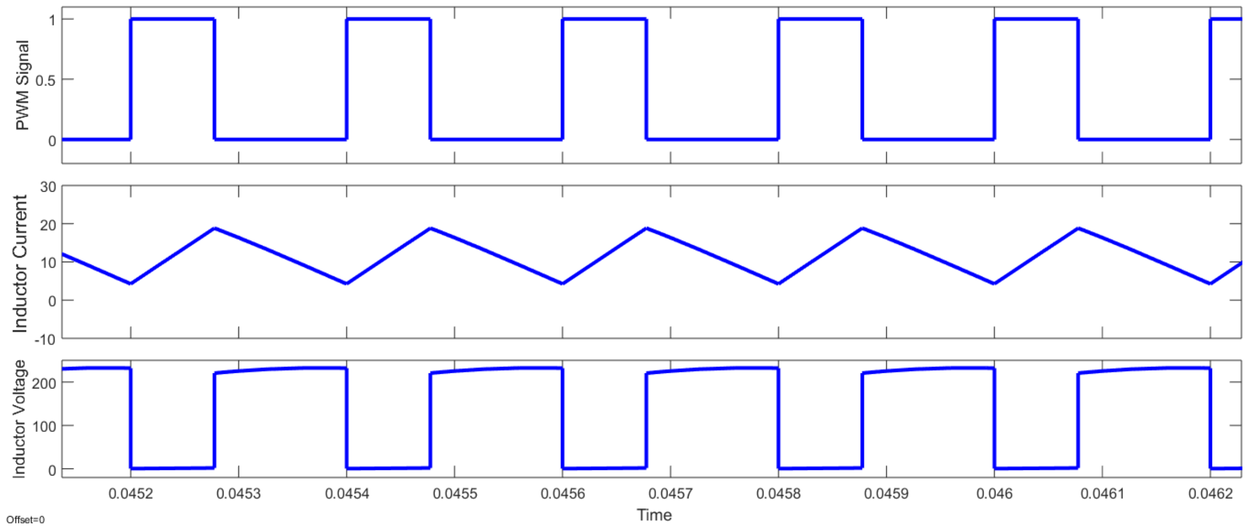

FIGURE.4.6 (A) WAVEFORM OF INDUCTOR VOLTAGE AND INDUCTOR CURRENT OF BOOST CONVERTER ON STEADY STATE.

The fig. (4.6 a.) above shows inductor current output waveform that obtained from the simulation is similar with the theoretical waveform stated in chapter 3. The output waveform that obtained is continuous conduction mode (CCM) which is the inductor current value greater than zero. Fig. (4.6 a.) Shows the inductor current output waveform from simulation.

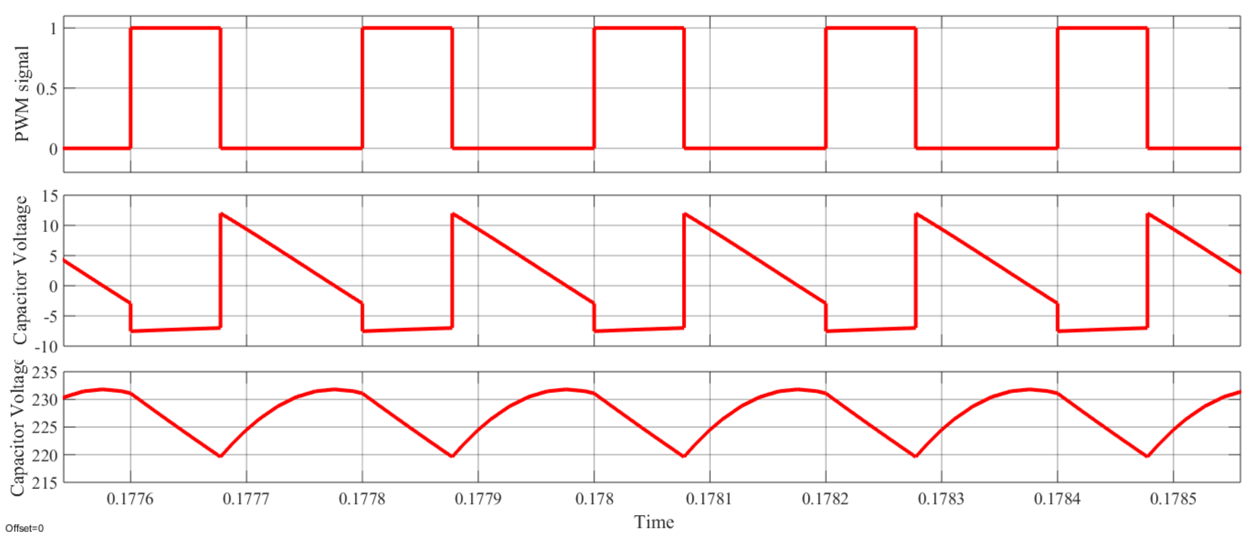

FIGURE 4.6 (B) WAVEFORM OF CAPACITOR VOLTAGE AND CAPACITOR CURRENT OF BOOST CONVERTER ON STEADY STATE

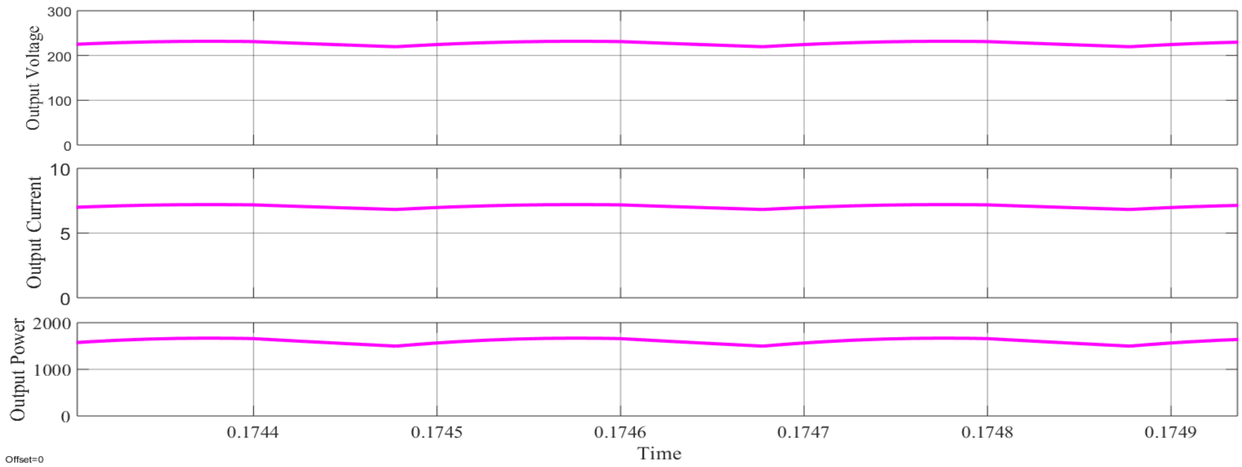

FIGURE 4.6 (C) WAVEFORM OF OUTPUT VOLTAGE, OUTPUT CURRENT AND OUTPUT POWER OF BOOST CONVERTER ON STEADY STATE

As shown from the simulation results in fig. (4.6 c.), a boost converter is designed to be operated in CCM is in order to step up a fluctuating solar panel voltage to a higher constant output voltage of 230V. In order to demand this requirement, the range of the duty cycle is between 0 to 38.78% due to the instability cause by the parasitic components. Based on the proposed design of the boost converter fig. 4.5, computer software MATLAB 2015a is used to simulate the designed boost converter's performance. The simulation results of the boost converter with input voltages and duty cycles are shown in Fig. 4.6 above. From the simulation results, the proposed converter is able to give a constant 230 V output voltage at 1658W loads. The boost converter is able to produce a constant output voltage of 230 V from a variable voltage of solar panel. The boost converter is able to deliver power with the highest efficiency of 95%.

4.5 Design of Fuzzy Logic Controller Parameters

Now a day, fuzzy logic controller has played an important role in the tracking of MPP in the PV system for any atmospheric conditions, in particular these tips of the thesis is designed to partial shade conditions. An important tips of FLC is robust and relatively simple to design over others an intelligence control system capable to extract MPP of PV system [58]-[60]. Additionally, it is an advantageous that it does not require the knowledge of an accurate plant model, be designed. On the other hand the designer needs expert knowledge of the PV system. The design and performance of the fuzzy system was tested in the Simulink/MATLAB2015a with the PV array.

4.5.1 PV Module with MPPT based Fuzzy Logic Controller

The fig. 4.7, shown below illustrates the basic diagram of a fuzzy logic based maximum power point tracker. As just looked from the figure, three state variables are sensed as an inputs of fuzzy controller; change of power (ΔP); change of current (CI) andΔP_m. FLC from measurements and simple numerical manipulation, gives the converter duty cycle (D) is fed to the converter through a pulse width modulator. This modulator drives the value of D to perform PWM that generates the control signals for the converter signals for firing the converter switch(s) [57].

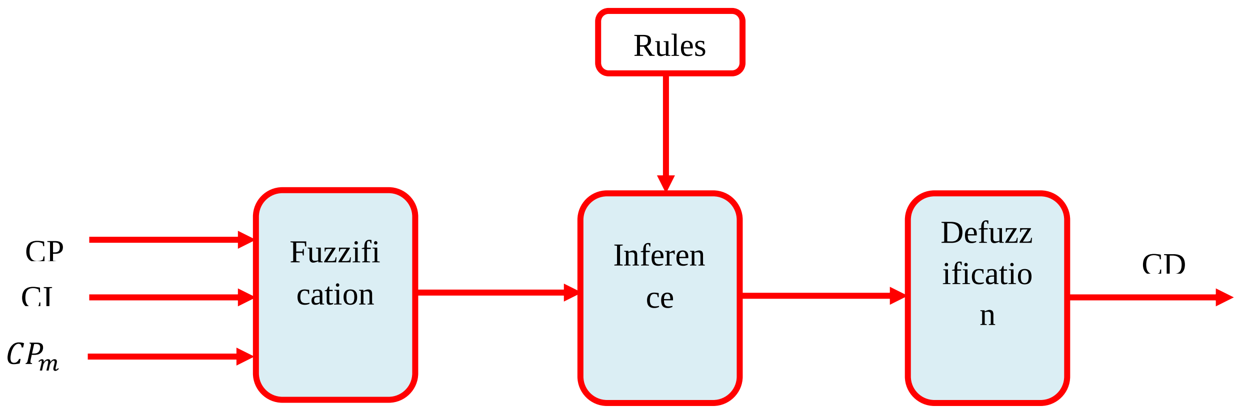

FIGURE 4.7 FUZZY MPPT INPUT AND OUTPUT VARIABLES

Where the inputs of the FLC can be expressed as:

$$CP(k) = P(k) - P(k-1) \qquad 4.22$$

$$CI(k) = I(k) - I(k-1) \qquad 4.23$$

$$CP_m = P_m - p(k) \qquad 4.24$$

Where P(k) is the present state power value

P(k-1) is the pervious state power value

I(k) is the present state current value

I(k-1) is the previous state current value

CP_m is the difference between the stored global maximum power (PM) and the current power, and P, I are the PV power and current respectively at instant k. CP is equal to zero at MPP.

In this thesis Max-Min Mamdami inference system have been used to compute the output to be defuzzified. In order to compute the outputs of fuzzy inference system for the inputs of CP(k) , CI(k) and $CP_m(k)$; the following steps has to be followed.

1. Fuzzifing the inputs using the input membership functions. (Take the input CP(k) ,I(k) and $CP_m(k)$ from fig. 4.8 shown below, is the proposed diagram in which this research going to optimize the outputs generated from the system. Then determine the degree to which they belongs to each of the appropriate fuzzy set via membership function which are NB, NS, PS, PB for input variables of CP(k) and CI(k) and PS ,PB for input variable CP_m. The important membership function shapes, triangular membership function are conducted and has been used to converts the crisp inputs gained in fig. 4.8 into fuzzy sets.

2. Combining the fuzzified inputs according to the fuzzy rules to establish a rule (here the used logical operate to perform this work is AND operation) to the inputs as a rule.

3. Finding the outputs of the rules the strength established in step two and the output membership function. The output is reshaped to a Min value according to the input combination rules.

4. Combining the consequences to get an output distribution (by combining output by mean of max operation)

5. Defuzzifying the output distribution

The proposed FLC is shown in the fig. (4.7); it is provided by three inputs, CP, CI, CP_m and one output CD is compared with the saw tooth waveform to generate the PWM signal to triggering the gate of the boost converter.

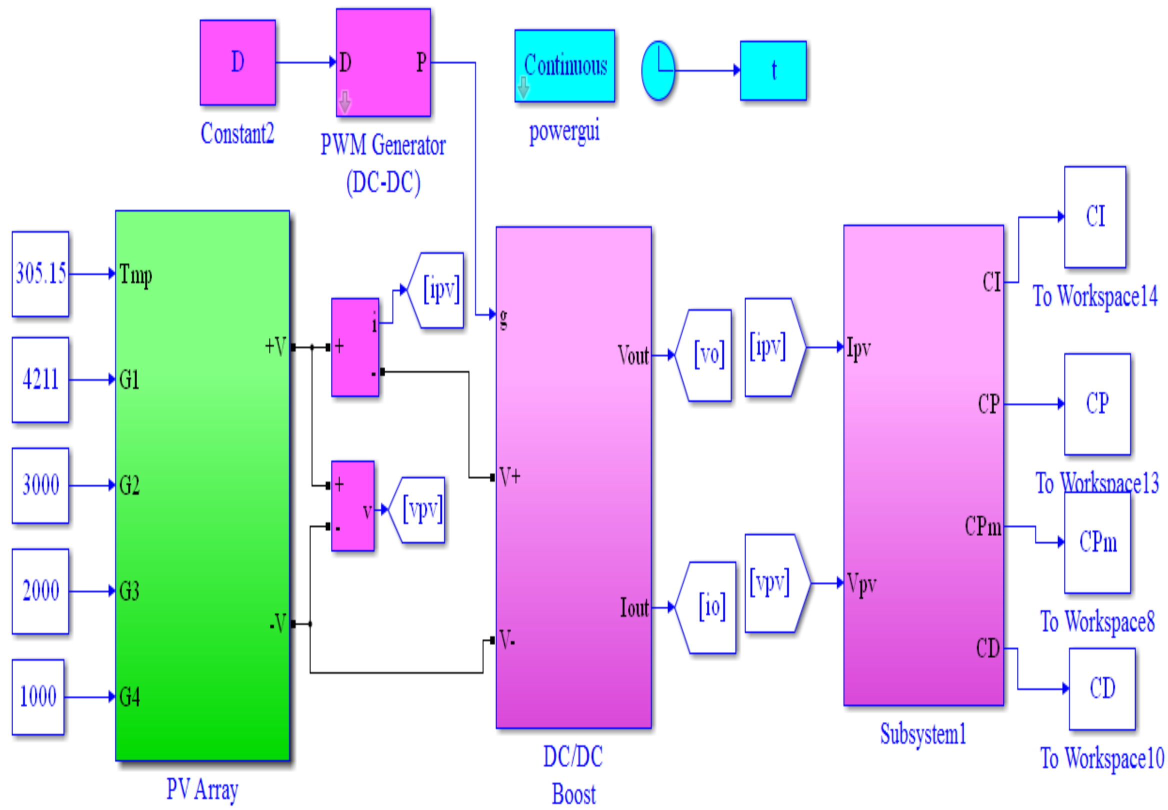

FIGURE 4.8 SIMULINK DIAGRAM OF THE PROPOSED SYSTEM WITHOUT MPPT CONTROLLER

4.5.1.1 Fuzzification mppt

It is the process of converting the actual inputs values CP, CI and CP_m into linguistic fuzzy set using membership functions as shown in fig. 4.7. The commonly used MF for the proposed controller is triangular MF. The each linguistic variable is expressed in terms of different linguistic values. The first two input linguistic variables, CP and CI are expressed by a linguistic value: NB, NS, PS, and PB, and the input variable CP_m is expressed by a linguistic value: PS and PB. The range of input linguistic variable CP, CI and CP_m are obtained as [-10 15]; [-1 0.1]; and [0 1657] respectively and the range of linguistic output variable CD became [-0.009, 0.001] in fig. 4.8 as shown from fig.4.9 and fig 4.10. Thus linguistic variables are defined by the following linguistic values.

Change of power, CP= {NB, NS, PS, PB}

Change of current, CI= {NB, NS, PS, PB}

CP_m = {PS, PB}

Change of duty cycle, CD= {NB, NM, NS, PS, PM, PB}

Those linguistic values are going to be converted into fuzzy set using triangular and trapezoidal MF as shown below in fig. 4.9 for uncontrolled proposed PV system as shown in fig 4.8. The values of CP, CI, CP_m are taken from fig 4.8 are fuzzified by the MF shown in fig. 4.9. For any values of linguistic variable CP, CI and CP_m over its universe of discourse are fuzzified by the appropriate MF (triangular or trapezoidal) of linguistic values in order to decide fuzzy rules made to control the system.

Therefore, the fuzzy set of input variables change of power, CP at the instant k, is defined by the following linguistic values:

Negative big = $\{(\mu_{NB}(CP(k)), CP(k)) \mid CP(k) \epsilon CP\}$

Negative small = $\{(\mu_{NS}(CP(k)), CP(k)) \mid CP(k) \epsilon CP\}$

Positive small = $\{(\mu_{PS}(CP(k)), CP(k)) \mid CP(k) \epsilon CP\}$

Positive big= $\{(\mu_{PB}(CP(k)), CP(k)) \mid CP(k) \epsilon CP\}$

Similarly, the fuzzy set of input variables change of current, CI at instant k, is defined by the following linguistic values:

Negative big= $\{(\mu_{NB}(CI(k)), CI(k)) \mid CI(k) \epsilon CI\}$

Negative small= $\{(\mu_{NS}(CI(k)), CI(k)) \mid CI(k) \epsilon CI\}$

Positive small= $\{(\mu_{PS}(CI(k)), CI(k)) \mid CI(k) \epsilon CI\}$

Positive big= $\{(\mu_{PB}(CI(k)), CI(k)) \mid CI(k) \epsilon CI\}$

Using the same fashion as above, the fuzzy set of input variables, CP_m at instant k, are defined by the following linguistic values:

Positive small= $\{(\mu_{PS}(CP_m(k)), CP_m(k)) \mid CP_m(k) \epsilon\ CP_m\}$

Positive big= $\{(\mu_{PB}(CP_m(k)), CP_m(k)) \mid CP_m(k) \epsilon\ CP_m\}$

As shown in the fig. 4.9 the membership function of each linguistic values are given, this can be converted into fuzzy set with the following membership function ranges stated bellow.

Form the fig. 4.9a) shows the universe of discourse of the input linguistic variable CP has [-8 15]. These input variables have linguistic values NB, NS, PS and PB. Thus each linguistic value also converted into fuzzy set triangular or trapezoidal MF stated in equation.4.25.

Therefore, for input linguistic variable CP:

$$\left.\begin{matrix}
\mu_{NB} = \begin{cases} 0 \ldots\ldots\ldots\ldots for CP \geq -1 \\ \dfrac{-(CP+1)}{7} \ldots\ldots\ldots\ldots for -8 \leq CP \leq -1 \\ 1 \ldots\ldots\ldots\ldots for CP \leq -8 \end{cases} \\
\mu_{NS} = \begin{cases} 0 \ldots\ldots\ldots\ldots for CP < -2, CP > 3 \\ \dfrac{CP+2}{2} \ldots\ldots\ldots\ldots for -2 \leq CP \leq 0 \\ \dfrac{-(CP-3)}{3} \ldots\ldots\ldots\ldots for 0 \leq CP \leq 3 \end{cases} \\
\mu_{PS} = \begin{cases} 0 \ldots\ldots\ldots\ldots for CP < 0, CP > 10 \\ \dfrac{CP}{5} \ldots\ldots\ldots\ldots for 0 \leq CP \leq 5 \\ \dfrac{10-CP}{5} \ldots\ldots\ldots\ldots for 5 \leq CP \leq 10 \end{cases} \\
\mu_{PB} = \begin{cases} 0 \ldots\ldots\ldots\ldots for CP < 6, CP > 15 \\ \dfrac{CP-6}{4} \ldots\ldots\ldots\ldots for 6 \leq CP \leq 10 \\ \dfrac{15-CP}{5} \ldots\ldots\ldots\ldots for 10 \leq CP \leq 15 \end{cases}
\end{matrix}\right\} \quad 4.25$$

Form the fig.4.9 b) the universe of discourse of the input linguistic variable CI has [-1 0.084]. These input variables have linguistic values NB, NS, PS and PB. Thus each linguistic value also converted into fuzzy set triangular and trapezoidal MF indicated in equation.4.26

Therefore, for input linguistic variable CI:

$$\left.\begin{matrix}
\mu_{NB} = \begin{cases} 0 \ldots\ldots\ldots\ldots\ldots\ldots\ldots\ldots . for CI \geq -0.02 \\ \dfrac{-100(CI+0.02)}{98} \ldots\ldots\ldots\ldots\ldots\ldots for -1 \leq CI \leq -0.02 \\ 1 \ldots\ldots\ldots\ldots\ldots\ldots\ldots\ldots\ldots for CI \leq -1 \end{cases} \\
\mu_{NS} = \begin{cases} 0 \ldots\ldots\ldots\ldots\ldots\ldots\ldots\ldots\ldots for CI < -0.5, CI > 0.0002 \\ 2(CI+0.5) \ldots\ldots\ldots\ldots\ldots\ldots\ldots for -0.5 \leq CI \leq 0 \\ -5000(CI-0.0002) \ldots\ldots\ldots\ldots\ldots\ldots . for 0 \leq CI \leq 0.0002 \end{cases} \\
\mu_{PS} = \begin{cases} 0 \ldots\ldots\ldots\ldots\ldots\ldots\ldots\ldots\ldots for CI < -0.01, CI > 0.0449 \\ 100(CI+0.01) \ldots\ldots\ldots\ldots\ldots\ldots\ldots\ldots .. for -0.01 \leq CI \leq 0 \\ \dfrac{-10000(CI-0.449)}{449} \ldots\ldots\ldots\ldots\ldots\ldots . for 0 \leq CI \leq 0.0449 \end{cases} \\
\mu_{PB} = \begin{cases} 0 \ldots\ldots\ldots\ldots\ldots\ldots\ldots\ldots\ldots for CI < 0.03 \\ \dfrac{1000(CI-0.03)}{54} \ldots\ldots\ldots\ldots\ldots\ldots\ldots for 0.03 \leq CI \leq 0.084 \\ 1 \ldots\ldots\ldots\ldots\ldots\ldots\ldots for CI > 0.08415 \end{cases}
\end{matrix}\right\} \quad 4.26$$

Similarly, form the fig. 4.9 c) the universe of discourse of the input linguistic variable CP_m has a range of [0 1657]. These input variables have linguistic values PS and PB. Thus each linguistic value also converted into fuzzy set triangular MF indicated in equation 4.27.

Therefore, for input linguistic variable CPm:

$$\left.\begin{array}{l}\mu_{PS}=\begin{Bmatrix}0.................................... for CP_m<0, CP_m>1657\\ \frac{CP_m}{300}.................................. for 0\le CP_m\le 300\\ \frac{800-CP_m}{500}............................ for 300\le CP_m\le 800\end{Bmatrix}\\ \mu_{PB}=\begin{Bmatrix}0.................................... for CP_m<400, CP_m>1657\\ \frac{CP_m-400}{750}................................ for 400\le CP_m\le 1150\\ \frac{1657-CP_m}{507}............................ for 10\le CP\le 15\end{Bmatrix}\end{array}\right\} \quad 4.27$$

Form the fig. 4.10 the universe of discourse of the output linguistic variable CD has [-0.008632 0.00091]. This output variables have linguistic values NB, NM, NS, PS, PM and PB. Thus each linguistic value also converted into fuzzy set similarly as done as for the input variables triangular and trapezoidal MF indicated in equation 4.28.

Therefore, for output linguistic variable CD:

$$
\left.\begin{array}{l}
\mu_{NB} = \begin{cases} 0 \ldots\ldots\ldots\ldots\ldots\ldots\ldots\ldots\ldots\ldots\ldots . for CD \geq -0.0001 \\ -117.2058(CD + 0.0001) \ldots\ldots\ldots for -0.008632 \leq CD \leq -0.0001 \\ 1 \ldots\ldots\ldots\ldots\ldots\ldots\ldots\ldots\ldots\ldots\ldots for CD \leq -0.008632 \end{cases} \\
\mu_{NM} = \begin{cases} 0 \ldots\ldots\ldots\ldots\ldots\ldots\ldots\ldots\ldots\ldots\ldots for CD < -0.003, CD > -0.0004 \\ 392.157(CD + 0.003) \ldots\ldots\ldots\ldots\ldots\ldots for -0.003 \leq CD \leq -0.00045 \\ -20000(CD + 0.0004) \ldots\ldots\ldots\ldots\ldots\ldots\ldots\ldots . for -0.00045 \leq CD \leq -0.0004 \end{cases} \\
\mu_{NS} = \begin{cases} 0 \ldots\ldots\ldots\ldots\ldots\ldots\ldots\ldots\ldots\ldots\ldots for CD < -0.0007, CD > 0.00015 \\ 1428.57(CD + 0.0007) \ldots\ldots\ldots\ldots\ldots\ldots\ldots\ldots\ldots for -0.0007 \leq CD \leq 0 \\ -\dfrac{100000(CD - 0.00015)}{15} \ldots\ldots\ldots\ldots\ldots\ldots\ldots . for 0 \leq CD \leq 0.00015 \end{cases} \\
\mu_{PS} = \begin{cases} 0 \ldots\ldots\ldots\ldots\ldots\ldots\ldots\ldots\ldots\ldots\ldots for CD < -0.0005, CD > 0.000499 \\ 1333.33(CD + 0.0005) \ldots\ldots\ldots\ldots\ldots\ldots\ldots for -0.0005 \leq CD \leq 0.00025 \\ -4016.06(CD - 0.000499) \ldots\ldots\ldots\ldots\ldots\ldots\ldots\ldots for 0.00025 \leq CD \leq 0.000499 \end{cases} \\
\mu_{PM} = \begin{cases} 0 \ldots\ldots\ldots\ldots\ldots\ldots\ldots\ldots\ldots\ldots\ldots for CD < 0.000317, CD > 0.00087 \\ 3535.569(CD - 0.000317) \ldots\ldots\ldots . for 0.000317 \leq CD \leq 0.0006 \\ \dfrac{-100000(CD - 0.00087)}{27} \ldots\ldots\ldots\ldots\ldots for 0.0006 \leq CD \leq 0.00087 \end{cases} \\
\mu_{PB} = \begin{cases} 0 \ldots\ldots\ldots\ldots\ldots\ldots\ldots\ldots\ldots\ldots\ldots for CD < 0.0006 \\ \dfrac{100000(CD - 0.0006)}{31} \ldots\ldots\ldots\ldots\ldots for 0.0006 \leq CD \leq 0.00091 \\ 1 \ldots\ldots\ldots\ldots\ldots\ldots\ldots\ldots\ldots\ldots\ldots for CD > 0.00091 \end{cases}
\end{array}\right\} \quad 4.28
$$

.

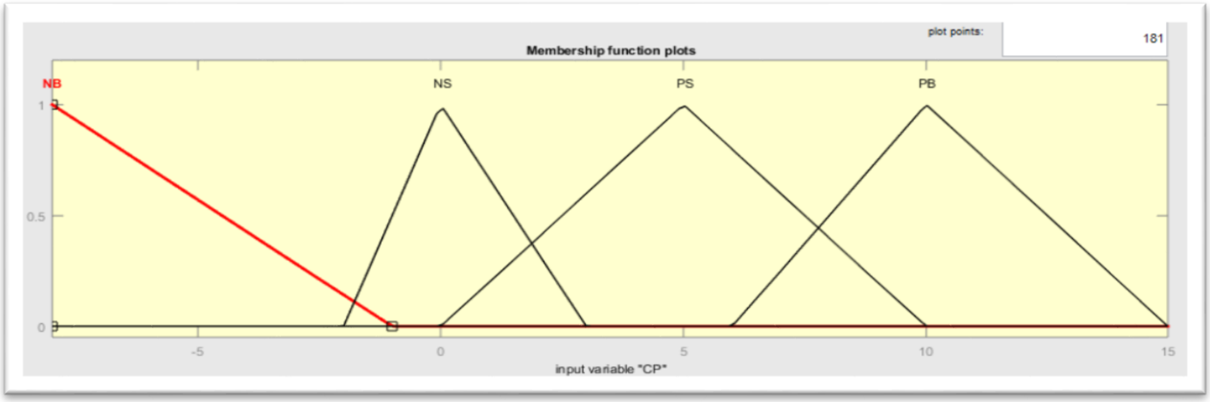

a

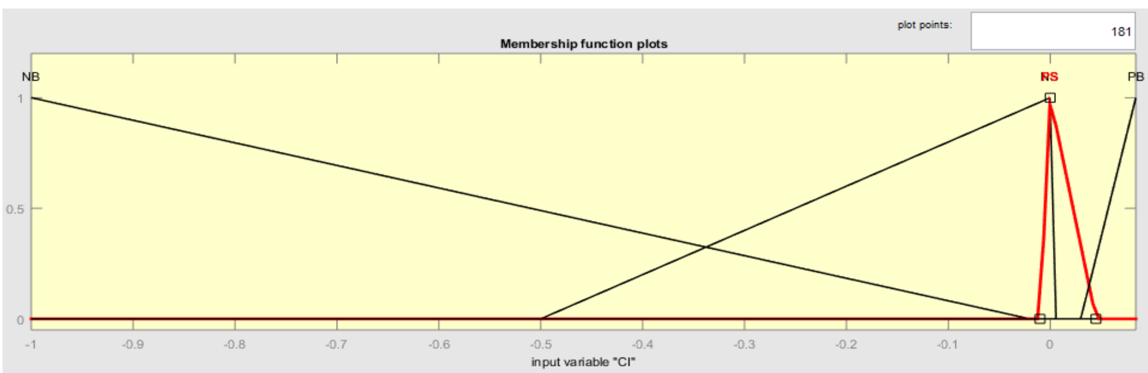

b

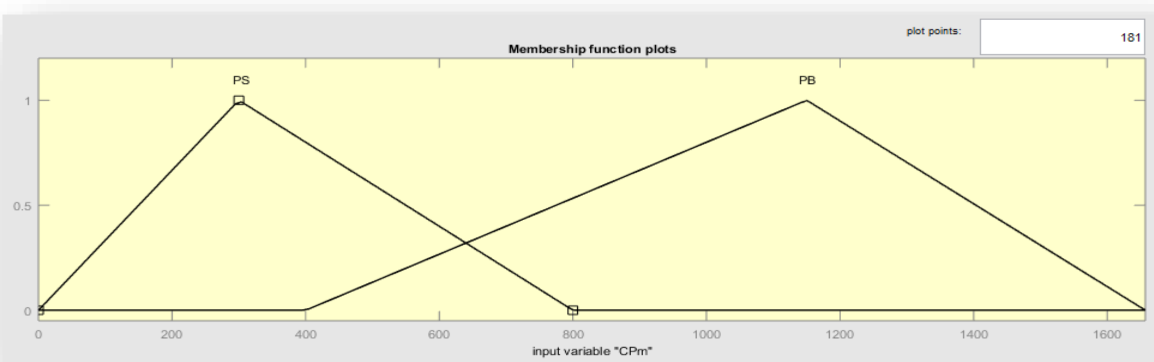

c

FIGURE 4.9 MEMBERSHIP FUNCTION OF a) CP, b) CI AND c) CP_m

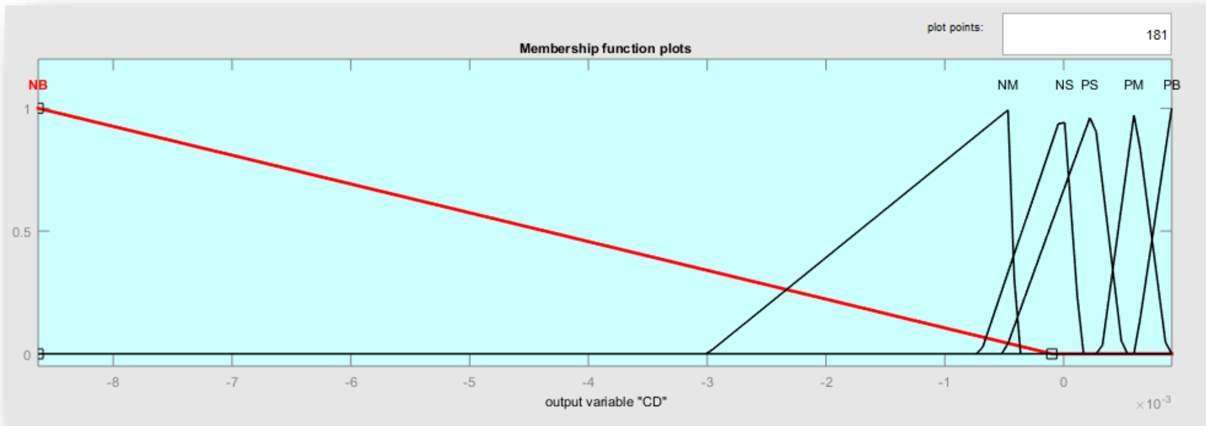

FIGURE 4.10 MEMBERSHIP FUNCTION CD

4.5.1.2 Fuzzy Inference Engine MPPT

As pointed in the previous chapter of this particular work, fuzzy rule base is a collection of IF……THEN rules that contain all the information for the controlled parameters. It is a set according to professional experience (or knowledge of the system) and the operation of the system control. To extract maximum possible power generated from the PV system, the fuzzy algorithm to be designed here contains 32 fuzzy control rules listed below in table 4.6.

Table 4.6 FLC Rules base

CP \ CI	NB	NS	PS	PB	CP_m
NB	PM	PM	NM	NM	PS
NS	PS	PS	NS	NS	
PS	NS	NS	PS	PS	
PB	NM	NM	PM	PM	
NS	PB	PB	PB	PB	PB
NB	PB	PB	PB	PB	
PS	PB	PB	PB	PB	
PB	PB	PB	PB	PB	

Where CP and CI are the universe of discourse of system defined by linguistic values NB, NS, PS, and PB by the fuzzy set on the range universe of discourse of CP and CI; and CP_m is the universe of discourse of system defined by linguistic values PS, and PB by the fuzzy set on the range universe of discourse, CP_m . Fuzzy rule base in table 4.7 can also be expressed in canonical form as:

- 1. If (CP is NB) and (CI is NB) and (CPm is PS) then (CD is PM) (1)
- 2. If (CP is NB) and (CI is NS) and (CPm is PS) then (CD is PM) (1)
- 3. If (CP is NB) and (CI is PS) and (CPm is PS) then (CD is NM) (1)
- 4. If (CP is NB) and (CI is PB) and (CPm is PS) then (CD is NM) (1)
- 5. If (CP is NS) and (CI is NB) and (CPm is PS) then (CD is PS) (1)
- 6. If (CP is NS) and (CI is NS) and (CPm is PS) then (CD is PS) (1)
- 7. If (CP is NS) and (CI is PS) and (CPm is PS) then (CD is NS) (1)
- 8. If (CP is NS) and (CI is PB) and (CPm is PS) then (CD is NS) (1)
- 9. If (CP is PS) and (CI is NB) and (CPm is PS) then (CD is NS) (1)
- 10. If (CP is PS) and (CI is NS) and (CPm is PS) then (CD is NS) (1)
- 11. If (CP is PS) and (CI is PS) and (CPm is PS) then (CD is PS) (1)
- 12. If (CP is PS) and (CI is PB) and (CPm is PS) then (CD is PS) (1)
- 13. If (CP is PB) and (CI is NB) and (CPm is PS) then (CD is NM) (1)
- 14. If (CP is PB) and (CI is NS) and (CPm is PS) then (CD is NM) (1)
- 15. If (CP is PB) and (CI is PS) and (CPm is PS) then (CD is PM) (1)
- 16. If (CP is PB) and (CI is PB) and (CPm is PS) then (CD is PM) (1)
- 17. If (CP is NB) and (CI is NB) and (CPm is PB) then (CD is PB) (1)
- 18. If (CP is NB) and (CI is NS) and (CPm is PB) then (CD is PB) (1)
- 19. If (CP is NB) and (CI is PS) and (CPm is PB) then (CD is PB) (1)
- 20. If (CP is NB) and (CI is PB) and (CPm is PB) then (CD is PB) (1)
- 21. If (CP is NS) and (CI is NB) and (CPm is PB) then (CD is PB) (1)
- 22. If (CP is NS) and (CI is NS) and (CPm is PB) then (CD is PB) (1)
- 23. If (CP is NS) and (CI is PS) and (CPm is PB) then (CD is PB) (1)
- 24. If (CP is NS) and (CI is PB) and (CPm is PB) then (CD is PB) (1)
- 25. If (CP is PS) and (CI is NB) and (CPm is PB) then (CD is PB) (1)
- 26. If (CP is PS) and (CI is NS) and (CPm is PB) then (CD is PB) (1)
- 27. If (CP is PS) and (CI is PS) and (CPm is PB) then (CD is PB) (1)
- 28. If (CP is PS) and (CI is PB) and (CPm is PB) then (CD is PB) (1)
- 29. If (CP is PB) and (CI is NB) and (CPm is PB) then (CD is PB) (1)
- 30. If (CP is PB) and (CI is NS) and (CPm is PB) then (CD is PB) (1)
- 31. If (CP is PB) and (CI is PS) and (CPm is PB) then (CD is PB) (1)

- 32. If (CP is PB) and (CI is PB) and (CPm is PB) then (CD is PB) (1)

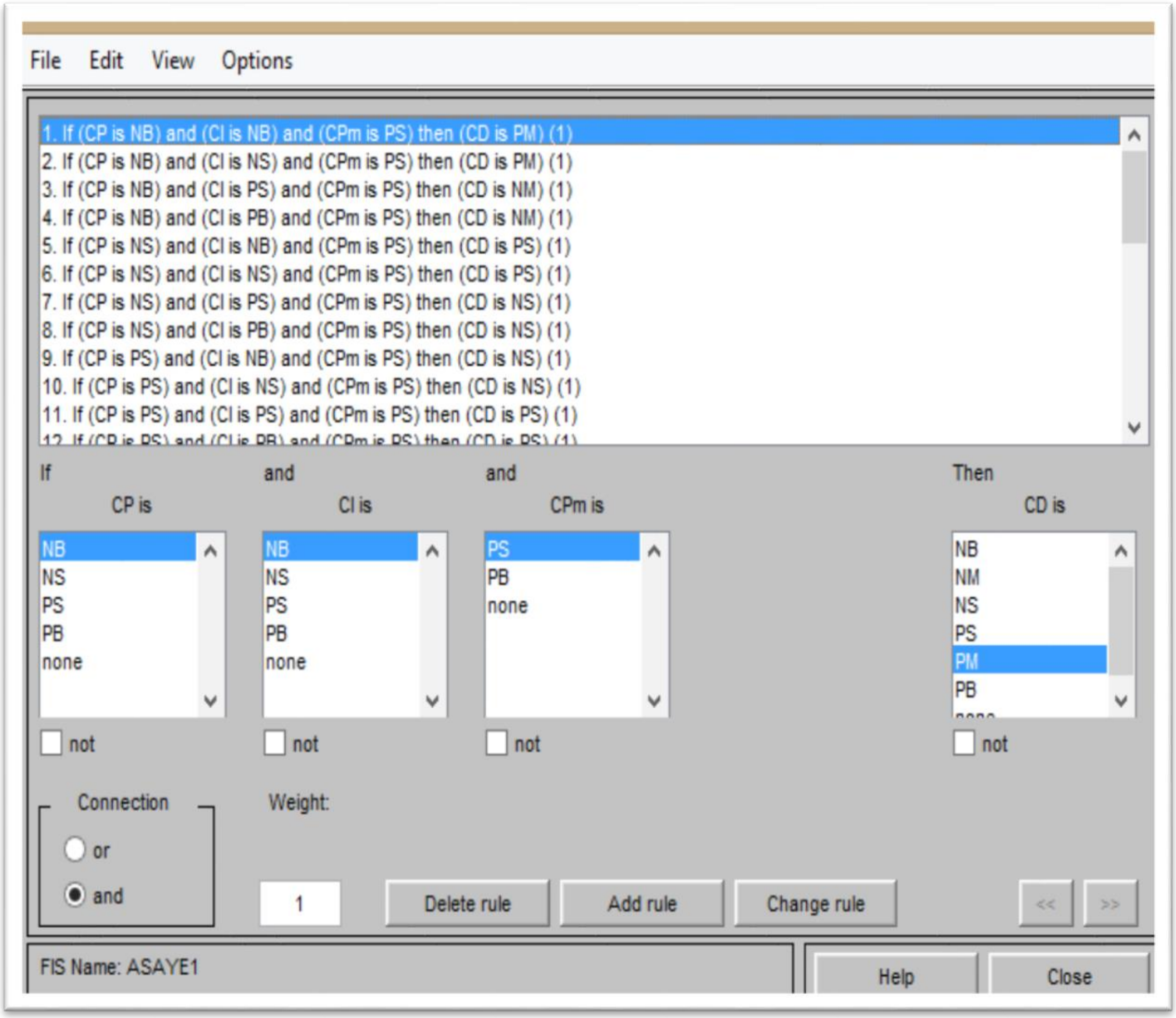

FIGURE 4.11 FUZZY RULE VIEWERS IMPLEMENTED IN MATLAB2015A

The canonical form Rules established from table 4.7 is implemented in the MATLAB 15a in order to track the maximum power point of the PV system for any shading patterns just as shown in the fig. 4.11 above as a rule viewer.

4.5.1.3 Defuzzification MPPT

Defuzzification evaluates the rules based on a set of control actions for a given fuzzy inputs set. This operation converts the inferred fuzzy control action into a crisp value at the output by forming the union of the outputs resulting from each rule. The center of area algorithm is used for defuzzification. Fig. 4.10 shows fuzzy membership of output CD.

Table 4.7 sample data taken from the proposed uncontrolled system in fig. 4.7

CI	-0.0121	-0.01868	-0.0038	0.031694	0.013284	-0.16736	-0.01363	0.081589	-0.05098
CP	0.6837	-1.7506	45.46	3.041493	1.243224	-11.01848	98.53456	7.783766	-4.79525
CPm	381	433.33	910.08	492.1608	471.5818	362.892	1558.465	484.3927	478.1277
CD	-0.000302	0.002359	-0.00559	0.000334	0.000147	-0.000951	-0.008631	0.0008715	-0. 00056

The crisp inputs of the system are found to be CI=0.0316947, CP=3.0414938, and CPm=492.16 are taken from uncontrolled system in table 4.8 column five with green paint .Then thus the crisp input vales of each input linguistic variables must be fuzzified in to fuzzy sets corresponding to their membership function.

For linguistic variable CP, crisp input to the system CP=0.6837, this is pass through MF negative small with fuzzy set with MF of $\frac{-(CP-3)}{3}$........ $for 0 \le CP \le 3$ and Positive small with fuzzy set of $\frac{CP}{5}$..... $for 0 \le CP \le 5$. i.e. $\mu_{NS,CP}(CP = 0.6837) = \frac{-(CP-3)}{3} = \frac{-(0.6837-3)}{3} = 0.7721$, and $\mu_{PS,CP}(CP = 0.6837) = \frac{CP}{5} = \frac{0.6837}{5} = 0.613674$.

For linguistic variable CP, crisp input to the system CP=-1.7506, this is pass through MF negative big with fuzzy set with MF of $\frac{-(CP+1)}{7}$... $for -8 \le CP \le -1$ and negative small with fuzzy set of $\frac{CP+2}{2}$... $for -2 \le CP \le 0$.

i.e. $\mu_{NB,CP}(CP=-1.7506=)\frac{-(CP+1)}{7}=\frac{-(-1.7506+1)}{7}=0.10722$,and

$\mu_{NS,CP}(CP=-1.7506=)\frac{(CP+2)}{2}=\frac{(-1.7506+2)}{2}=0.1247$

For linguistic variable CP, crisp input to the system CP=45.46, this is pass through MF positive big with fuzzy set with MF of $0....forCP<6, CP>15$. i.e. $\mu_{PB,CP}(CP=45.46)=0$

For linguistic variable CP, crisp input to the system CP=3.04149, this is pass through MF Positive small with fuzzy set of $\frac{CP}{5}...for 0 \le CP \le 5$.

i.e. $\mu_{PS,CP}(CP=0.6837)=\frac{CP}{5}\frac{0.6837}{5}=0.608298$

For linguistic variable CP, crisp input to the system CP=1.24322, this is pass through MF negative small with fuzzy set with MF of $\frac{-(CP-3)}{3}....for 0 \le CP \le 3$ and Positive small with fuzzy set of $\frac{CP}{5}......for 0 \le CP \le 5$.

i.e. $\mu_{NS,PS}(CP=1.24322)=\frac{-(CP-3)}{3}=\frac{-(1.24322-3)}{3}=0.58559$,and

$\mu_{PS,CP}(CP=1.24322)=\frac{CP}{5}=\frac{1.24322}{5}=0.248644$

For linguistic variable CP, crisp input to the system CP= -11.01848, this is pass through MF negative big with fuzzy set with MF of $1.....forCP \le -8$ i.e. $\mu_{NB,CP}(CP=-11.01848)=1$.

For linguistic variable CP, crisp input to the system CP=98.5345636, this is pass through MF positive big with fuzzy set with MF of $0....forCP<6, CP>15$ .i.e. $\mu_{PB,CP}(CP=98.5345636)=0$.

For linguistic variable CP, crisp input to the system CP=7.783766, this is pass through MF positive small with fuzzy set with MF of $\frac{10-CP}{5} .... for 5 \leq CP \leq 10$, and Positive big with fuzzy set of $\frac{CP-6}{4} ..... for 6 \leq CP \leq 10$.

i.e. $\mu_{PS,CP}(CP = 7.783766) = \frac{10-CP}{5} = \frac{10-7.783766}{5} = 0.44324$,and

$\mu_{PB,CP}(CP = 7.783766) = \frac{CP-6}{4} = \frac{7.783766-6}{4} = 0.44594$.

For linguistic variable CP, crisp input to the system CP=4.79524, this is pass through MF positive small with fuzzy set with MF of $\frac{CP}{5} ..... for 0 \leq CP \leq 5$

i.e. $\mu_{PS,CP}(CP = 4.79524) = \frac{CP}{5} = \frac{4.79524}{5} = 0.959$.

The each crisp inputs CI given in table 4.8 is also converted into fuzzy set pairs as the same fashion above for CP using fuzzy MF of CI given in equation 4.26.

For linguistic variable CI, crisp input to the system CI=-0.0121, this is pass through MF negative small with fuzzy set with MF of $2(CI + 0.5) ..... for -0.5 \leq CI \leq 0$. i.e. $\mu_{NS,CI}(CI = -0.0121) = 2(CI + 0.5) = 2(-0.0121 + 0.5) = 0.9758$.

For linguistic variable CI, crisp input to the system CI=--0.01868, this is pass through MF negative small with fuzzy set with MF of $2(CI + 0.5) ..... for -0.5 \leq CI \leq 0$. i.e. $\mu_{NS,CI}(CI = -0.01868) = 2(CI + 0.5) = 2(-0.01868 + 0.5) = 0.96264$.

For linguistic variable CI, crisp input to the system CI= - 0.0038, this is pass through MF negative small with fuzzy set with MF of $2(CI + 0.5) ..... for -0.5 \leq CI \leq 0$ and Positive small with fuzzy set of MF of $100(CI + 0.01) .... for -0.01 \leq CI \leq 0$ i.e. $\mu_{NS,CI}(CI = -0.0038) = 2(CI + 0.5) = 2(-0.0038 + 0.5) = 0.9924$ and

$\mu_{PS,CI}(CI = 0 - 0.0038) = 100(CI + 0.01) = 100(-0.0038 + 0.01) = 0.62$.

For linguistic variable CI, crisp input to the system CI=0.0316947, this is pass through MF positive small with fuzzy set with MF of $\frac{-10000(CI-0.449)}{449}.....for 0 \le CI \le 0.0449$ and Positive big with fuzzy set of MF of $\frac{1000(CI-0.03)}{54}.....for 0.03 \le CI \le 0.084$. i.e.

$$\mu_{PS,CI}(CI=0.0316947)=\frac{-10000(CI-0.449)}{449}=\frac{-10000(0.0316947-0.449)}{499}=0.2941 \text{and}$$

$$\mu_{PB,CI}(CI=0.0316947)=\frac{1000(CI-0.03)}{54}=\frac{1000(0.0316947-0.03)}{54}=0.0313833.$$

For linguistic variable CI, crisp input to the system CI=0.013284634, this is pass through MF positive small with fuzzy set with MF of $\frac{-10000(CI-0.449)}{449}.....for 0 \le CI \le 0.0449$. i.e.

$$\mu_{PS,CI}(CI=0.013284634)=\frac{-10000(CI-0.449)}{449}=\frac{-10000(0.013284634-0.449)}{499}=0.70412.$$

For linguistic variable CI, crisp input to the system CI=-0.167365, this is pass through MF negative big with fuzzy set of MF of $\frac{-100(CI+0.02)}{98}......for -1 \le CI \le -0.02$ and negative small with fuzzy set with MF of $2(CI+0.5).....for -0.5 \le CI \le 0$. i.e.

$$\mu_{NB,CI}(CI=0.167365)=\frac{-100(CI+0.02)}{98}=\frac{-100(0.167365+0.02)}{98}=0.15037 \text{and}$$

$$\mu_{NS,CI}(CI=0.167365)=2(CI+0.5)=2(0.167365+0.5)=0.66527.$$

For linguistic variable CI, crisp input to the system CI=-0.0136296, this is pass through MF negative small with fuzzy set with MF of $2(CI+0.5).....for -0.5 \le CI \le 0$.

i.e. $\mu_{NS,CI}(CI=0.0136296)=2(CI+0.5)=2(0.0136296+0.5)=0.97274.$

For linguistic variable CI, crisp input to the system CI=0.081589, this crisp value is pass through MF positive big with fuzzy set with MF of $\frac{1000(CI-0.03)}{54}.....for 0.03 \le CI \le 0.084$. i.e.

$$\mu_{PB,CI}(CI=0.081589)=\frac{1000(CI-0.03)}{54}=\frac{1000(0.081589-0.03)}{54}=0.95535.$$

For linguistic variable CI, crisp input to the system CI= -0.050984166, this is pass through MF negative big with fuzzy set of MF of $\frac{-100(CI+0.02)}{98}.....for -1 \le CI \le -0.02$ and negative small with fuzzy set with MF of $2(CI+0.5).....for -0.5 \le CI \le 0$.i.e.

$$\mu_{PB,CI}(CI=-0.050984166)=\frac{-100(CI+0.02)}{98}=\frac{-100(-0.050984166+0.02)}{98}=0.0316 \text{ and}$$

$$\mu_{NS,CI}(CI=-0.050984166)=2(CI+0.5)=2(-0.050984166)=0.898.$$

Similarly, each crisp inputs CPm given in table 4.8 is also converted into fuzzy set pairs with the same terminology above like CP using fuzzy MF of CI given in equation 4.27.

For linguistic variable CPm, crisp input to the system CPm=381, this is pass through MF positive small with fuzzy set of MF of $\frac{800-CP_m}{500}......for 300 \le CP_m \le 800.$ i.e.

$$\mu_{PS,CP_m}(CP_m=381)=\frac{800-CP_m}{500}=\frac{800-381}{500}=0.838.$$

For linguistic variable CPm, crisp input to the system CPm=433.33, this is pass through MF positive small with fuzzy set of MF of $\frac{800-CP_m}{500}......for 300 \le CP_m \le 800$ and positive big with fuzzy set with MF of $\frac{CP_m-400}{750}.....for 400 \le CP_m \le 1150.$

i.e. $\mu_{PS,CP_m}(CP_m=433.33)=\frac{800-CP_m}{500}=\frac{800-433.33}{500}=0.73334.$ and

$$\mu_{PB,CP_m}(CP_m=433.33)=\frac{CP_m-400}{750}=\frac{433.33-400}{750}=0.04444.$$

For linguistic variable CPm, crisp input to the system CPm=910.08, this is pass through MF positive big with fuzzy set with MF of $\frac{CP_m-400}{750}.....for 400 \le CP_m \le 1150$.i.e.

$$\mu_{PB,CP_m}(CP_m=910.08)=\frac{CP_m-400}{750}=\frac{910.08-400}{750}=0.6801.$$

For linguistic variable CPm, crisp input to the system CPm=492.16, this is pass through MF positive small with fuzzy set of MF of $\frac{800-CP_m}{500}.....for 300 \leq CP_m \leq 800$ and positive big with fuzzy set with MF of $\frac{CP_m-400}{750}.....for 400 \leq CP_m \leq 1150.$

i.e. $\mu_{PS,CP_m}(CP_m = 492.16) = \frac{800-CP_m}{500} = \frac{800-492.16}{500} = 0.61568$ and

$\mu_{PB,CP_m}(CP_m = 492.16) = \frac{CP_m-400}{750} = \frac{492.16-400}{750} = 0.12288.$

For linguistic variable CPm, crisp input to the system CPm=471.5818, this is pass through MF positive small with fuzzy set of MF of $\frac{800-CP_m}{500}.....for 300 \leq CP_m \leq 800$ and positive big with fuzzy set with MF of $\frac{CP_m-400}{750}.....for 400 \leq CP_m \leq 1150.$

i.e. $\mu_{PS,CP_m}(CP_m = 471.5818) = \frac{800-CP_m}{500} = \frac{800-471.5818}{500} = 0.65683$ and

$\mu_{PB,CP_m}(CP_m = 471.5818) = \frac{CP_m-400}{750} = \frac{471.5818-400}{750} = 0.09544.$

For linguistic variable CPm, crisp input to the system CPm=362.892, this is pass through MF positive small with fuzzy set of MF of $\frac{800-CP_m}{500}.....for 300 \leq CP_m \leq 800.$ i.e.

$\mu_{PS,CP_m}(CP_m = 362.892) = \frac{800-CP_m}{500} = \frac{800-362.892}{500} = 0.8742.$

For linguistic variable CPm, crisp input to the system CPm=1558.465, this is pass through MF positive big with fuzzy set with MF of $\frac{1657-CP_m}{507}.....for 10 \leq CP \leq 15.$ i.e.

$\mu_{PB,CP_m}(CP_m = 1558.46) = \frac{1657-CP_m}{507} = \frac{1657-1558.465}{507} = 0.194349.$

For linguistic variable CPm, crisp input to the system CPm=484.39, this is pass through MF positive small with fuzzy set of MF of $\frac{800-CP_m}{500}.....for 300 \leq CP_m \leq 800$ and positive big with fuzzy set with MF of $\frac{CP_m-400}{750}.....for 400 \leq CP_m \leq 1150.$

i.e. $\mu_{PS,CP_m}(CP_m = 484.39) = \frac{800 - CP_m}{500} = \frac{800 - 484.39}{500} = 0.63122$ and

$\mu_{PB,CP_m}(CP_m = 484.39) = \frac{CP_m - 400}{750} = \frac{484.39 - 400}{750} = 0.11252.$

For linguistic variable CPm, crisp input to the system CPm=478.1277, this is pass through MF positive small with fuzzy set of MF of $\frac{800 - CP_m}{500} ..... for 300 \le CP_m \le 800$ and positive big with fuzzy set with MF of $\frac{CP_m - 400}{750} ..... for 400 \le CP_m \le 1150.$

i.e. $\mu_{PS,CP_m}(CP_m = 478.1277) = \frac{800 - CP_m}{500} = \frac{800 - 478.1277}{500} = 0.643744$ and

$\mu_{PB,CP_m}(CP_m = 478.1277) = \frac{CP_m - 400}{750} = \frac{478.1277 - 400}{750} = 0.10417.$

Each crisp outputs CD given in table 4.8 is also converted into fuzzy set pairs with the same terminology above like crisp inputs given in equation 4.28.

For linguistic variable CD, crisp input to the system CD=-0.000302, this is pass through MF negative big with fuzzy set of MF of $-117.2058(CD + 0.0001).... for -0.008632 \le CD \le -0.0001$, negative small with fuzzy set with MF of $1428.57(CD + 0.0007)..... for -0.0007 \le CD \le 0$, and positive small with fuzzy set with MF of $1333.33(CD + 0.0005)..... for -0.0005 \le CD \le 0.00025$. i.e.

$\mu_{NB,CD}(CD = 0.000302) = -117.2058(CD + 0.0001) = -117.2058(0.000302 + 0.0001) = 0.0236755,$

$\mu_{NS,CD}(CD = 0.000302) = 1428.57(0.000302 + 0.0007) = 0.56857,$ and

$\mu_{PS,CD}(CD = 0.000302) = 1333.33(0.000302 + 0.0005) = 0.2639999.$

For linguistic variable CD, crisp input to the system CD=0.0002359, this is pass through MF positive small with fuzzy set with MF of $1333.33(CD + 0.0005)..... for -0.0005 \le CD \le 0.00025.$ .i.e.

$\mu_{PS,CD}(CD = 0.0002359) = 1333.33(0.0002359 + 0.0005) = 0.9812.$

For linguistic variable CD, crisp input to the system CD=-0.00559, this is pass through MF negative big with fuzzy set with MF of $-117.2058(CD + 0.0001).... for -0.008632 \le CD \le -0.0001$.i.e.

$\mu_{NB,CD}(CD = -0.00559) = -117.2058(CD + 0.0001) = -117.2058(-0.00559 + 0.0001) = 0.6434598$

For linguistic variable CD, crisp input to the system CD=0.00033456, this is pass through MF positive small with fuzzy set of MF o $-4016.06(CD - 0.000499).... for 0.00025 \le CD \le 0.000499,$

and positive medium with fuzzy set with MF of $3535.569(CD-0.000317)..........for 0.000317 \le CD \le 0.0006$. i.e.

$\mu_{PS,CD}(CD=0.00033456)=-4016.06(0.00033456-0.000499)=0.6604$ and

$\mu_{PM,CD}(CD=0.00033456)=3535.569(0.00033456-0.000317)=0.06208$.

For linguistic variable CD, crisp input to the system CD=0.00014757, this is pass through MF negative small with fuzzy set with MF of $-\frac{100000(CD-0.00015)}{15}......for 0 \le CD \le 0.00015$, and positive small with fuzzy set with MF of. $1333.33(CD+0.0005)......for -0.0005 \le CD \le 0.00025$,i.e.

$\mu_{NS,CD}(CD=0.00014757)=-\frac{100000(CD-0.00015)}{15}=-\frac{100000(0.00014757-0.00015)}{15}=0.016$,

and $\mu_{PS,CD}(CD=0.00014757)=1333.33(0.00014757+0.0005)=0.8634245$

Therefor the crisp input to fuzzy value for each linguistic variables are summarized as follows:

I, The fuzzy sets to linguistic variable cp for uncontrolled PV systems given in table 4.8.

NB(cp)={(0.10722,-1.7506);(1,-11.01848)}

NS(cp)={(0.7721,0.6837);(0.1447,1.7506);(0.58559,1.24322)}

PS(cp)={(0.13674,0.6837);(0.608298,3.04149);(0.248644,1.24322);(0.44324,7.783766);(0.959,4.79524)}

PB(cp)={(0,45.45);(0,98.5345636);(0.44594,7.7833766)}

II. The fuzzy sets to linguistic variable ci for uncontrolled PV systems given in table 4.8.

NB(ci)={(0.15037,-0.167365);(0.0316,-0.05098416)}

NS(ci)={(0.9758,-0.0121);(0.9624,-0.01868);(0.9924,-0.0038);(0.66527,-0.167365);(0.97274,-0.0136296);(0.898,-0.050984166)}

PS(ci)={(0.62,-0.0038);(0.2941,0.0316947);(0.70412,0.013284634)}

PB(ci){(0.0313833,0.0316947);(0.95535,0.081589)}

III. The fuzzy sets to linguistic variable CP_m for uncontrolled PV systems given in table 4.8.

PS(CPm)={(0.838,381);(0.73334,433.33);(0.61568,492.16);(0.65683,471.5818);(0.8742,362.892);(0.63122,484.39);(0.643744,478.1277)}

PB(cp_m)={(0.04444,433.33);(0.6801,910.08);(0.12288,492.16);(0.09544,471.5818);(0.194349,1558.465);(0.11252,484.39);(0.10417,478.1277)}

Step 1: determine the activation degrees of the antecedent parts of rules FR1 to FR32 at for each particular point:

For the crisp inputs (0.6837,-0.0121, 380) the following fuzzy relations are drawn:

6. (CP is NS) and (CI is NS) and (CPm is PS)

10. (CP is PS) and (CI is NS) and (CPm is PS)

μ_{R_6}(0.6837,-0.0121, 380)= $\min[\mu_{NS}(0.6837), \mu_{NS}(-0.0121), \mu_{PS}(380)]$

μ_{R_6}(0.6837,-0.0121, 380)= min [0.7721, 0.97558, 0.838] =0.7721

$\mu_{R_{10}}$(0.6837,-0.0121, 380)= $\min[\mu_{PS}(0.6837), \mu_{NS}(-0.0121), \mu_{PS}(380)]$

$\mu_{R_{10}}$(0.6837,-0.0121, 380)=min [0.13674, 0.97558, 0.838] =0.13674

Step 2: applying the Mamdani (*min*) implication, activation degrees of the consequent parts of rules FR^6 and FR^{10} become:

μ_{FR^6}(0.6837,-0.0121, 380, u)= $\min[\mu_{R_6}(0.6837, -0.0121, 380), \mu_{CD}(CD)]$

For linguistic variable CP, crisp input to the system CP=3.04149, this is pass through MF of positive small with fuzzy set with MF of $\mu_{PS}(CP = 3.04149) = \frac{CP}{5}..... for 0 \le CP \le 5.$

Therefore, $\mu_{PS}(CP = 3.04149) = \frac{3.04148}{5} = 0.608298$

Similarly, fuzzy set for the corresponding crisp value of input CI=0.0316947

$$\mu_{PS}(CI = 0.0316947) = \frac{-10000(CI - 0.449)}{449} = \frac{-10000(0.0316947 - 0.449)}{499} = 0.2941$$

$$\mu_{PB,CI}(CI = 0.0316947) = \frac{1000(CI - 0.03)}{54} = \frac{1000(0.0316947 - 0.03)}{54} = 0.0313833$$

Similarly, fuzzy set for the corresponding crisp value of input CPm=492.16

$$\mu_{PS,CP_m}(CP_m = 492.16) = \frac{800 - CP_m}{500} = \frac{800 - 492.16}{500} = 0.61568$$

$$\mu_{PB,CP_m}(CP_m = 492.16) = \frac{CP_m - 400}{750} = \frac{492.16 - 400}{750} = 0.12288$$

Fuzzy set for the corresponding crisp value of output CD=0.00033456 is calculated using MF of CD defined in equation 4.28 as follows:

$$\mu_{PS,CD}(CD = 0.00033456) = -4016.06(0.00033456 - 0.000499) = 0.6604$$

$$\mu_{PM,CD}(CD = 0.00033456) = 3535.569(0.00033456 - 0.000317) = 0.06208.$$

The next step is to define the rule-base that maps the inputs CI, CP and CPm to the output *CD,* which is defined by the fuzzy set in the above step using the rules table 4.7 for these particular specific points.

If CP is PS and CI is PS and CPm is PS THEN CD is PS

$$\mu_{R_{CP,CI,CP_m}}(3.04149, 0.0316947, 492.16) = Min\left(\mu_{CP}(3.04149), \mu_{CI}(0.03169), \mu_{CP_m}(492.16)\right)$$

$$\mu_{R_{CP,CI,CP_m}}(3.04149, 0.0316947, 492.16) = Min\begin{pmatrix}\mu_{PS}(CP = 3.04149), \mu_{PS}(CI = 0.03169), \\ \mu_{PS}(CP_m = 492.16)\end{pmatrix}$$

$$\mu_{R_{CP,CI,CP_m}}(3.04149, 0.0316947, 492.16) = Min(0.608298, 0.2941, 0.61568) = 0.2941$$

Finally, the fuzzy inference of this fuzzy rule is given as follows:

$$\mu_{FR^{11}}(3.04149, 0.0316947, 292.16, \mu_{CD}) = Min\left(\mu_{R_{11}}(3.04149, 0.0316947, 492.16)\right)$$

If CP is PS and CI is PB and CPm is PB THEN CD is PB

$$\mu_{R_{CP,CI,CP_m}}(3.04149, 0.0316947, 492.16) = Min\left(\mu_{PS,CP}(3.04149), \mu_{PB,CI}(0.03169), \mu_{PB,CP_m}(492.16)\right)$$

$$\mu_{R_{CP,CI,CP_m}}(3.04149, 0.0316947, 492.16) = Min\begin{pmatrix}\mu_{PS}(CP = 3.04149), \mu_{PB}(CI = 0.03169), \\ \mu_{PB}(CP_m = 492.16)\end{pmatrix}$$

$$\mu_{R_{CP,CI,CP_m}}(3.04149, 0.0316947, 492.16) = Min(0.608298, 0.316947, 0.12288) = 0.12288$$

4.6 P&O MPPT

P&O algorithm is the conventional maximum power tracking system and functioning based on the "hill climbing" method. It is also very popular and most commonly used in practice because of its simplicity in algorithm and ease of implementation. Additionally, it is the most efficient MPPT algorithm at uniform shade condition, but when partial shading occurred at the surface of the array its tracking potential going poor. In this research, P&O algorithm was proposed along with FLC for comparison.

It can be seen From P-V characteristics curve in fig. 4.11, the voltage and power are increasing from point A to point B, the converse is true for point B to A; and power from point C to point B increases, voltage decreases from point B to point C, power decreases and voltage incrementing. P&O algorithm is initiated by applying the perturbed voltage, ΔV to change the operating condition of the PV array. This is achieved by changing duty cycle of boost converter, increases (decreases) the power when operating on the left of the MPP and decreases (increases) the power when on the right of the MPP. Therefore, if there is an increase in power, the subsequent perturbation should be kept the same to reach the MPP and if there is a decrease in power, the perturbation should be reversed. The change of output power at the present and the previous sampling interval is subsequently compared. Based on the instantaneous output power of the two sampling intervals, the MPPT control system can decide to regulate the PV array to be operated either at larger or lower operating voltage. The PV array will pursue numerous of iteration process but eventually the PV system will be operated at a particular optimum power point. At this stage, PV array will be generating maximum output power. Fig. 4.13 shows the flowchart of this algorithm [114]-[115].

Table 4.8 Conditions for the operation of p&o algorithm

Case	**Condition**	**Action on PV array**	Duty cycle
I	$Pk>Pk-1$ and $Vk>Vk-1$	Operating voltage is increased by ΔV	Decrease
II	$Pk>Pk-1$ and $Vk<Vk-1$	Operating voltage is decreased by ΔV	Increase
III	$Pk<Pk-1$ and $Vk>Vk-1$	Operating voltage is decreased by _V	Increase
IV	$Pk<Pk-1$ and $Vk<Vk-1$	Operating voltage is increased by _V	Decrease

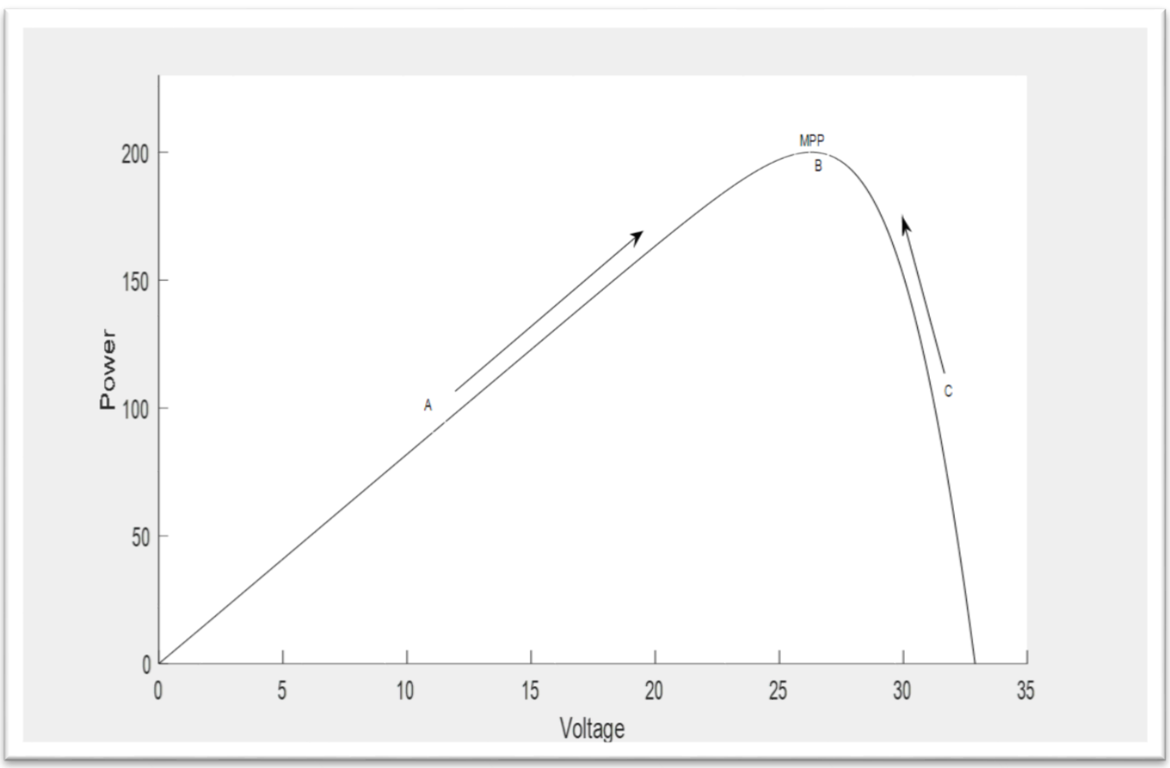

FIGURE 4.12 P-V CURVE OF PV MODULE AT 1000 W/M2 AND 25OC

There are some limitations that reduce its MPPT efficiency. First, it cannot determine when it has actually reached the MPP. Instead, it oscillates the operating point around the MPP after each cycle and slightly reduces PV efficiency under the constant irradiance condition. Second, it can fail under in cases of rapidly changing atmospheric conditions as a result of moving clouds and under the conditions of partial shade [114].

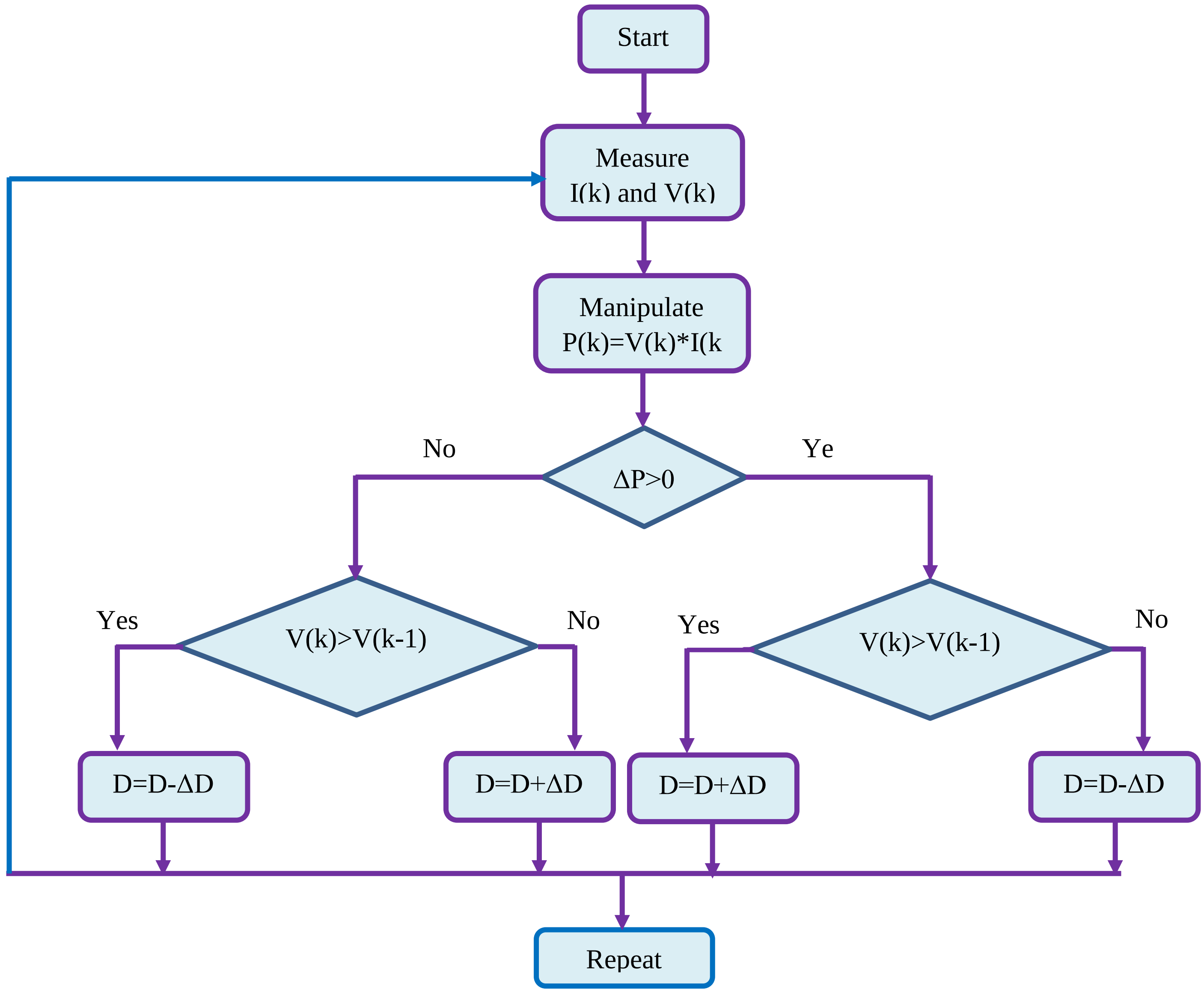

FIGURE 4.13 P&O ALGORITHM FLOWCHART

The performance of the algorithm is affected by the choice of the magnitude (ΔD) of the converter switching duty cycle. Large perturbations cause large output power fluctuations around the MPP while small perturbations slow down the algorithm [114]-[116]. This limitation can be overcome by FLC system.

CHAPTER 5

SIMULATION AND DISCUSION OF RESULTS

5.1 Simulation results

This chapter shows MATLAB2015a simulations perform comparative tests between the P&O, fuzzy MPPT algorithm with direct coupling of PV system. Simulations verify the functionality of MPPT with a resistive load. Some selected results are presented which show the simulation results of PV and load, with operating point at 305.15K temperature and for uniform 4211 $\frac{W}{m^2}$ irradiance and three shading patterns shown in fig.5.1.

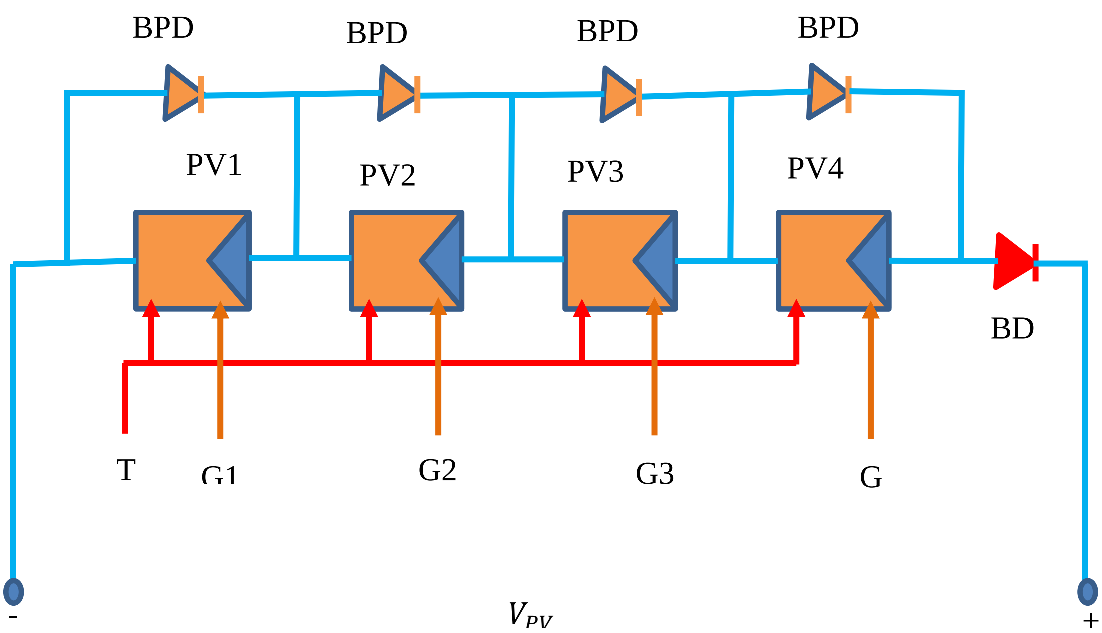

FIGURE 5.1 THE PROPOSED SYSTEM CONFIGURATION

In this section, the simulations were performed on a PV system for comparing the MPPT algorithms in terms of their efficiency, harmonic oscillation based on simulations in the MATLAB/Simulink software. The comparison results are summarized in a table. The PV system used in the simulations is shown in Fig. 5.3. This system consists of four KC200GT solar module which provides a maximum power of 3190 W, a DC–DC boost converter operating at 25 kHz, a filter inductance of 742.588 µH, a filter capacitor of 48.579 µF and a resistive load of 32.2 Ω. The input of the power converter is connected to the PV panel, the output is connected to the resistive load and the control signal generated by each MPPT technique fed to a PWM for controlling the boost converter's ideal switches. The system was simulated in MATLAB/SIMULINK 2015a software environment. When one or more of the PV cell is shaded in PV system then it can act as an electrical load. This shaded PV cells or string absorbs an important quantity of electrical energy generated by other normal PV cells receiving high irradiation and converting into heat. This physical phenomenon is kwon to be hotspot. This condition can be solved by the addition of bypass diode between specific number of cells or modules in series circuits as fig. 5.1.

5.2 Simulation results of PV generation for various shading pattern (SP) without MPPTs

In this particular section of the thesis PV generation system is simulated in MATLAB2015a for various weather conditions. The PV system is configured from 4 KC200GT PV modules in series connections. As shown in the fig. 5.1 above, each PV modules has get different solar radiations and evaluates the performance of the proposed system for different shading patterns. Hence the proposed MPPT in this thesis is mainly proposed for SP4 with blue P-V curve given in the fig. 5.2. However, the system is going to be tested for SP1, SP2 and SP3 to check the flexibility of the proposed system for varying weather condition.

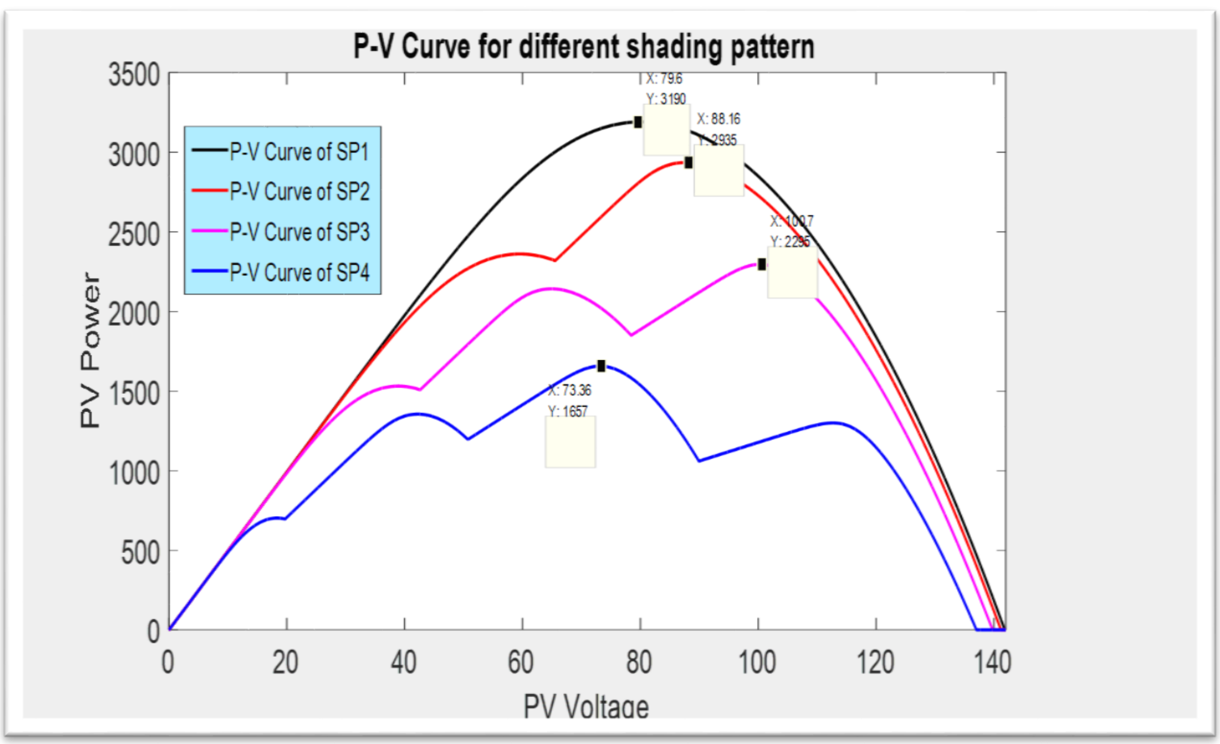

FIGURE 5.2 POWER GENERATED FROM THE PV SYSTEM FOR DIFFERENT SHADING PATTERNS

As just seen from fig. (5.2) the capacity of PV system generation is different for different shading patterns. The PV system has generates a maximum power of 3190.175W under SP1 (or uniformly shaded system) with one maximum peak (GMPP); 2935.2W under SP2 with one LMPP and one GMPP; 2295.3W under SP3 with two LMPP and one GMPP; and 1656.7W under SP4 with three LMPP and one GMPP. An efficient MPPT has been proposed to extract these maximum powers with the fastest steeling time to reach GMPP and low oscillation around the steeling time and after steady state.

5.3 Simulation of PV generation under partial shade with FLC MPPT and P&O MPPT controller

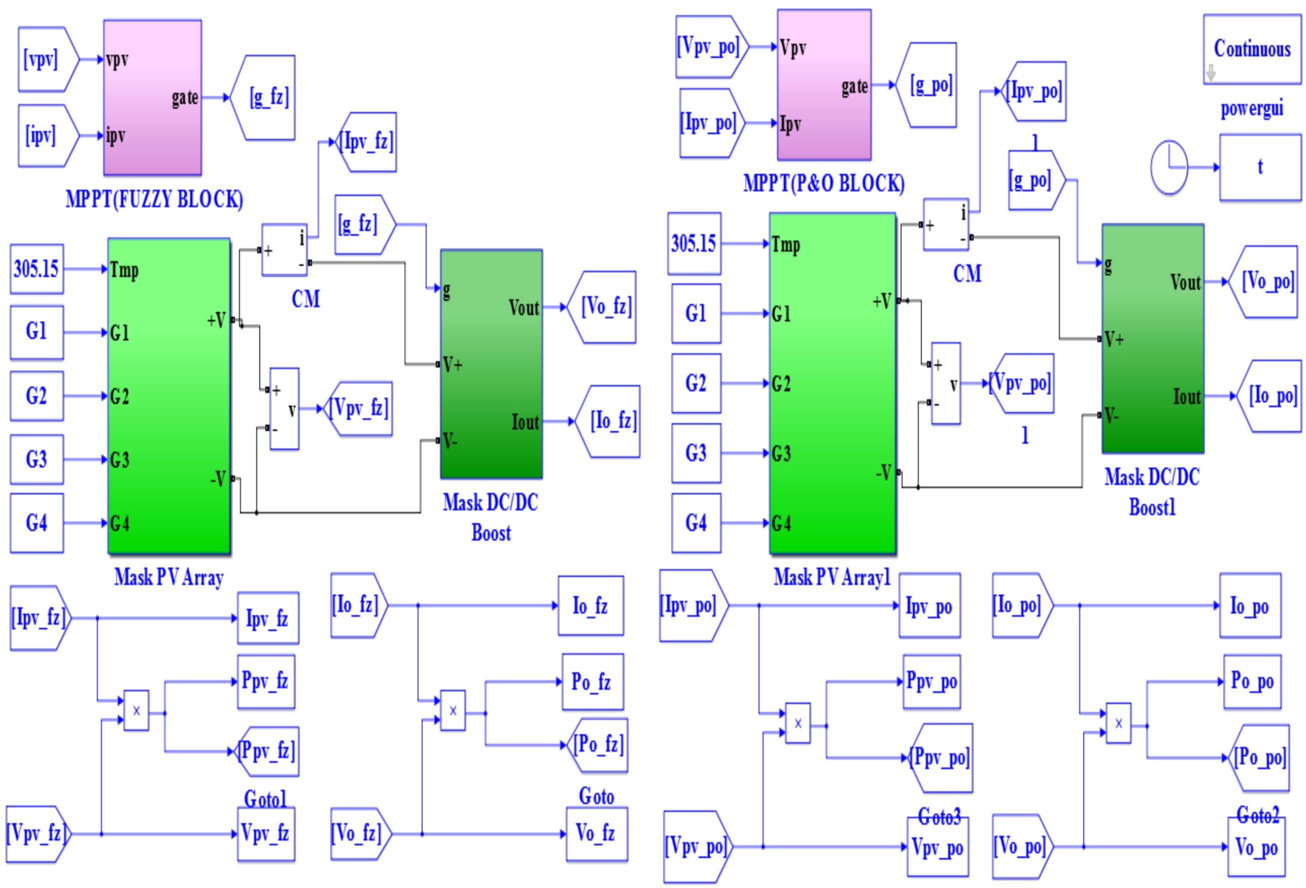

FIGURE 5.3 SIMULINK DIAGRAM OF THE PROPOSED SYSTEM WITH P&O AND FLC BY MATLAB2015A FOR DIFFERENT SP

The proposed system is tested under varying distributed radiation levels of four shading patterns with radiation level of SP1=[G1=4211, G2=4211, G3=4211, G4=4211]; SP2=[G1=4211 , G2=4211, G3=4211, G4=3000]; SP3=[G1=4211, G2=4211, G3=3000, G4=2000]; and SP4=[G1=4211, G2=3000, G3=2000, G4=1000]; and at the selected site temperature of 305.15k for the PV1, PV2 ,PV3 and PV4 connected in series configuration shown in the fig. 5.3 with P&O and FLC. Analyze the results obtained with the proposed system, FLC and the comparative testing system, P&O MPPT algorithm.

5.4 Result of PV generation under uniform radiation

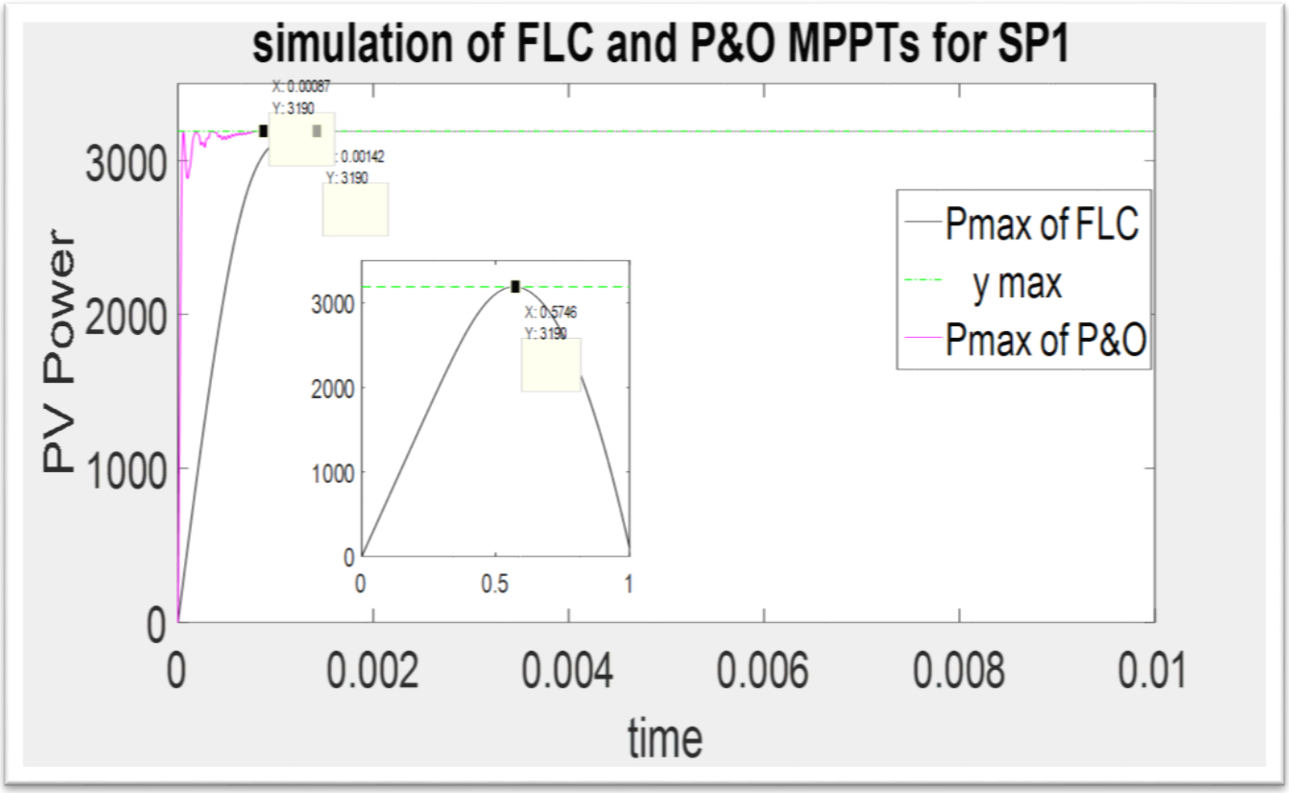

FIGURE 5.4 SIMULATION RESULTS OF MAXIMUM POWER EXTRACTED FROM FLC AND P&O MPPT

The PV system with shading pattern (SP1) can generate a maximum power of 3190.175W. Therefore the proposed system in fig. 5.3 above for this particular shading pattern is expected to extract those maximum powers. This configuration in fig 5.3 with this shading pattern (SP1 or uniformly illuminated conditions) is with P&O MPPT controller extracted a maximum power of 3190.143W with tracking efficiency of 99.999% i.e. with almost negligible power loss shown from fig. 5.4. Additionally, FLC MPPT can also extract maximum power of 3190.126W with 99.998% tracking efficiency. Those entire quantitative figures validates that those MPPT algorithms (both FLC and P&O) extracts available possible power generated from the PV system (i.e. 3190.175). P&O MPPT controller reach maximum power point faster than FLC MPPT controller (i.e. the P&O have been better steeling time (0.00087 sec) than the steeling time of FLC MPPT (0.001413 sec)) even if; there is high harmonics oscillation for a very short period of time around its steady state (or until it reaches MPP). FLC MPPT controller reached MPP slowly compared to P&O MPPT. This confirms P&O MPPT better than FLC when the PV array is under uniform shading condition. The main challenge is for a large PV farm, there is no probability of getting uniform illumination over all surface of the module of the PV system because of the shadow of the threes, poles roofs and it might be dusts on some parts of the module. All other important parameters of this PV system are stated in table 5.1 bellow quantitatively.

Table 5.1 the performance evaluation of various parameters for uniformly illuminate PV array.

Parameter	Results obtained from MPPT Algorithm for shading pattern (SP1)	
	P&O MPPT	FLC MPPT
Pmax,ref (Pmpp)	3190.175	3190.175
Pmppt	3190.143	3190.126
Vmax,ref (Vmpp)	80.1526	80.1526
Vmppt	80.1353	79.8727
Imax,ref (Impp)	39.8013	39.8013
Imppt	39.9403	39.5224
Ts	0.00087	0.001413
Tracking efficiency (%)	99.999	99.998
Oscillation (%)	0.0958	0.03135

5.5 Result of PV generation under shading pattern (SP2)

Similarly, the performance evaluation of the corresponding optimization techniques for this shading condition has been done using MATLAB 20151a. The PV system comprises of four KC200GT multi-crystalline PV modules connected in series. The schematic diagram of the PV string and preset shade patterns are shown in SIMULINK fig. 5.3. For the performance comparisons, P&O MPPT technique also implemented along with the proposed techniques, FLC MPPT.

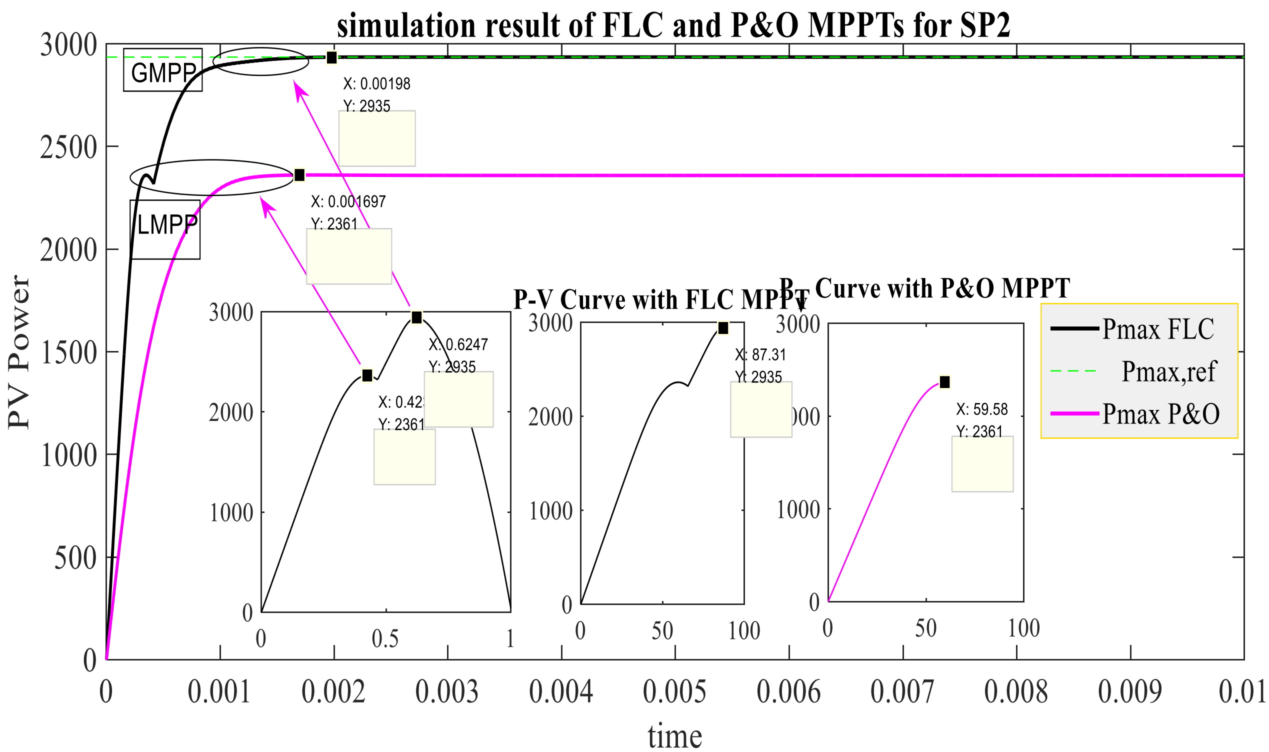

FIGURE 5.5 SIMULATION RESULTS OF MAXIMUM POWER EXTRACTED FROM FLC AND P&O MPPT

The PV system with shading pattern (SP2) could generate a maximum power of 2935.2W. In a sense, the proposed system in fig. 5.3 above for this particular shading pattern (G1=4211, G2=4211, G3=4211, G4=3000) is expected to extract that maximum power. The result in fig.5.5 shows that, the configuration in fig 5.3 with this shading patterns (SP2) with FLC MPPT controller is extracted a maximum power of 2935.101W with tracking efficiency of 99.996% i.e. with almost negligible power loss shown from fig. 5.5. In short the proposed algorithm is extracted the expected power from the PV system. However; P&O MPPT algorithm can be extracted a power of 2360.752W with 80.427% tracking efficiency. This result also shows that P&O can only extracts the first peaks of multi peaks partially shaded PV system shown in fig.5.5. To sum up, overall result indicates that 19.573% (100-80.427) of generated power from the PV system is not extracted by P&O MPPT algorithm (or 0.19573*2935.2=574.5W power is lost due to conventional MPPT algorithm). Those entire quantitative figures validates that those MPPT algorithms with FLC potentially extracted available power generated from the PV system (i.e. 2935.101W). Therefore FLC MPPT controller is more efficient than P&O MPPT controller. This confirms FLC MPPT controller is used to get the optimal power form the system during shading pattern (SP2) condition. All other important parameters of this PV system are stated in table 5.2 quantitatively for both MPPT algorithms.

Table 5.2 the performance evaluation of various parameters of the PV system for SP2 condition.

Parameter	Results obtained from MPPT Algorithm for shading pattern (SP2)	
	P&O MPPT	FLC MPPT
Pmax,ref (Pmpp)	2935.2	2935.2
Pmppt	2360.752	2935.101
Vmax,ref (Vmpp)	87.4263	87.4263
Vmppt	59.59	87.339
Imax,ref (Impp)	33.5732	33.5732
Imppt	39.6166	33.6059
Ts	0.001697	0.00198
Tracking efficiency (%)	80.427	99.996
Oscillation (%)	0.1143	0.005689

5.6 Result of PV generation under shading pattern (SP3)

As similar fashion to shading pattern SP2, the performance of the corresponding optimization techniques for this shading condition has been done using MATLAB 20151a. The PV system comprises of four KC200GT multi-crystalline PV modules connected in series. The schematic diagram of the PV string and preset shade patterns are given in fig. 5.3. For the performance comparisons propose P&O MPPT technique also implemented along with the proposed techniques, FLC MPPT.

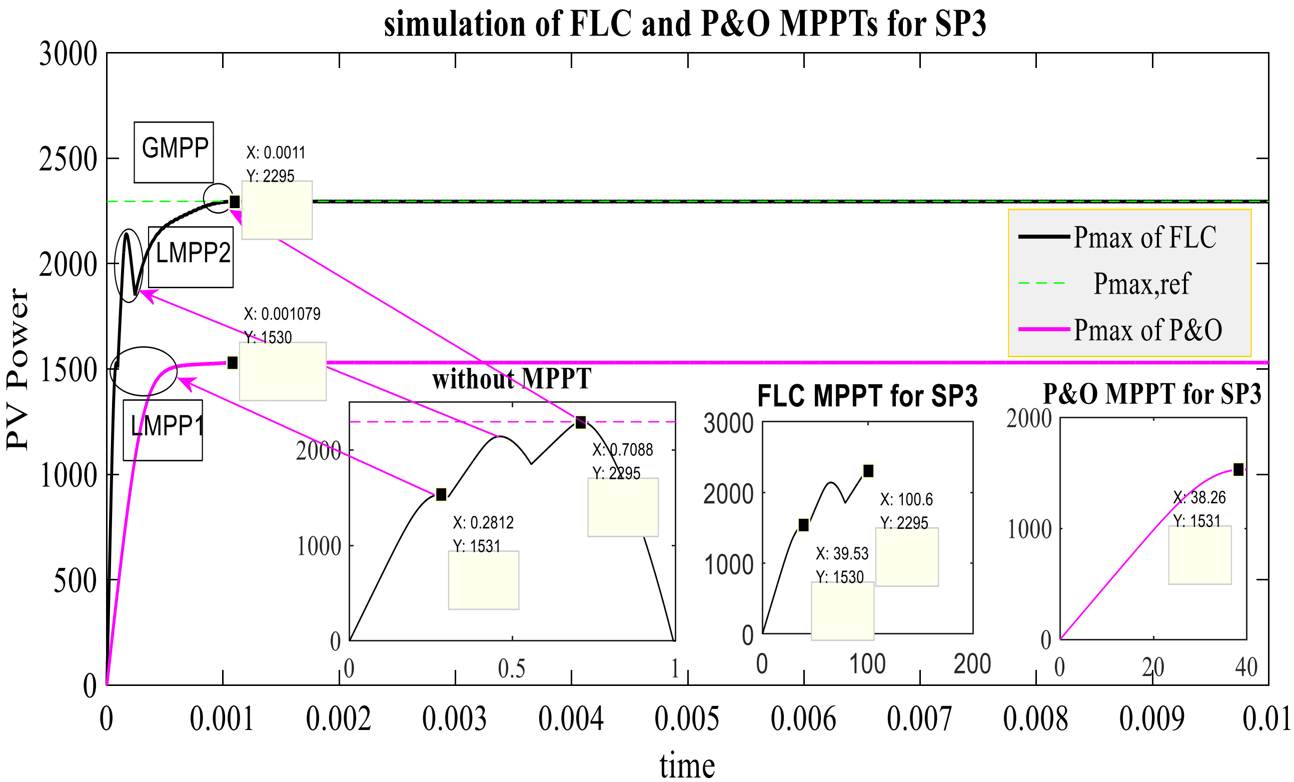

FIGURE 5.6 SIMULATION RESULTS OF MAXIMUM POWER EXTRACTED FROM FLC AND P&O MPPT

The PV system with shading pattern (SP3) is generates a maximum power of 2295.3W at its GMPP. Therefore, the proposed system in fig. 5.3 above for this particular shading pattern (SP3) (G1=4211, G2=4211, G3=3000, G4=2000) is expected to extract that maximum powers. The configuration in fig 5.3 with shading patterns (SP3) using FLC MPPT controller could extracted a maximum power of 2295.2W with tracking efficiency of 99.995%. This result proved that the FLC MPPT algorithm capable of extracting almost the available maximum powers the PV system can generate. It means that FLC MPPT algorithm can found the GMMP with negligible power loss of partially shaded PV system with two LMPPTs and one GMPPT as shown from fig. 5.6. However, P&O MPPT could extract maximum power of 1531.589W with tracking efficiency of 66.727%. This conventional MPPT algorithm is able to only track the first power peaks from a number of LMPPs and one GMPPT. It cannot search the GMPPT the PV system has. This indicates that it is impossible to extract 33.273% (100-66.727) of the generated power from the PV system with P&O MPPT algorithm (i.e. 0.33273*2295.3=763.715W power is lost or not extracted by this algorithm). That entire quantitative figure ensures that MPPT algorithms with FLC extracted a potential available power generated from the PV system (i.e. 2295.3W). Therefore FLC MPPT controller is going more efficient than P&O MPPT controller accordingly the system goes more shading patterns. The result confirms; FLC MPPT controller is used to extract the optimal available power form the system during shading pattern (SP3) condition. All other important parameters of this proposed PV system along with P&O MPPT are stated in table 5.3 bellow quantitatively.

Table 5.3 the performance evaluation of various parameters of the PV system for SP3 condition.

Parameter	Results obtained from MPPT Algorithm for shading pattern (SP3)	
	P&O MPPT	FLC MPPT
Pmax,ref (Pmpp)	2295.3	2295.3
Pmppt	1531.589	2295.208
Vmax,ref (Vmpp)	100.19	100.19
Vmppt	38.9188	100.3386
Imax,ref (Impp)	22.9095	22.9095
Imppt	39.3534	22.8745
Ts	0.001079	0.0011
Tracking efficiency (%)	66.727	99.995
Oscillation (%)	0.1327	0.0598

5.7 Result of PV generation under shading pattern (SP4)

The performance of the FLC optimization techniques and P&O algorithm for this shading condition has been done using MATLAB 20151a. The PV system composed of four KC200GT multi-crystalline PV modules connected in series configuration. The configuration of the PV string and preset shade patterns are given in fig. 5.3. The comparative study is done between the proposed optimization system, FLC and conventional P&O MPPT algorithm.

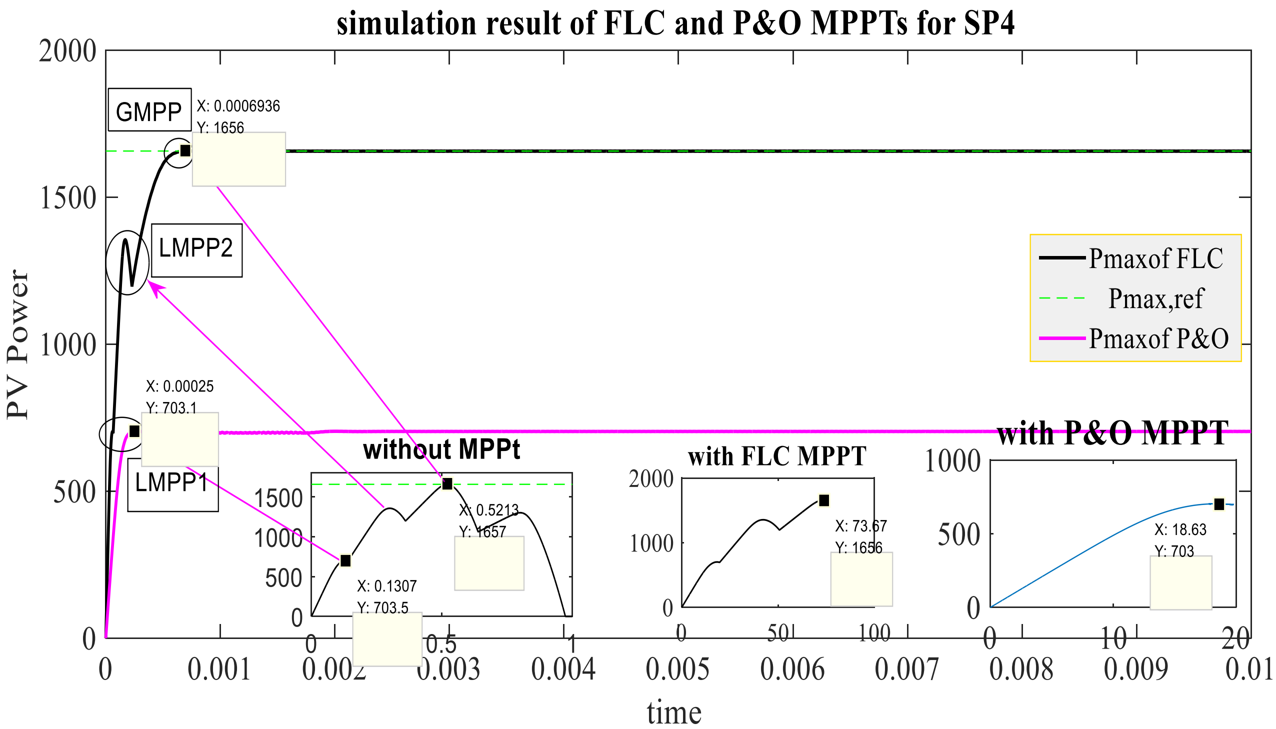

FIGURE 5.7 SIMULATION RESULTS OF MAXIMUM POWER EXTRACTED FROM FLC AND P&O MPPT

The PV system with shading pattern (SP4) can generates a maximum power of 1656.7W. Nevertheless; this partial shading condition of the PV system has been three local maxima with first local maxima of 703.5 W and one global maxima of 1656 W. It is clearly seen from the simulation results in the fig. 5.7, the proposed MPPT system is almost all the power generated by the PV system. This is simply shows that FLC algorithm can be able to extract the power at GMPP of 1656 W with tracking efficiency of 99.986%. It confirms that this optimization system is almost zero power loss. However, P&O MPPT can extracted maximum power of 703.5154W with tracking efficiency of 47.4648%.This is the first local maximum power point (LMPP). This proves P&O MPPT algorithm is unable to search global maximum power point (GMPP) of the maximum generated power from the PV system. This indicates that it is impossible to extract 52.5352% (100-47.4648) of the generated power or GMP from the PV system (i.e. 0.525352*1656.7=870.35W (or more than half of the generated power) is lost or not extracted by this algorithm). The above quantitative figure ensures that MPPT algorithms with FLC extracted available power generated from the PV system (i.e. 1656 W). Therefore FLC MPPT controller is more efficient than P&O MPPT controller as the system exposed to more shading patterns. This confirms FLC MPPT controller is used to extract the optimal available power (global maximum power) form the PV system under any condition. All other important parameters of this proposed PV system along with P&O MPPT are stated in table 5.4 bellow numerically.

Table 5.4 the performance evaluation of various parameters of the PV system for SP4 condition.

	Results obtained from MPPT Algorithm for shading pattern (SP4)	
	P&O MPPT	FLC MPPT
Pmax,ref (Pmpp)	1656.7	1656.7
Pmppt	703.5154	1656.484
Vmax,ref (Vmpp)	73.0073	73.0073
Vmppt	18.0158	73.6033
Imax,ref (Impp)	22.69169	22.69169
Imppt	39.0279	22.50084
Ts	0.00025	0.0006936
Tracking efficiency (%)	47.4648	99.986
Oscillation (%)	0.884	0.0367

5.8 Comparisons of P&O MPPT and FLC MPPT for SP1, SP2, SP3, and SP4

The table 5.5 the charts in fig 5.8-5.12 below shows clear comparison of all important parameters of the PV system with P&O and FLC MPPT for all shading parameters.

5.8.1 Tracking efficiency of the PV system

The efficiency of the MPPT technique is a very important consideration for special PV system applications such as the power supply used in space stations and satellites. It can be determined by the following equation:

$$\eta = \frac{P_{mppt}}{P_{\max}} * 100\% \qquad 5.1$$

The simulation results indicate the proposed has the best efficiency as compared to conventional P&O algorithms shown in table 5.5 bellow.

The quantitative figure shown above in section 5.4-5.7, is summarized below in table 5.5, and used to draw the conclusions of the proposed system.

Table 5.5 the performance evaluation and comparison of various parameters for different shading pattern PV array.

Parameter	Results obtained from MPPT Algorithm for different shading patterns							
	SP1		SP2		SP3		SP4	
	P&O	FLC	P&O	FLC	P&O	FLC	P&O	FLC
Pmax,ref (Pmpp)	3190.175	3190.175	2935.2	2935.2	2295.3	2295.3	1656.7	1656.7
Pmppt	3190.143	3190.126	2360.752	2935.101	1531.589	2295.208	703.5154	1656.484
Vmax,ref (Vmpp)	80.1526	80.1526	87.4263	87.4263	100.19	100.19	73.0073	73.0073
Vmppt	80.1353	79.8727	59.59	87.339	38.9188	100.3386	18.0158	73.6033
Imax,ref (Impp)	39.8013	39.8013	33.5732	33.5732	22.9095	22.9095	22.69169	22.69169
Imppt	39.9403	39.5224	39.6166	33.6059	39.3534	22.8745	39.0279	22.50084
Ts	0.00087	0.001413	0.01697	0.00198	0.001079	0.0011	0.00025	0.0006936
Tracking efficiency (%)	99.999	99.998	80.427	99.996	66.727	99.995	47.4648	99.986
Oscillation (%)	0.0958	0.03135	0.1143	0.005689	0.1327	0.0598	0.884	0.0367

Depending on table 5.5, it is possible to show the comparison of each parameters of the PV system using charts.

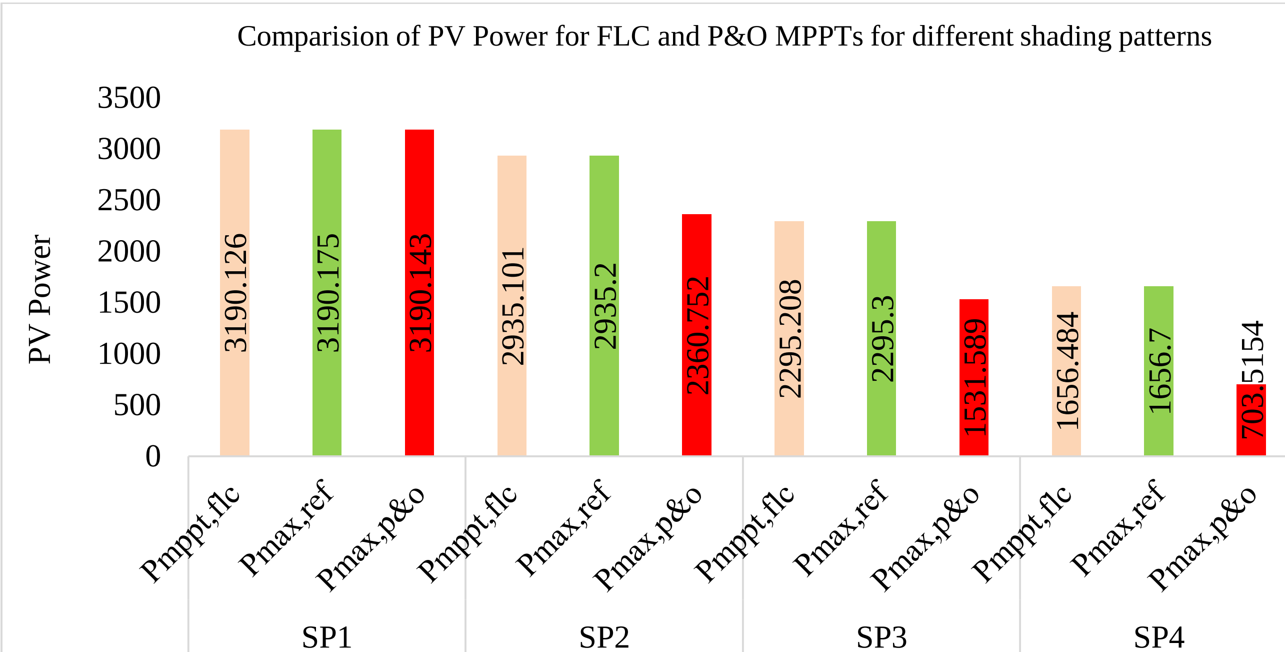

FIGURE 5.8 COMPARISON OF PV POWER FOR FLC AND P&O MPPTS FOR DIFFERENT SHADING PATTERN

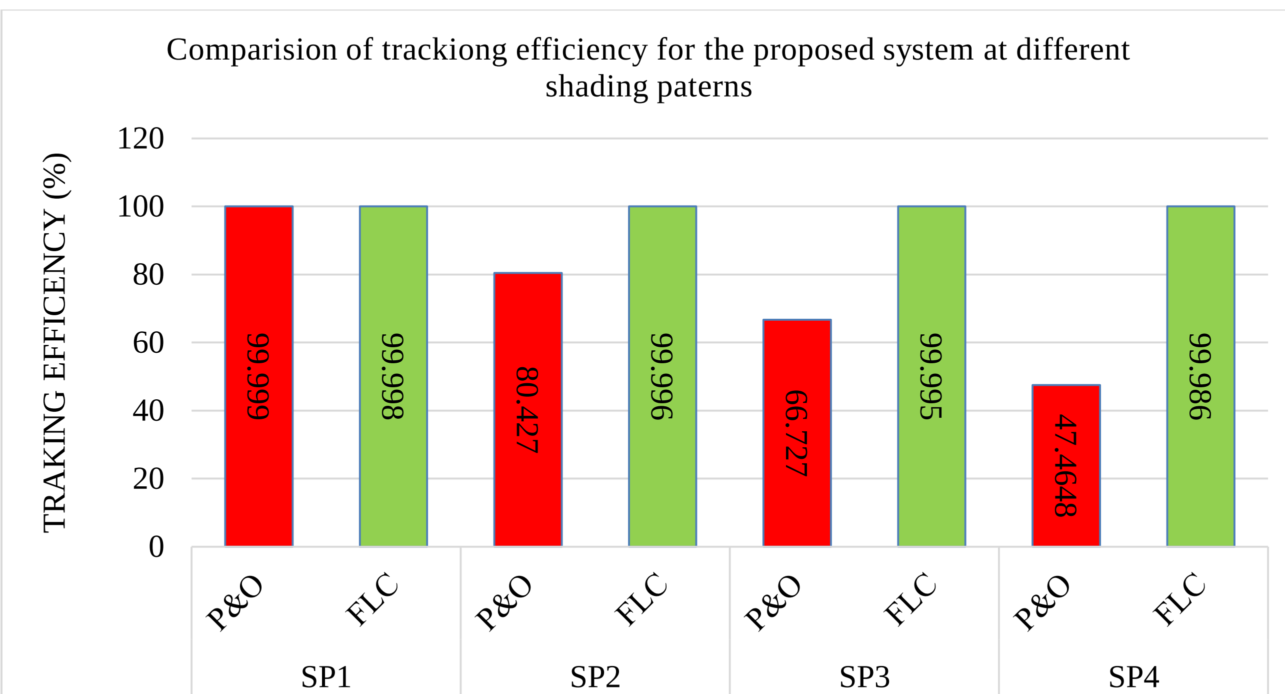

FIGURE 5.9 COMPARISON OF PERCENTAGE TRACKING EFFICIENCY FOR FLC AND P&O MPPTS FOR DIFFERENT SHADING PATTERN

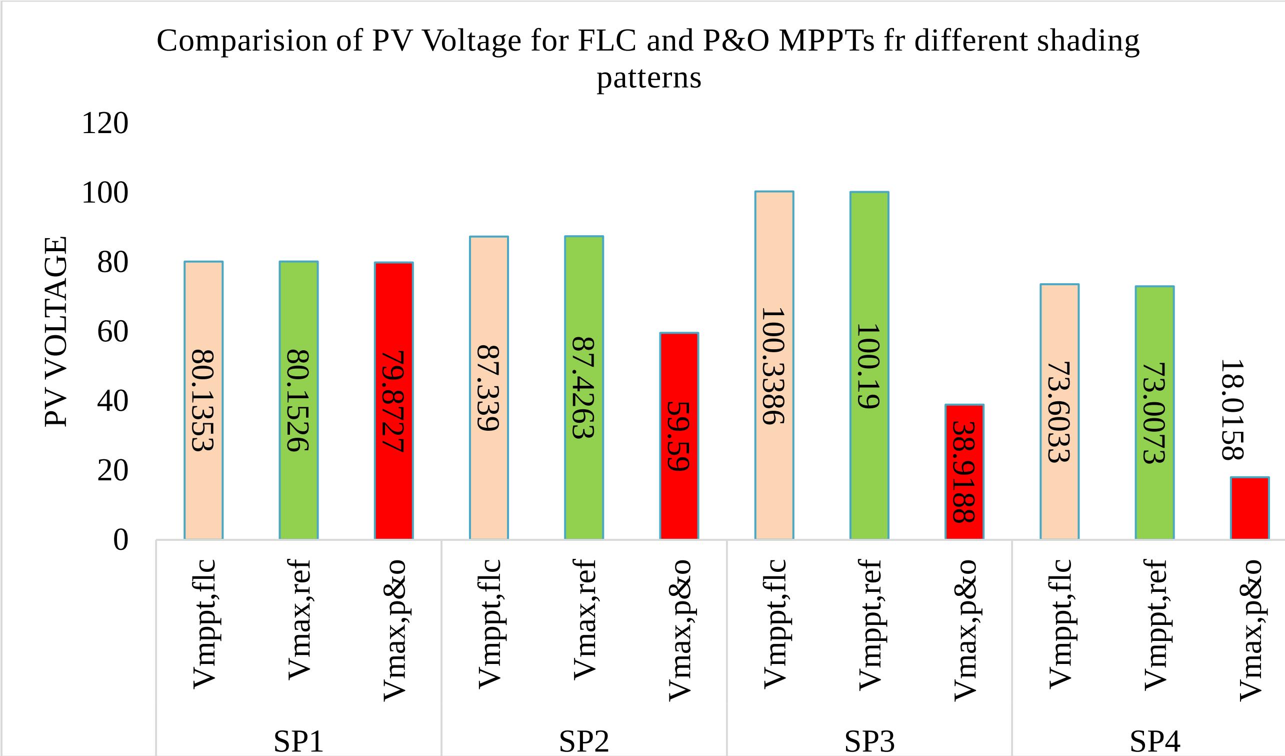

FIGURE 5.10 COMPARISON OF PV VOLTAGE FOR FLC AND P&O MPPTS FOR DIFFERENT SHADING PATTERN

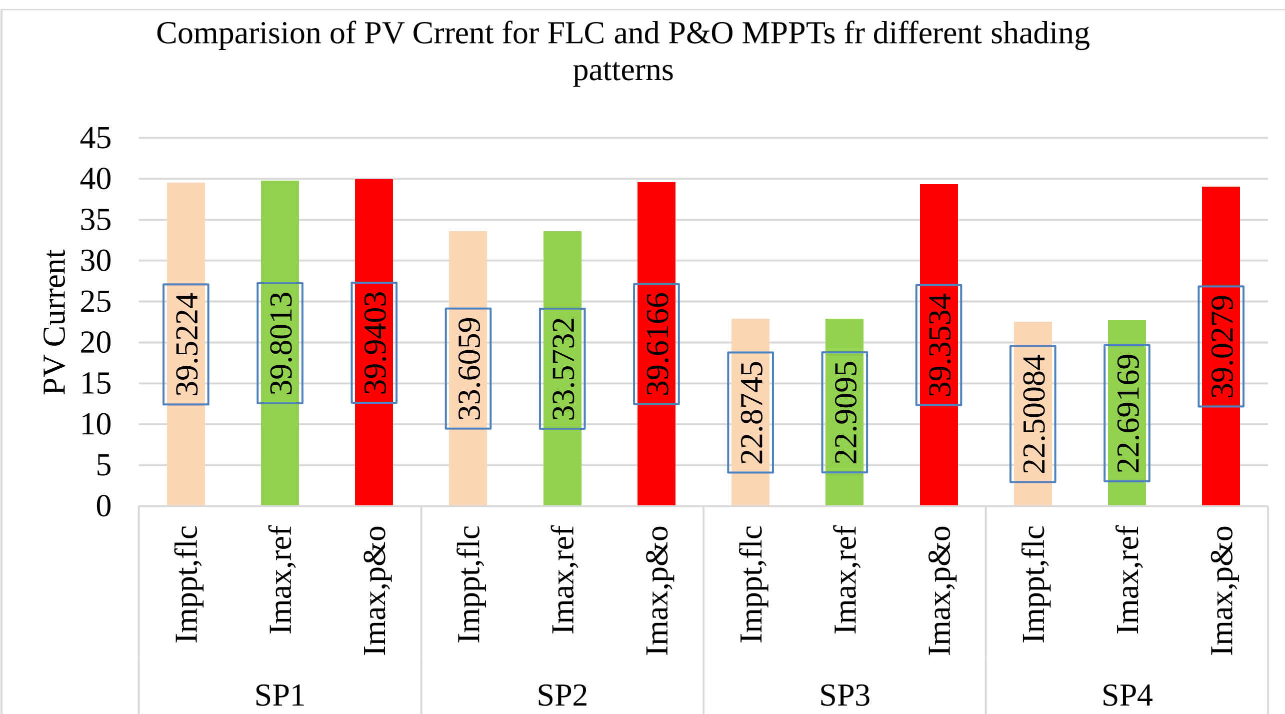

FIGURE 5.11 COMPARISON OF PV CURRENT FOR FLC AND P&O MPPTS FOR DIFFERENT SHADING PATTERN

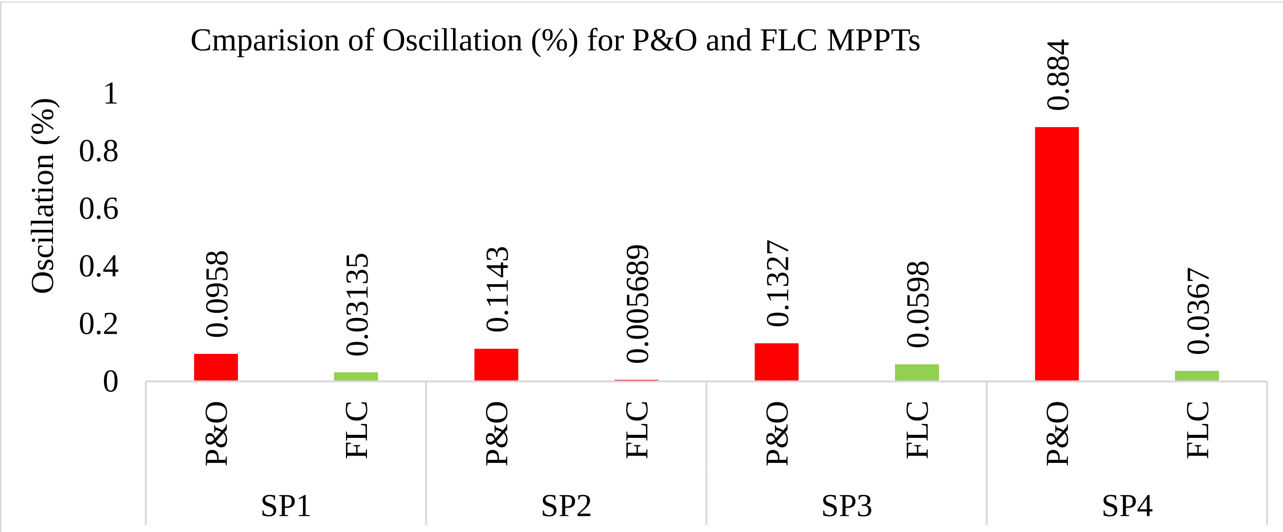

FIGURE 5.12 COMPARISONS OF HARMONIC OSCILLATION FOR FLC AND P&O MPPTS FOR DIFFERENT SHADING PATTERN

CHAPTER 6

CONCLUSION AND RECOMMENDATION

6.1 Conclusion

The fuzzy logic controller offers a good response to changes in cell temperature and solar radiation, and a controller alters the duty cycle of a DC-DC converter as a control parameter. Results of simulation tests indicate that the proposed system increases the system's efficiency. The model is simulated in a MATLAB/Simulink 15a environment by first varying the solar radiation and then varying the temperature. The output power and voltage obtained from the fuzzy logic-based MPPT system is greater than that obtained from a conventional P&O MPPTs of solar module.

The graph and the charts in chapter five shows that conventional controller P&O is not applicable MPPT controller when the system under various partial shading conditions and get more worst as the PV system exposed to partial shading. In other word, the result confirms that P&O MPPT is not flexible for different atmospheric condition (it extracts only the first local maximum power point/LMPP). Conversely, FLC MPPT controller can extract all the power/ global maximum power generated from the PV system. FLC is flexible and sensitive for varying weather condition (different shading pattern). This validates that FLC controller is flexible to varying weather condition seen from the results of SP1 to SP4 in chapter 5. FLC MPPT is robust and high tracking efficiency for any partial shading pattern.

Moreover, alternations in solar radiation and temperature do not have any impact on the system's performance levels, further indicating that the overall system efficiency has been enhanced using FLC based MPPT system.

6.2 Recommendation

The purpose of a photovoltaic power system is to provide generated available potential power. This can be done through MPPT technique. In this thesis, FLC algorithm is used to extract the global maximum power of the PV system under partial shade condition. But, it is challenging to determine the range of linguistic values of each linguistic variables and to establish a number of rules of the controller. i.e. it too hard determining the accurate values of lower and upper limits of a linguistic values, NB, NM, NS, ZE, PS, PM, and PB of each linguistic variables CP, CI and CPm in the proposed system. Therefore, I strongly recommended that the future work could include, using optimization techniques that reduce the rules of the controller and minimize the challenge of determinations of lower and upper limits of linguistic values of each linguistic variables. The drawbacks of the system mentioned here can be solved using controllers such as genetic algorithm with fuzzy controller. It can be used in the control algorithm to tune the membership functions so that the inexact reasoning characteristics of the FLC are sufficient to control a system that requires precise control actions.

Reference

[1] K.Ogimito; I. Kaizuka; Y. Ueda; and T.Oozeki, "A Goof fit Japan's Solar Power Program and Prospects for the New Power System," *IEEE Power and Energy Manganize,* Vols. 11, no. 2, pp. 65-74, 2013.

[2] J. Traube, F.Lu, D.Maskimovic, J.Mossoba, M.Kromer, P.Faill, S.Katz, B.Borowy, S.Nicolas and L. Casey, "Mitigation of Solar Irradiance Intermittency in Photovoltaic Power Systems with Integrated Electric -Vehivle Charging Functionality," *IEEE Tran. Power Elec.,* Vols. 28, no. 6, pp. 3058-3067, June 2013.

[3] W.Xiao, N. Ozog and W.G. Duford , "Topology study of photolatic interface for maximum power point tracking," *IEEE Trans. Ind. Electron,* Vols. 54, no. 3, pp. 1696-1704, 2007.

[4] W. Jung, G. Yu and J. Chosi, "Improved perturbation and observation method of MPPT cotrol for photovoltaic power systems," *IEEE Photovoltaic Specialist Conference,* pp. 1788-1791, 2005.

[5] W.Xiao and W.G. Dunford, "A Modefied addaptive hill climbing MPPT method for photovoltaic power system," *in Power Electronic Specialists Conference,* pp. 1788-1791, 2005.

[6] M. Shahidehpour and F. Schwarts, "Dont't let the sun go dowon on PV[Photovoltaic System]," *IEEE Power and Energy Manganize,* Vols. 2, no. 3, pp. 40-48, 2004.

[7] X. Yang, Y. Song, G. Wang and W. Wang, "A Comprehesive Reviw on the Development of Sustainable Energy Stratagy and Implementation in China," *IEEE Tran. Sustainable Energy,* Vols. 1, no. 2, pp. 57-65, 2010.

[8] Ocran, T.A.et al, " Artifical Neural Network Maximum Power Point Tracker for Solar Electric Vehicle," *Tsinghua Science & Technology,* Vols. 10, no. 2, pp. 204-208, 2005.

[9] X. Wang, J. Byrne, L. Kurdgelashvilil & A. Barnett, "Introduction of High Effecient Photovoltaics:," *on the way to becoming a major electric source* , 2012.

[10] R. Kadir, J. Gaubert and G. Champesionis, "An improved maximum power point trucking for phototovoltaic gird-connected inverter based on voltage -oriented control," *IEEE Trans. Ind. Electron,* vol. 58, pp. 66-75, 2011.

[11] A.Mahmoud, H.Mashaly, S. Kandi, H. EL Khasahab and M.Nashed, "fuzzy logic implementation for photovoltaic maximum power tracking," *2000.IECON 2000 26th Annual conference of IEEE ,2000* , pp. 735-740.

[12] A.Sarfari and S. Mekhilef, "incremental conductance MPPT mthod for PV systems," *Canadian Conference on Electrical and Computer Engineering (CCECE),* pp. 345-347, 2011.

[13] H.Abouobaida and M.Chekaoui, "Comparative study of maximum power point tracks for fast changing inviromental conditions," *in Multimedia coputing and systems (ICMCS),* pp. 1131-1135, 2012.

[14] AN.A. Ali, M.H. Mostafa and T. Abdel-Moneim, "A Survey of maximum PPT tehniques of PV systems," *proceeding of the IEEE Energy tech.,* pp. 1-17, 2012.

[15] A. Zbeeb, V. Devabhaktuni, A. Sebak, and L. Maheshwari, "A New microcontroller-based MPPT algorithm for photovoltaic applications," *Int. Conference on Energy and Enviroment,* 2009.

[16] A. Yaadani and P.P. Dash , "A control method and characterization of dynamics for photovoltaic (PV) system interfaced with distribution network," *IEEE Trans. Power Del.,* vol. 24, pp. 1538-1551, 2009.

[17] S. Park, G. Cha, Y. Jung and C. Won, "Design and application of PV generation system using a sof-switcing boost converter with SARC," *IEEE Trans. Ind. Electron,* vol. 57, pp. 512-522, 2010.

[18] H. Abidi, A. Abdelghani nd D.M ontesinos-Miracle, "MPPT algorithm and photovoltaic array emulator using DC/DC converters," *IEEE Mediterranean Electro Technical Conference,* pp. 567-572, 2012.

[19] Q. Zhang, X. Sun, Y. Zhong and M. Matsui, "A novel topology for solving the partial shading problems in potovoltaic power generation system," *in Power Electronics and Motion control Conference,2009. IPEMC'09. IEEE 6th I nternaational*, pp. 1689-1698, 2009.

[20] P. Pate and V.Agarwal, "Maximum power point tracking scheme for PV systems oprating under partially shaded conditions," *IEEE Trans. Ind. Electron.*, vol. 55, pp. 1689-1698, 2008.

[21] S. Jain and V. Agarawal, "A new algorithm for rapid tracking of approximate maximum power point in photovoltaic systems," *IEEE Power Electronics Letters,* vol. 2, pp. 16-19, 2004.

[22] K. Ishaque and Z. Salam, "A deterministic particle swarm optimizaton maximum point tracker for photovoltaic system under partial shading condition," *IEEE Trans. Ind. Electron.*, vol. 60, pp. 3195-3206, 2013.

[23] M.S. Ismail, M. Monghavvemi and T.M.I. Mahlia, "Characterization of PV Panel clees and global optimization of its moodel parameters using genetic algorithm," *energy Convers. Manag. 73*, pp. 10-25, 2010.

[24] D. Shmilovitz and Y. Levron, "Distributed maximum power point tracking in phtovoltaic systems-Emerging Architectures and Control Methods," *ATKAFF*, vol. 53 NO. 2, pp. 142-155, 2012.

[25] J. D. Bastiidas_Rodriguez, E. Franco, G. Petrone, C.A. Ramos-Paja and G. Spagnuolo, "Maximum power point tracking artictures for photovoltaic system in mismatching cnditions. a review," *INT. Power Electron*, Vols. 7, Iss 6, pp. 1396-1413, 2014.

[26] "Renewable Energy Policy Network For The 21th Century," *Renewable Global Status Report,* 2012.

[27] "Volker Quasching,2005. Understanding renewable energy systems.UK and USA:Earthscan.," *ISBN:1844071286.*, 2005.

[28] Gilbert M. Masters, "Renewable and efficient electric power systems.," *Canadian: John Wiley & Sons, Inc. ISBN: 9780470745601*, p. 2004.

[29] Paul A. Lynn, "Electricity from sun light: An introduction to photovoltaic. United Kingdom," *John Wiley and Sons, Ltd. ISBN: 9780470745601*, 2010.

[30] Deutsche Gesellschaft Fur Sonnenenergie, "Planning and installing photovoltaic systems: aguide for installers, architects and engineers.UK and USA: Earthscan.," *ISBN : 9781844074426*, 2008.

[31] Tark Salmi, Mounir Bonzguenda, Adel Gastil and A. masmoundi, "Matlab/Simulink based Modeling of solar Photovoltaic cell," *international journal of renewable energy research* , vol. 2 no. 2, pp. 213-218, 2012.

[32] " Photovoltaics: design and installation manual. Canada: Fourth Printing.," *Solar energy International. ISBN: 0865715203*, 2004..

[33] S. Rahman, N. S. Oni and Q. A. Ibn Masud, "Design of a Charge Controller Circuit with Maximum Power Point Tracker for Photovoltaic System," *Dept. of Electrical & Electronic Engineering, BRAC university*, Dec. 2012.

[34] Akihiro Oi, "Design and Simulation of Photovoltaic Water Pumping System," *Master of Science Thesis, California Polytechnic State University*, 2005..

[35] J. M. Enrique, J. M. Andujar and M. A. Bohorquez, " A reliable, fast, and low cost maximum power point tracker for photovoltaic applications," *Solar Energy*, Vols. vol. 84, no. 1, pp. 79 - 89 , 2010..

[36] "F. Sick and T. Erge, Photovoltaic in buildings: a design handbook, International Energy Agency (1996).".

[37] P. Chen, "AN IMPROVED MAXIMUM POWER POINT TRACKING ALGORITHM USING FUZZY LOGIC CONTROLLER FOR PHOTOVOLTAIC APPLICATIONS," *Master of Science in Engineering in lyles colage of engineering California, Fresno,* pp. 13-14, August 2015.

[38] J.A. Gow and C. Manning, "Development of a photovoltaic array model for use in power-electronics simulation studies," *in Proc. IEE Electric power applications,* Vols. vol. 146, no. 2, pp. 193-200, March 1999.

[39] "International Energy Agency (IEA)-PVPS Trends in photovoltaic applications. [Online].," *Available: www.iea-pvps.org,* Sept 2009.

[40] "Photovoltaics: design and installation manual. Canada: Fourth Printing. ISBN: 0865715203.," *Solar energy International,* , 2004..

[41] R.B. Koad, "An improved Maximum Power Point Tracking For PV System," *Doctor of Philosophy Department of Electronic and Computer Engineering College of Engineering, Design and Physical Sciences Brunel University London,* pp. 23-28, January 2017.

[42] E. V. Paraskevadaki and S. A. Papathanassiou, "Evaluation of MPP voltage and power of mc-Si PV modules in partial shading conditions," *IEEE Trans. Energy Convers,* vol. vol. 26, pp. 923-932., 2011.

[43] Mao, M, Zhang, L, Duan, Q et al., " A Two-Stage Particle Swarm Optimization Algorithm for MPPT of Partially Shaded PV Arrays.," *International Journal of Green Energy,* vol. 14 (8)., no. ISSN 1543-5075, pp. 694-702., 2017.

[44] "Maximum Power Point Tracking in Power System," *A.M.A. Motaleb,* pp. 23-35, 2010.

[45] S. R. Potnuru, D. Pattabiraman, S. I. Ganesan and N. Chilakapati, "Positioning of PV panels for reduction in line losses and mismatch losses in PV array," *Renewable Energy,* vol. 78, pp. 264-275, 2015.

[46] T. L. Kottas, Y. S. Boutalis and A. D. Karlis, "New maximum power point tracker for PV arrays using fuzzy controller in close cooperation with fuzzy cognitive networks," *IEEE Trans. Energy Convers,* vol. 21, p. 2006, 793-803.

[47] Z. Liang, R. Guo, J. Li and A. Q. Huang, "A high-efficiency PV module integrated dc/dc converter for PV energy harvest in freedom systems," *IEEE Trans. Power Electron,* Vols. 26, no. 3, pp. 897 -909, 2011.

[48] V. Phimmasone, Y. Kondo, T. Kamejima and M. Miyatake, "Evaluation of extracted energy from PV with PSO-based MPPT against various types of solar irradiation changes," *in Electrical Machines and Systems (ICEMS) International Conference,* pp. 487-492, 2010.

[49] S. Hadji, J. Gaubert and F. Krim, "Maximum power point tracking (MPPT) for photovoltaic systems using open circuit voltage and short circuit current," *in 3rd International Conference on Systems and Control,* pp. 87-92, 2013.

[50] N. Khaehintung and P. Sirisuk, "Application of maximum power point tracker with self-organizing fuzzy logic controller for solar-powered traffic lights," *in 2007 7th International Conference on Power Electronics and Drive Systems,* pp. 642-646, 2007.

[51] M. Abdulaziz, S. Aldobhani and R. John, "Maximum power point tracking of PV system using ANFIS prediction and fuzzy logic tracking," *in Power Electronics and Drive Systems, 2003. PEDS 2003. the Fifth International Conference on,,* 2008.

[52] Spagnuolo, and M. Vitelli, "Perturb and observe MPPT technique robustness improved," *in Proc. IEEE Int. Symp. Ind. Electron,* Vols. 3, no. 1, pp. 845-850, May 2004.

[53] T. Esram and P. L. Chapman,, "Comparison of photovoltaic array maximum power point tracking techniques," *IEEE Transactions on Energy Conversion EC,* vol. 22, p. 439, 2007.

[54] B. Subudhi and R. Pradhan, "A comparative study on maximum power point tracking techniques for photovoltaic power systems," *IEEE Transactions on Sustainable Energy,* vol. 4,

pp. 89-98, 2013.

[55] Sera, Dezso, et al., "On the perturb-and-observe and incremental conductance MPPT methods for PV systems," *Photovoltaics, IEEE Journal of,* vol. 3.3, pp. 1070-1078.

[56] M. Lokanadham and K. V. Bhaskar, "Incremental conductance based maximum power point tracking (MPPT) for photovoltaic system," *International Journal of Engineering Research and Applications (IJERA),* vol. 2, pp. 1420-1424, 2015.

[57] H. N. Zainudin and S. Mekhilef, "Comparison study of maximum power point tracker techniques for PV systems," *in Proceedings of the 14th International Middle East Power Systems Conference (MEPCON'10), Cairo University, Egypt,,* pp. 750-755, 2010.

[58] Y. Jung, J. So, G. Yu and J. Choi, "Improved perturbation and observation method (IP&O) of MPPT control for photovoltaic power systems," *in Conference Record of the Thirty-First IEEE Photovoltaic Specialists Conference*, pp. 1788-1791, 2005.

[59] Y. Hsiao and C. Chen, "Maximum power tracking for photovoltaic power system," *in Industry Applications Conference, 2002. 37th IAS Annual Meeting. Conference Record of the,,* pp. 1035-1040, 2002.

[60] X. Liu and L. A. Lopes, "An improved perturbation and observation maximum power point tracking algorithm for PV arrays," *in Power Electronics Specialists Conference, 2004. PESC 04. 2004 IEEE 35th Annual,* pp. 2005-2010, 2004.

[61] D. Hohm and M. Ropp, "Comparative study of maximum power point tracking algorithms using an experimental, programmable, maximum power point tracking test bed," *in Photovoltaic Specialists Conference, 2000. Conference Record of the Twenty-Eighth IEEE,* pp. 1699-1702, 2000.

[62] F. Liu, S. Duan, F. Liu, B. Liu and Y. Kang, "A variable step size INC MPPT method for PV systems,," *IEEE Trans. Ind. Electron,* vol. 55, pp. 2622-2628, 2008.

[63] Chen, Yie-Tone, Zhi-Hao Lai, and Ruey-Hsun Liang, "A novel auto-scaling variable step-size MPPT method for a PV system," *Solar Energy*, vol. 102, pp. 247-256, 2014.

[64] K. Kobayashi, I. Takano, andY. Sawada, "A study on a two stage maximum power point tracking control of a photovoltaic system under partially shaded insolation conditions," *in Proc. IEEE Power Eng. Soc. General Meeting*, vol. 4, pp. 2612-2617, Jul. 2003.

[65] Y.-H. Liu, S.-C. Huang, J.-W. Huang and W.-C. Liang, "A particle swarm optimization-based maximum power point tracking algorithm for PV systems operating under partially shaded conditions," *IEEE Trans. Energy Conver.*, Vols. 27, no. 4, pp. 1027-1035, 2012.

[66] M. Sheraz and M. A. Abido, "An efficient MPPT controller using differential evolution and neural network," *in Power and Energy (PECon), 2012 IEEE International Conference on*, pp. 378-383, 2012.

[67] M. A. S. Masoum, H. Dehbonei, and E. F. Fuchs, "Theoretical and experimental analyses of photovoltaic systems with voltage and current based maximum power-point tracking," *IEEE Trans. Energy Convers*, Vols. 17, no.4, pp. 514-522, 2002.

[68] N. Femia, G. Petrone, G. Spagnuolo and M. Vitelli, "Optimization of perturb and observe maximum power point tracking method," *IEEE Trans. Power Electron*, Vols. 20, no. 4, pp. 963-973, 2005.

[69] E. Koutroulis and F. Blaabjerg, "A new technique for tracking the global maximum power point of PV arrays operating under partial-shading conditions," *IEEE J. Photovoltaics*, Vols. 2, no. 2, pp. 184-190, 2012.

[70] K. Ishaque, Z. Salam and G. Lauss, "The performance of perturb and observe and incremental conductance maximum power point tracking method under dynamic weather conditions," *Appl. Energy*, vol. 119, pp. 228-236, 2014.

[71] C. Rodriguez and G. A. J. Amaratunga, "Analytic solution to the photovoltaic maximum power point problem," *IEEE Trans. Circuits Syst. I, Reg. Papers*, Vols. 54, no. 9, pp. 2054-

2060, 2007.

[72] J. Ahmad, "A fractional open circuit voltage based maximum power point tracker for photovoltaic arrays," *in Software Technology and Engineering (ICSTE), 2010 2nd International Conference on,* vol. 1, pp. 247-250, 2010.

[73] T. Noguchi, S. Togashi, and R. Nakamoto, "Short-current pulse-based maximum-power-point tracking method for multiple photovoltaic-and converter module system," *IEEE Trans. Ind. Electron,* Vols. 49, no. 1, pp. 217-223, 2002.

[74] T. Tafticht, K. Agbossou, M. L. Doumbia, and A. Ch´eritia, "An improved maximum power point tracking method for photovoltaic systems," *Renew. Energy,* Vols. 33, no. 7, pp. 1508-1516, 2008.

[75] M. Sheraz and M. A. Abido, "An efficient MPPT controller using differential evolution and neural network," *in Power and Energy (PECon), 2012 IEEE International Conference on,* pp. 378-383, 2012.

[76] Chin, Chia Seet, et al., ""Optimization of partially shaded PV array using fuzzy MPPT," *Humanities, Science and Engineering (CHUSER), 2011 IEEE Colloquium on. IEEE,* 2011.

[77] Syafaruddin, E. Karatepe and T. Hiyama, "Artificial neural network-polar coordinated fuzzy controller based maximum power point tracking control under partially shaded conditions," *IET Renewable Power Generation,* Vols. 3, no. 2, pp. 239-253, 2009.

[78] C. Larbes, S.M. A¨ıt Cheikh, T. Obeidi, and A. Zerguerras, "Genetic algorithms optimized fuzzy logic control for the maximum power point tracking in photovoltaic system," *Renew. Energy,* vol. 34, pp. 2093-2100, 2009.

[79] Sheraz, Muhammad, and Mohammed A. Abido, "An efficient MPPT controller using differential evolution and neural network," *Power and Energy (PECon), 2012 IEEE International Conference on. IEEE,* 2012.

[80] Y. J. Wang and P. C. Hsu, "Analytical modelling of partial shading and different orientation of photovoltaic modules," *IET Renew. Power Gener*, Vols. 4, no. 3, pp. 272-282, 2010.

[81] D. Nguyen and B. Lehman, "An adaptive solar photovoltaic array using model-based reconfiguration algorithm," *IEEE Trans. Ind.Electron*, Vols. 55,no 7, pp. 2644-2654, 2008.

[82] K. Ishaque, Z. Salam, M. Amjad, and S. Mekhilef, "An improved particle swarm optimization (PSO)-based MPPT for PV with reduced steady-state oscillation," *IEEE Trans. Power Electron.*, Vols. 27, no. 8, pp. 3627-3638, 2012.

[83] T. L. Nguyen and K.-S. Low, "A global maximum power point tracking scheme em-ploying DIRECT search algorithm for photovoltaic systems," *IEEE Trans. Ind. Electron*, Vols. 57, no. 10, pp. 3456-3467, 2010.

[84] L.-R. Chen, C.-H. Tsai, Y.-L. Lin, and Y.-S. Lai, "A biological swarm chasing algorithm for tracking the PV maximum power point," *IEEE Trans. Energy Convers*, Vols. 25, no. 2, pp. 484-493, 2010.

[85] B. N. Alajmi, K. H. Ahmed, S. J. Finney and B. W. Williams, "A maximum power point tracking technique for partially shaded photovoltaic systems in microgrids," *IEEE Trans. Ind. Electron.*, Vols. 60, no. 4, pp. 1596-1606, 2013.

[86] Y.H. Ji, D.Y. Jung, J.G. Kim, J.H. Kim, T.W. Lee, and C.Y. Won, "A real maxi-mum power point tracking method for mismatching compensation in PV array under par-tially shaded conditions," *IEEE Trans. Power Electron.*, Vols. 26, no. 4, pp. 1001-1009, 2011.

[87] Á.-A. Bayod-Rújula and J.-A. Cebollero-Abián, "A novel MPPT method for PV sys-tems with irradiance measurement," *Sol. Energ*, vol. 109, pp. 95-104, 2014.

[88] Sundarabalan, C. K., K. Selvi, and K. Sakeenathul Kubra, "Performance Investigation of Fuzzy Logic Controlled MPPT for Energy Efficient Solar PV Systems," *Power Electronics and Renewable Energy Systems. Springer India*, pp. 761-770, 2015.

[89] Mohamed, Azah, and M. A. Hannan, "Hardware implementation of fuzzy logic based maximum power point tracking controller for PV systems," *Power Engineering and Optimization Conference (PEOCO), 2010 4th International. IEEE*, 2010.

[90] Takun, Pongsakor, Somyot Kaitwanidvilai, and Chaiyan Jettanasen, "Maximum power point tracking using fuzzy logic control for photovoltaic systems," *Proceedings of International MultiConference of Engineers and Computer Scientists.Hongkong.,* 2011.

[91] Noman, Abdullah M., Khaled E. Addoweesh, and Hussein M. Mashaly, "fuzzy logic control method for MPPT of PV systems," *IECON 2012-38th Annual Conference on IEEE Industrial Electronics Society. IEEE,* 2012.

[92] Cheikh, MS Aït, et al., "Maximum power point tracking using a fuzzy logic control scheme," *Revue des energies Renouvelables,* Vols. 10, no. 3, pp. 387-395, 2007.

[93] Choudhury, Subhashree, and Pravat Kumar Rout, "Adaptive Fuzzy Logic Based MPPT Control for PV System under Partial Shading Condition," *International Journal of Renewable Energy Research (IJRER),* Vols. 5, no. 4, pp. 1252-1263, 2015.

[94] Ismail, NF Nik, et al, "Fuzzy logic controller on DC/DC boost converter," *Power and Energy (PECon), 2010 IEEE International Conference on. IEEE*, 2010.

[95] T. Yu and T. Chien, "Analysis and simulation of characteristics and maximum power point tracking for photovoltaic systems," *in Power Electronics and Drive Systems, 2009. PEDS 2009. International Conference on,,* pp. 1339-1344, 2009.

[96] A. Woyte, J. Nijs, and R. Belmans, "Partial shadowing of photovoltaic arrays with different system configurations: literature review and field test results," *Solar Energy,* vol. 74, pp. 217-233, 2003.

[97] G. Venkateswarlu, C. H. Jhansi & P. S. Raju, "Fuzzy logic based maximum power point tracking techingue for partially shaded photovoltaic system," *International Journal of*

Electrical and Electronics Engineering (IJEEE), vol. 3, pp. 49-60, 2014.

[98] C.S. Chin, M.K. Tan, P. Neelakantan, B.L. Chua and K.T.K. Teo, "Optimization of partially shadedd PV arrary using fuzzy MPPT," *IEEE Colloquium on Humanities, Science and Engineering Research (CHUSER 2011),* 2011.

[99] M.A. Sasi, "Fuzzy logic control of MPPT Controller for PV system," *Faculty of Engineering and Applied Science,* 2017.

[100] Luis Castafier and Santiago Silvestre, "Modelling photovoltaic systems using pSpice.," *England: John Wiley & Sons Ltd. ISBN: 0470845279.,* 2002.

[101] Antonio Luque and Steven Hegedus, Handbook of photovoltaic science and engineering, England: John Wiley & Sons Ltd. ISBN: 0470845279., 2002.

[102] M. R. AlRashidi, K. M. El-Naggar and M. F. AlHajri, "Parameters estimation of double diode solar cell model.," *World academy of science, engineering and technology,* pp. 100-103, 2013.

[103] G.H. Yordanov, O.M. Midtgård and T.O. Saetre, "Two diode model revisited: parameters extraction from semi-log plots of I-V data.," *25th european photovoltaic solar energy conference and exhibition/5th world conference on photovoltaic energy conversion,,* pp. 4156-4163, 2010.

[104] P. Rodrigues, J. R. Camacho and F. B. Matos, "The application of trust region method to estimate the parameters of photovoltaic modules through the use of single and double exponential models," *Proceedings of the international conference on renewable energies and power quality, (ICRERPQ'11)..*

[105] M. G. Villalva, J. R. Gazoli and E. Ruppert, "Modeling and circuit-based simulation of photovoltaic arrays," *Barzilian journal of power electronics,* Vols. 14, no. 1, pp. 35-45, 2009.

[106] Basil M. Hamed and Mohammed S. El-Moghany, "Fuzzy controller design using FPGA for photovoltaic maximum power point tracking," *International journal of advanced research in*

artificial intelligence (IJARAI), Vols. 1, no. 3, pp. 14-21, 2012.

[107] L.A Zedah, "Outline of New Approach of the Analysis of Complex System and Decision," *IEEE Transactions System, Man, Cybern.,* Vols. SMC-3, no.1, pp. 146-151, 1963.

[108] KC200GT solar cell data sheet..

[109] Marcelo Gradella Villalva, Jonas Rafael Gazoli, and Ernesto Ruppert Filho, "Comprehensive approach to modeling and simulation of photovoltaic arrays," *IEEE transactions on power electronics,*, Vols. 24, no. 5, pp. 1198-1208, 2009.

[110] S. Narediran, S.K. Sahoo and R. Das, "Control and analysis of MPPT techinques for maximizing power extraction and elliminating oscilations in PV system.," *international energy journal 16,* pp. 107-118, 2016.

[111] K. Ishaque, Z. Salam and H. Taheri, "Accurate MATLAB Simulink PV System Simulator based on a Two-Diode Model,," *Journal of Power Electronics,* Vols. 11, no. 2, pp. 179-187, 2011.

[112] Furkan Dinçer and Mehmet Emin Meral, "Critical factors that affecting efficiency of solar cells.," *smart grid and renewable energy,* Vols. 1, no.1, pp. 47-50, 2010.

[113] M. Ravi Kumar, B. Bala Sai Babu, and M. Seshu, "Estimation of Average Solar Radiation on Horizontal and Tilted Surfaces for Vijayawada Location," *IOSR Journal of Electrical and Electronics Engineering (IOSR-JEEE,* vol. 11, no. 3, pp. 45-53, 2016.

[114] Bih Lii Chua and Aroland Kiring, " Fuzzy Logic Based MPPT for PV Array under Partially Shaded Conditions," *International Conference on Advanced Computer Science Applications and Technologies,* 2012.

[115] Wankhede, R. B., and U. B. Vaidya, "Energy Comparison of MPPT Techniques Using Cuk," *Energy 1.6,* 2014.

Appendix

Implementation of the Newton Raphson Method

The following functions is developed using MATLAB to compute various functions or find the parameters needed to proposed of model the photovoltaic.

```
% this function is design to solve the nonliear equation related %
ot the photovoltaic current and photovoltaic voltage, by % applying
the Newton Method.
Iscn=8.21;  //nomial short circuit current
Vocn=32.9;  //nomial open circuit voltage
Imp=7.61;   //maximum current @ mpp
Vmp=26.3;   // maximum votage @ mpp
Pmax_e=Vmp*Imp;  // experimental maximum power
Kv=-0.123;       // voltage coefficient of nomial open circuit
Ki=3.18e-3;      //current coefficient of short circuit current
Ns=36;           // series connected cells in a single module
Np=1;            //series connected cells in a single module
K=1.38065e-23;   //boltzman's constant
q=1.60217646e-19;// charge of electron
a=1.3;           // diode identity constant
%%nomial values
Gn=1000;         //radiation @ STC
Tn=25+273.15;    //temperature @ STC
%%adjusting algorithm
%the model is adjusted at the for the following test condition
T=32+273.15;      // operating temperature
G=4211;           // operating radiation
Vtn=(K*Tn)/q;     // terimal voltage @ STC temperature
Vt=(K*T)/q;       // termial voltage at operating temperature
Ion=Iscn/(exp(Vocn*a*Ns*Vtn)-1);
Io=Ion;
%reference values of Rs and Rp
Rs_max=(Vocn-Vmp)/Imp;
Rp_min=Vmp/(Iscn-Imp)-Rs_max;
%initial guess of Rs and Rp
Rp=Rp_min;
Rs=0;
tol=0.001;
P=(0);
error=inf; %dummy value
%Iterative process for Rsand Rp until Pmax,model=Pmax,experimental
while(error>tol)
    %Temperature and irradiance effect on the current
    dT=T-Tn;
    Ipvn=(Rs+Rp)/Rp*Iscn;
    Ipv=(Ipvn+Ki*dT)*G/Gn;
```

```
    Isc=(Iscn+Ki*dT)*G/Gn;
    %increments Rs
    Rs=Rs+0.01;
    %Parallel Resistance
    Rp=Vmp*(Vmp+Imp*Rs)/(Vmp*Ipv-
Vmp*Io*exp((Vmp+Imp*Rs)/Vt/Ns/a)+Vmp*Io-Pmax_e);
    %Solving the I-V equation for several (V,I)pairs
    clear V
    clear I
    V=0:0.3:350;  %voltage vector
    I=zeros(1,size(V,5)); %current vector

    for j=1 :size(V,5) % calculates for all voltage values
        % solves g=I-f(I,V)=0 with Newntonn_Raphson
        g(j)=Ipv-Io*(exp((V(j)+I(j)*Rs)/Vt/Ns/a)-1)-
(V(j)+I(j)*Rs)/Rp-I(j);
        while(abs(g(j)>0.001))
            g(j)=Ipv-Io*(exp((V(j)+I(j)*Rs)/Vt/Ns/a)-1)-
(V(j)+I(j)*Rs)/Rp-I(j);
            glin(j)=-Io*Rs/Vt/Ns/a*exp((V(j)+I(j)*Rs)/Vt/Ns/a)-
Rs/Rp-1;
    I_(j)=I(j)-g(j)/glin(j);
    I(j)=I_(j);
        end
    end
    for j=1:size(V,2)
        %calculates power using the I-V equation
        p=(Ipv-Io*(exp((V+I.*Rs)/Vt/Ns/a)-1)-(V+I.*Rs)/Rp).*V;
        Pmax_m=max(p);
        error=(Pmax_m-Pmax_e);
    end
    end %while(error>tol)m
    %% outputs
    fprintf('model info:\n');
    fprintf('Rp_min=%f',Rp_min);
    fprintf('\n Rp=%f',Rp);
    fprintf('Rs_max=%f',Rs_max);
    fprintf('\n Rs=%f',Rs);
    fprintf('\n a=%f',a);
    fprintf('\n T=%f',T - 273.15);
    fprintf('\n G=%f',G);
    fprintf('\n Pmax,m=%f(model)',Pmax_m);
    fprintf('\n Pmax,e=%f(experimental)',Pmax_e);
    fprintf('\n tol=%f',tol);
    fprintf('\n P_error=%f',error);
    fprintf('\n Ipv=%f',Ipv);
    fprintf('\n Isc=%f',Isc);
    fprintf('\n Ion=%f',Ion);
```